SOUTHERN JOURNAL OF RESEARCH

ISSN (P): 2789-7583
ISSN (O): 2789-7591

INSTITUTE OF SOUTHERN PUNJAB MULTAN, PAKISTAN

VOLUME: 03 | ISSUE: 01 | JAN-JUN | 2023

SOUTHERN JOURNAL OF RESEARCH

INSTITUTE OF
SOUTHERN PUNJAB
MULTAN, PAKISTAN

ISSN (P): 2789-7583
ISSN (O): 2789-7591

Editorial and Advisory Board

Editorial Team

Author's Guidelines

The Journal is devoted to promoting the rapid dissemination of original research papers in the relevant disciplines of particular importance. The primary emphasis will be placed on original research contributions, preliminary communications, and reviews on current developments containing full details presented from Social, Natural, Behavioral Sciences, Engineering, and Languages. It will bring together researchers from different specializations. SJR will be a peer-reviewed multidisciplinary International Journal that will be bi-annually published by the Institute of Southern Punjab (ISP), Multan (Pakistan). SJR will be purely an academic Journal and will cover both applied and theoretical issues of all disciplines in the English Language. Likely subscribers will be the Universities, Research Institutions, and individual researchers. Authors are requested to read these instructions carefully before formatting the manuscript.

Organization of the Manuscript

The title should be clear, informative, and concise and should be centered and typed in bold with Arial font and size of 15pt. Author's name is to be bold and centered below the title in the form: Given name (or initial) and family name in Times New Roman and size of 10pt. Author affiliations (department, faculty & institutional information) must be provided below the names in Times New Roman and font size of 10pt. A maximum 4-5 keywords must be mentioned below the abstract. The article should be prepared in Times New Roman, and font size of 10pt with a line spacing of 1.5. All the main headings will be bold, Times New Roman with 11pt font size, whereas, subheadings should be bold and italics. The body of the article should be organized in the following manner: Introduction, Materials and Methods, Results, Discussion, Acknowledgement, and References. Template for research articles is available on the website: https://sjr.isp.edu.pk/index.php/journal/index.

Authors are requested to follow the same guidelines for the submission of a manuscript. All illustrations must be in the form of Photographs and must be numbered in sequence. Each illustration must be referred to in the text. It should be provided with the caption giving sufficient information for the figure without reference to the text. All text and illustrations must be within the allowed area as per the attached template. Tables are often an economic way of presenting data. All tables must be numbered in sequence with Latin numerals both in the text and in the heading of each table. The heading should be informative for the table to be understood without reference to the text. These are inserted in the appropriate place in the text. References should be placed at the end of the manuscript in APA style. These should be in the general form as: Aslam, M., Shafigh, P., & Jumaat, M. Z. (2016). Drying shrinkage behavior of structural lightweight aggregate concrete. *Journal of Cleaner Production*, 127, 183-194.

Double-Blind Peer Review Policy

This journal uses a double-blind review, which means that both the reviewer and author identities are concealed from the reviewers, and vice versa, throughout the review process. To facilitate this, authors need to ensure that their manuscripts are prepared in a way that does not give away their identity. To help with this preparation please submit the Title Page containing the Author's details and Blinded Manuscript with no author details as 2 separate files.

Ethical Issues

The corresponding Author on behalf of joint authors will submit an undertaking that: The contents of the paper are original but not plagiarized. The paper submitted to SJR has not been previously published and is not under consideration for publication in any other medium. Authors who do not comply with these guidelines and policies of the Higher Education Commission (HEC) may be liable for punitive action. The paper is submitted in SJR solely from a research point of view under no compulsion. Additionally, no financial involvements affect this submission of research.

Correspondence and Submission

A copy of the manuscript should be submitted to the: Editor-in-Chief, Southern Journal of Research (SJR), Institute of Southern Punjab, 9-KM Bosan Road, Multan, Pakistan.

Submission is made online: https://sjr.isp.edu.pk/index.php/journal/index.

For further queries, contact: sjr@isp.edu.pk.

Copyright Notice

The policy for copyright shall be clearly stated in the author guidelines and the copyright holder named on all published articles. Likewise, licensing information shall be clearly described in guidelines on the website, and licensing terms shall be indicated on all published articles, both HTML and PDFs. If authors are allowed to publish under a Creative Commons license, then any specific license requirements shall be noted. Any policies on posting final accepted versions or published articles on third-party repositories shall be clearly stated.

Privacy Statement

The names and email addresses entered in this journal site will be used exclusively for the stated purposes of this journal and will not be made available for any other purpose or to any other party.

Disclaimer

The opinions expressed in the Southern Journal of Research (SJR) are those of the authors and contributors, and do not necessarily reflect those of the journal management, advisory and editorial boards. Papers published are processed through double-blind peer-review by respective subject experts/specialists and language experts. Neither the Institute of Southern Punjab, (ISP) nor the editors of SJR can be held responsible for errors nor any consequences arising from the use of the information contained in SJR, instead; should errors be reported directly to the corresponding author of the articles.

Table of Contents

Southern Journal of Research Vol. 3(1), 2023

Symmetric Effect of Financial Market Development, Government Transparency and Trade openness on Macroeconomic Stability: Cross-country evidence

Muhammad Hussain

Xidian University, Shaanxi, China

Abstract

This paper investigates the effect of financial market development, government transparency, and trade openness on macroeconomic stability by utilizing a panel data of 75 countries over the period from 2007 to 2017. Quantile Regression method is applied for estimation, the findings reveal that financial market development is favorable for the macroeconomic stability. The results also shows that government transparency and trade openness is positively and significantly associated with the macroeconomic stability. Gross Domestic Product (GDP) is utilized as control variable which is also positive and significant with macroeconomic stability. Furthermore, for robustness, the main panel is divided into three sub-panel on the basis of country risk (low-risk, moderate-risk, and high-risk) and adopted same statistic technique. The results shows that independent variables of the study have a significant and positive association with macroeconomic stability at various quantiles. However, financial market development and government transparency are important factor than trade openness. It is recommended that optimal level of policies for financial development and government transparency should be designed and formulated for economic stability in the country. It is suggested for the future research to focus on financial openness for further study on macroeconomic stability.

Keywords: Financial Market Development, Government Transparency, Trade openness, Macroeconomic Stability, Quantile Regression, Panel Data Analysis, Sub-Panel (country risk).

Email: hussain.hed@gmail.com

1. Introduction

A sound financial system can reduce the market anomalies, reduce the cost of capital, and improve the overall economic performance (Adeoye & Isumaila, 2022; Ahmed, 2013). In a globalized economy, trading activities are important and fundamental element for economic development (Touwen, 2021). These economic activities ignite the volume of investment through economic freedom and trade openness which is essential for a sound macroeconomic environment (Ehigiamusoe et al., 2020). Macroeconomic instability is curbing and restricting to develop their economies, especially the developing economies is seriously suffering locally and regionally. The governments of these economies are trying to deal and manage the related economic factors to improve their macroeconomic stability (Weller & Zulfiqar, 2013).

Financial market development is very important factor to enhance the savings and investment which increase the overall firms' productivity (Sever, 2019). Existing evidences are available that financial market development from the financial intermediation plays important role in mobilizing and redistribution of financial resources which contributes to the country's economic growth (Brychko et al., 2021). A developed financial system is essential for macroeconomic stability by relaxing credit constraints on

firms and households (Nyalihama & Kamanzi, 2022). Trade openness is an approach where governments provide a free trade and less restrictions on trade of goods and services which is positively increase the economic growth Kaplan & Yaprakli, 2014). The macroeconomic stability indicators are very important factors for economic growth and development (Vasylieva et al., 2018). So, it is also believed that governments can stable its macroeconomic indicators by less restricted economic activities which will not only boost up the income level of individual but also productivity in a country.

Countries which have implemented sound transparency system, and easy business operating policies have achieved a better position globally. To eradicate the corruption element in a country, governments have to formulate and implement different strategic policies which will enhance the transparency. Government transparency build a confidence among investors. For example, foreign direct investment is basic need especially for the developing countries. Investors trust on government initiatives not on just announcements. The improving transparency and accountability have a positive influence on decision making for local and foreign investors (Schmaljohann, 2013). On the other hand, Şıklar and Kocaman (2018) has suggested that macroeconomic stability is important for foreign direct investment. Hence, it is believed that through financial market development, trade openness, and government transparency, the stability in macroeconomic indicators can be achieved.

Existing literatures builds a positive link between financial development and economic growth (Eren et al., 2019; Ibrahim & Alagidede, 2018). A very few contemporary existing literatures are available that tested the direct relationship between financial market development on macroeconomic stability. Previously, macroeconomic stability is tested with financial development of the West African Region by utilizing a panel data, this study confirms that there is a positive impact of macroeconomic stability on the financial market development. By applying cointegration analysis, VECM, and Granger Causality test, argued that to attract high volume of the foreign direct investment, the macroeconomic stability should be strengthened (Şıklar & Kocaman, 2018). However, Nyalihama and Kamanzi (2022) have argued that financial development has a positively and significantly impact on macroeconomic stability. Previously, transparency of central banks is investigated with financial stability by using a panel data of 110 countries over the period from 2000 to 2011, and found that too high transparency is not beneficial for the financial stability (Horváth & Vaško, 2016). Williams (2014) has documented that in democratic countries, the transparency has a positive and significant impact on macroeconomic stability. The impact of trade openness is investigated by Ma et al., (2022) using quarterly Chinese data over the period from 2005 to 2020, and found that the impact of trade openness on macroeconomic volatility is differ in different situation.

Based on the above research arguments, we believed that financial market development, government transparency, and trade openness have a direct positive impact on macroeconomic stability. In prior studies, these variables are tested with different factors (Eren et al., 2019; Ibrahim & Alagidede, 2018; (Şıklar & Kocaman, 2018; Horváth & Vaško, 2016). Similarly, Shaohua et al., (2021) have investigated these variables by considering the macroeconomic stability as independent variable. However, in this study, we have considering macroeconomic stability as dependent variable while financial market development, trade openness, government transparency as independent variable. Moreover, quantile regression will be a good contribution in existing literature on macroeconomic stability. Secondly, this panel data is further divided into three sub-

panels based on country risk which is also previously overlooked, and will also provide a help for the policymakers in formulating different policies.

2. Methodology

In this research study, a panel data consisting 75 countries globally are utilized over the period from 2007 to 2017. Further, this panel data is divided into sub-panel based on country risk i.e low-risk, medium-risk, and high-risk to investigated the effect of financial market development, government transparency, and trade openness on macroeconomic stability. Secondary data is utilized which is collected from global competitiveness index (GCI). Macroeconomic stability is considered as dependent variable which is the third pillar of GCI, and measured with country credit rating, government debt, inflation, gross national savings, and government budget balance. Whereas financial market development is considered as independent variable which is eight pillar of GCI which is measured with legal rights, regulation of security exchanges, soundness of banks, venture capital availability, ease of access to banks, financing through local equity markets, affordability of financial services, and financial services meeting business needs. Government transparency is measured with degree of accessibility of information for business. Trade openness is measured with imports plus exports as percentage of gross domestic product. However, gross domestic product (GDP) is considered as control variable for this study. According to the linear regression, it explains that how much dependent variable changes with change in a particular variable. However, in quantile regression, it estimates the changes in various quantile. Thus, quantile regression methodology is utilized in this study. For this short panel data, it is assumed that data is stationary at level. Quantile regression is a non-linear parametric method which is widely used by the researchers when the data is not normally distributed. For this purpose, Jarque-Bera (JB-test) is utilized to test the normality of the data. For robustness, the main panel data is divided into three sub-panels based on country risk which is a novel contribution in existing literature on macroeconomic stability.

3. Results and Discussion

Descriptive statistics of dependent variable and independent variable are shown in Table-1 as below. The average score of macroeconomic stability (MES) of the selected countries is 4.712. Burundi is showing the instable macroeconomic situation whereas Norway has shown the strong macroeconomic stability indicators among countries of this study. The mean value of financial market development is 4.212, and the maximum value is 6.40 and minimum value is 2.10. Gambia has the most developed financial market whereas Mauritania is the least developed country. On average, the transparency government is 4.288. Mauritania also has weak government transparency, and Singapore is the most transparency government among countries. The average value of trade openness is 87.484. Singapore has the less restricted economic policy and easy to operate economic activities whereas Norway has the strict policy towards trade openness.

3.1 Descriptive Statistics

The descriptive statistics is also showing that Jarque-Bera Test of all variables are significant which mean that the data is not normally distributed. For further analysis, a non-parametric test is applied. Hence, quantile regression is utilized which fulfill all its assumptions.

Table 1. Summary Statistics

Variable	Mean	S.D	Min	Max	Skew:	Kurtos:	JB-test

MES	4.712	0.874	1.000	6.840	-0.397	3.677	37.454***
FMD	4.212	0.762	2.100	6.400	0.158	2.748	5.645***
TRANSP:	4.288	0.763	2.471	6.322	0.306	2.813	14.121***
TRDOPN:	87.484	60.611	20.722	437.326	2.616	11.451	3396199***
GDP	17643.96	22160.80	172.495	123514.2	1.955	7.345	1175.21***

Source: Authors

3.2. Quantile Regression Estimates

Quantile regression methodology allows to understand the relationship between variables which are outside mean value. This method is helpful to test the non-linear relationship with predicator variables. The following Table presents the results of each variable for the full sample of countries.

Table 2: Quantile Regression Estimates (Full Sample)

Variables	QR(Median)	Q10	Q20	Q30	Q40	Q50	Q60	Q70	Q80	Q90
FMD	0.089*** (0.034)	0.141*** (0.071)	0.162*** (0.049)	0.110*** (0.040)	0.073*** (0.035)	0.089*** (0.034)	0.062** (0.034)	0.024 (0.033)	-0.016 (0.039)	-0.035 (0.047)
GTranp:	0.285*** (0.050)	0.209** (0.122)	0.204*** (0.058)	0.268*** (0.048)	0.275*** (0.046)	0.285*** (0.050)	0.214*** (0.054)	0.257*** (0.049)	0.261*** (0.049)	0.342*** (0.073)
TradeOp	0.001*** (0.000)	0.002*** (0.004)	0.002*** (0.004)	0.002*** (0.003)	0.001*** (0.004)	0.001*** (0.004)	0.001*** (0.004)	0.001*** (0.004)	0.000 (0.000)	-0.001 (0.000)
GDP	9.020*** (01.400)	1.350*** (2.100)	1.130*** (1.390)	1.040*** (1.250)	9.090*** (1.280)	9.020*** (1.400)	9.940*** (1.750)	7.550*** (1.760)	7.110*** (2.140)	4.970*** (2.130)
Intercept	2.838*** (0.222)	1.770*** (0.355)	2.163*** (0.242)	2.414*** (0.2100)	2.769*** (0.213)	2.838*** (0.222)	3.422*** (0.249)	3.631*** (0.220)	4.099*** (0.229)	4.309*** (0.353)
Observ:	825									
JB-test	66.983***									
R^2	0.166									
Adj: R^2	0.162									

Source: Author's own explanation

Note: Values in parenthesis are the robust standard errors. However, *, **, and *** indicate significance at the 10%, 5%, and 1% levels, respectively. (FMD=Financial Market Development, GTransp=Government Transparency, TradeOp=Trade Openness, GDP=Gross Domestic Product)

From the above results, it is found that according to QR(Median) all the independent variables have positive and significant impact on macroeconomic stability. According to this result, as financial market development increases in a particular country, this will bring a positive change to stable the economic indicators (beta=0.089, p-value<0.05). Government transparency is also showing positive results on dependent variable of the study. It showing that 1% increase in implementation of government transparency, will bring 28% increase in macroeconomic stability which is a big change. So, it is important factor for an economy that facing instability in the economy indicators. However, as per the results of trade openness, it is shows that trade openness is not brining a big positive change in stability but a very slight

positive change on dependent variable. The co-efficient of beta of gross domestic product is showing a positive and significant change on macroeconomic stability. The full sample of panel data is consisting of 825 observations. Jarque-Bera Test is showing significant results which is showing the quantile regression is meeting basic assumption. R-squared is 16.60% which is describing that overall impact of explanatory variables on dependent variable. However, Adjusted R-squared is 16.20%.

Furthermore, the table is also reporting the results of different quantiles i.e., 10, 20, 30, 40, 50, 60, 70, 80, and 90 percent quantiles. It is found that financial market development is gradually increasing its impact on stability up to 50 percent quantile, after that its impact is insignificant. However, government transparency is resulting a good positive contribution for the soundness of macroeconomic indicators throughout the quantiles. Although, it is found that trade openness has a positive and significant impact at various quantiles but its impact on macroeconomic stability is too low (beta=0.002, p-value<0.05). It is found that trade openness is not an effective factor to influence the macroeconomic stability. Gross domestic product is also contributing better on macroeconomic stability.

3.3 Robustness Checks

For robustness checks, the full sample panel is divided into three sub-panels i.e low-risk, medium-risk, and high-risk. Based on this technique, find slightly different results based on country's risk. Same methodology is adopted to find results.

Table 3: Quantile Regression Estimates (Low-Risk)

Variables	**Q10**	**Q20**	**Q30**	**Q40**	**Q50**	**Q60**	**Q70**	**Q80**	**Q90**
FMD	0.065 (0.092)	0.121* (0.077)	0.133*** (0.077)	0.167*** (0.068)	0.180*** (0.062)	0.124*** (0.061)	0.164*** (0.061)	0.205*** (0.073)	0.152** (0.091)
GTranp:	0.344*** (0.144)	0.339*** (0.113)	0.201*** (0.106)	0.173*** (0.089)	0.103 (0.073)	0.092 (0.071)	0.069 (0.072)	0.090 (0.091)	0.114 (0.159)
TradeOp	0.001 (0.001)	0.003*** (0.001)	0.002* (0.003)	0.001 (0.001)	0.001 (0.004)	-0.001 (0.004)	-0.001 (0.004)	-0.000 (0.000)	-0.001** (0.000)
GDP	9.080*** (1.480)	9.650*** (1.220)	8.510*** (1.300)	0.000*** (1.500)	0.000*** (1.230)	0.000*** (1.160)	0.000*** (1.190)	0.000*** (2.010)	0.000*** (6.360)
Intercept	1.546*** (0.601)	1.439*** (0.510)	2.299*** (0.496)	2.564*** (0.446)	2.936*** (0.398)	3.468*** (0.405)	3.526*** (0.408)	3.493*** (0.529)	3.980*** (0.787)
Observ:	407								
JB-test	38.417***								
R^2	0.109								
Adj: R^2	0.100								

Source: Author's own explanation

Note: Values in parenthesis are the robust standard errors. However, *, **, and *** indicate significance at the 10%, 5%, and 1% levels, respectively. (FMD=Financial Market Development, GTransp=Government Transparency,

TradeOp=Trade Openness, GDP=Gross Domestic Product)

Table 4: Quantile Regression Estimates (Medium-Risk)

Variables	Q10	Q20	Q30	Q40	Q50	Q60	Q70	Q80	Q90
FMD	0.327***	0.236***	0.136***	0.099	0.020	-0.041	-0.089	-0.08***	-0.094
	(0.102)	(0.093)	(0.068)	(0.077)	(0.073)	(0.074)	(0.071)	(0.068)	(0.103)
GTranp:	0.215	0.151	0.153**	0.176***	0.192***	0.164***	0.222***	0.311***	0.413***
	(0.223)	(0.111)	(0.089)	(0.085)	(0.083)	(0.082)	(0.086)	(0.075)	(0.082)
TradeOp	0.013***	0.011***	0.009***	0.006***	0.006***	0.006***	0.003	0.002	0.002
	(0.002)	(0.002)	(0.002)	(0.001)	(0.001)	(0.002)	(0.002)	(0.002)	(0.002)
GDP	1.860***	1.680***	1.220***	5.310	3.590	2.190	-4.220	-8.590	-1.440
	(8.090)	(6.860)	(5.440)	(5.160)	(5.200)	(5.300)	(6.210)	(6.450)	(6.070)
Intercept	-0.050	1.161**	2.116***	2.708***	3.167***	3.731***	4.241***	4.699***	4.147***
	(0.861)	(0.626)	(0.527)	(0.498)	(0.499)	(0.472)	(0.444)	(0449)	(0.750)
Observ:	198								
JB-test	6.649***								
R^2	0.100								
Adj: R^2	0.081								

Source: Author's own explanation

Note: Values in parenthesis are the robust standard errors. However, *, **, and *** indicate significance at the 10%, 5%, and 1% levels, respectively. (FMD=Financial Market Development, GTransp=Government Transparency, TradeOp=Trade Openness, GDP=Gross Domestic Product).

Table 5: Quantile Regression Estimates (High-Risk)

Variables	Q10	Q20	Q30	Q40	Q50	Q60	Q70	Q80	Q90
FMD	0.479***	0.327***	0.284***	0.242***	0.172***	0.183***	0.148***	0.048	0.106
	(0.144)	(0.071)	(0.070)	(0.063)	(0.050)	(0.047)	(0.048)	(0.055)	(0.090)
GTranp:	-0.211	-0.087	0.022	0.079	0.137*	0.169***	0.126***	0.151***	-0.072
	(0.142)	(0.132)	(0.111)	(0.102)	(0.085)	(0.080)	(0.077)	(0.076)	(0.097)
TradeOp	0.002***	0.002***	0.002***	0.002***	0.002***	0.002***	0.002***	0.002***	0.002
	(0.001)	(0.001)	(0.001)	(0.001)	(0.001)	(0.001)	(0.001)	(0.001)	(0.002)
GDP	1.880***	1..460***	1.260***	1.220***	1.130***	1.020***	8.840***	6.180***	9.140
	(4.350)	(2.440)	(2.210)	(2.151)	(2.110)	(2.100)	(2.340)	(2.030)	(2.000)
Intercept	2.234***	2.718**	2.752***	2.858***	3.115***	3.098***	3.652***	4.317***	5.519***
	(1.036)	(0.439)	(0.355)	(0.364)	(0.378)	(0.402)	(0.441)	(0.478)	(0.489)
Observ:	208								
JB-test	12.907***								
R^2	0.215								
Adj: R^2	0.199								

Source: Author's own explanation

Note: Values in parenthesis are the robust standard errors. However, *, **, and *** indicate significance at the 10%, 5%, and 1% levels, respectively. (FMD=Financial Market Development, GTransp=Government Transparency, TradeOp=Trade Openness, GDP=Gross Domestic Product).

For low-risk countries, the impact of financial market development is significant and positive throughout the various quantiles which was not observed in the full sample panel. Similarly, government transparency is found positive up to 40th quantile, and later on insignificant impact on macroeconomic stability which is also inconsistent with the main panel. However, the results of trade openness are consistent with the main panel. However, the results of medium-risk panel data are consistent with the full sample panel. As per the results of high-risk countries, the impact of financial market development is found positive and significant up to 70 percent quantile which is almost consistent with main panel. However, the government transparency is found inconsistent with the main panel, and also found inverse results with low-risk panel data. Interestingly, the trade openness factor is showing its silent features with on macroeconomic stability in the main global panel as well as in the sub-panels.

4. Conclusion and Policy Implications

The objective of this study is to assess the impact of financial market development, government transparency, and trade openness on macroeconomic stability. For this purpose, a panel data consisting of 75 countries of the world is utilized and quantile regression method is applied for estimates. For robustness checks, the main global panel is divided into three sub-panels based on country's risk (low-risk, medium risk, and high-risk). The results of all the independent variables have found positive and significant relationship with macroeconomic stability by using full main panel data. However, the results of sub-panels are different from the main panel except medium-risk countries. Hence, the expansion in financial markets through provision of financial services may introduced and strengthen the macroeconomic stability. Similarly, the results also indicates that government transparency is contributing to stabilize the output in medium-risk countries. However, the features of trade openness towards macroeconomic stability are silent. Interestingly, the results of low-risk countries and high-risk countries are showing opposite results. The co-efficient of beta of financial market development has positively and significantly increasing gradually with increasing quantiles for low-risk countries and vice versa in high-risk countries. The co-efficient beta of government transparency is decreasing positively and significantly on macroeconomic stability for low-risk countries whereas for high-risk countries, this impact is started negatively and gradually improving its impact significantly and positively on macroeconomic stability. However, trade openness has shown its silent impact. Based on the results it is concluded that for medium-risk level countries, financial market development and government transparency factors are important instead of trade openness to stable macroeconomic indicators. However, from the results of low-risk and high-risk countries, it is concluded that high-risk countries must revisit their policies towards government transparency. It is recommended for the researchers to test the impact of financial openness on macroeconomic stability.

References

Adeoye, B. W., & Isumaila, O. S. (2022). Stock Market Liquidity and Economic Growth: Empirical Evidence from Nigeria. *Romanian Journal of Economics*, *54*(1 (63)), 80-94.

Ahmed, A. D. (2013). Effects of financial liberalization on financial market development and economic

performance of the SSA region: An empirical assessment. *Economic Modelling*, *30*, 261-273.

Brychko, M., Bilan, Y., Lyeonov, S., & Mentel, G. (2021). Trust crisis in the financial sector and macroeconomic stability: a structural equation modelling approach. *Economic Research-Ekonomska Istraživanja*, *34*(1), 828-855.

Ehigiamusoe, K. U., Lean, H. H., & Chan, J. H. (2020). Influence of macroeconomic stability on financial development in developing economies: Evidence from West African region. *The Singapore Economic Review*, *65*(04), 837-856.

Eren, B. M., Taspinar, N., & Gokmenoglu, K. K. (2019). The impact of financial development and economic growth on renewable energy consumption: Empirical analysis of India. *Science of the Total Environment*, *663*, 189-197.

Horváth, R., & Vaško, D. (2016). Central bank transparency and financial stability. *Journal of Financial Stability*, *22*, 45-56.

Ibrahim, M., & Alagidede, P. (2018). Effect of financial development on economic growth in sub-Saharan Africa. *Journal of Policy Modeling*, *40*(6), 1104-1125.

Kaplan, F., & Yaprakli, S. (2014). The impacts of institutions, openness and macroeconomic stability on economic growth: a panel data analysis on middle income countries. *Istanbul University Econometrics and Statistics e-Journal*, (20), 104-123.

Ma, Y., Jiang, Y., & Yao, C. (2022). Trade openness, financial openness, and macroeconomic volatility. *Economic Systems*, *46*(1), 100934.

Nyalihama, C., & Kamanzi, C. (2022). Impact of financial systems development on macroeconomic stability in Rwanda.

Schmaljohann, M. (2013). *Enhancing foreign direct investment via transparency? Evaluating the effects of the EITI on FDI* (No. 538). Discussion paper series.

Sever, C. (2019). *Finance and Productivity* (Doctoral dissertation).

Shaohua, Z., Yahya, F., Pham, H., & Waqas, M. (2021). Do transparency and anti-monopoly policies matter for financial development? Evidence from a panel ARDL-PMG approach. *Journal of Applied Economics*, *24*(1), 1-16.

Şıklar, İ., & Kocaman, M. (2018). FDI and macroeconomic stability: The Turkish case. *European Financial and Accounting Journal*, *13*(1), 19-40.

Şıklar, İ., & Kocaman, M. (2018). FDI and macroeconomic stability: The Turkish case. *European Financial and Accounting Journal*, *13*(1), 19-40.

Touwen, L. J. (2021). *Extremes in the archipelago: Trade and economic development in the outer islands of Indonesia, 1900-1942*. Brill.

Vasylieva, T. A., Lieonov, S. V., Liulov, O. V., & Kyrychenko, K. I. (2018). Macroeconomic stability and its impact on the economic growth of the country.

Weller, C. E., & Zulfiqar, G. (2013). Financial market diversity and macroeconomic stability. *Working Paperswp332, Political Economy Research Institute, University of Massachusetts at Amherst*.

Williams, A. (2014). The effect of transparency on output volatility. *Economics of Governance*, *15*(2), 101-129.

Impact of Working Capital Management on Corporate Performance. A Case-study of Automobile, Chemical, Food, and Pharmaceutical Sector of Pakistan

Muhammad Asif[1], Muhammad Farooq[1], Sonia Hassan[2]*, Ghulam Fareed Khan[3]

[1]Department of Management Sciences, The Islamia University, Bahawalpur, Pakistan
[2]Department of Business Administration, Bahauddin Zakariya University, 60000 Multan, Pakistan
[3]Department of Business Administration, Zhejiang University, China

Abstract. There is no hidden secret that working capital management policies do impact profitability but to what extent this is still a debatable issue. The capital structure theories suggest that apart from the firm size, the sensitivity of working capital management policies varies among different business sectors. The present study aims to investigate variation in working capital policies of the Automobile, Chemical, Food, and pharmaceutical sectors of Pakistan. Firm performance is measured through Return on Assets and Shareholders wealth is measured through Return on Equity. We find that the chemical sector aggressively manages working capital with the mean value of the Net Trade Cycle is 21 days. The results also suggest that aggressive working capital policy does not show any association with a firm's profitability while the opposite does harm a firm's performance.

Keywords: Capital Management; Corporate Performance; Automobile; Pakistan's Economy.
Email: soniahassan@isp.edu.pk

1. Introduction

The present study emphasizes to study the working capital practices of the Automobile, Chemical, Food, and pharmaceutical sectors of the economy and its contribution to the profitability of the same as well. Working capital management proved to be an important area of corporate finance in the last decades especially its importance recognized in the era of economic downturn 2007-08. Because of its growing importance in the world of corporate finance, the CFO Magazine publishes reports on working capital management performance in many countries.

Investment in working capital always remains one of the important decisions that was taken by the financial manager. Several theories help managers to resolve this puzzle successfully. This decision is important as it has a direct impact on firm value. Haq et al. (2011) concluded that a firm's profitability is affected by the working capital policy adopted by the financial manager. Working capital in the simplest way can be defined as the ability of the company to meet its day-to-day operations (Charitou, Elfani, & Lois, 2010). The efficient management of working capital ensures not only the continuity in the operation of the business but also ensures to pay short-term debt and upcoming operational expenses. It consists of the management of inventories, accounts receivables, accounts payable, and cash.

Numerous theories evolved to understand the relation between working capital and firm performance. One school of thought argued that investment in working capital has a positive impact on firm performance. This is

because this will allow firms to increase sales as well as get discounts under early payments. Excess investment in stock also gives shelter against price fluctuations, reduces order cost, and the possibility of reduced sale due to stock out situation. On the other hand, overinvestment in stock increases financing costs. So eventually high-interest cost leads to bankruptcy.

Corporate managers have three ways to deal with working capital namely Conservative, aggressive and moderate policy of working capital management. Each one has a unique effect on a firm's profitability, liquidity, and risk. In the conservative approach, the firm makes excess investment in the current asset so this approach is less risky and less profitable as well. In an aggressive approach, the firm made less investment in the current asset. This approach increases the profitability and as well as risk as well. Moderate approaches manage the way between these two sides of the coin. In this approach, the firm tries to manage a permanent portion of the current portion with long-term funds while the rest of the portion of current assets with short-term financing.

It is important to note that working capital policies vary from organization to organization keeping in view the nature of business. For instance, manufacturing industries have to maintain spare parts and equipment resultantly heavy investment in the current assets. While services need not make heavy investments in current assets. In this context, it is implied that working capital policy significantly impacts shareholders' value.

Financing constraints of an organization change the optimum level of working capital and its possible association with the profitability of the organization. This is not supported by the seminal work of Modigliani and Miller in which they claim that in a perfect capital market, firms are independent with financing and investment decisions regarding their value. After that extensive literature on capital market imperfection evolved. Researchers concluded that market imperfection increases the cost of external financing as compared to internally generated funds. Fazzari et al. (1988) argue that the number of financial factors like availability of retained earnings, access to the capital market, and cost of financing put the effect of firm's investment in working capital. Fazzari and Petersen (1993) concluded that investment in working capital is more sensitive to financial constraints. To our knowledge, our paper is the first one to analyze the impact of financing constraints on this relationship. Based on findings we concluded that managers put concentration on other areas of finance to increase shareholder's value as working capital has the least impact on a firm's profitability. To the best of our knowledge, this is the first attempt to take the four diverse economic sectors simultaneously to analyze the possible impact of working capital management on a firm's profitability.

2. Literature Review

Nadiri (1969) was among the pioneers who firstly study the role of working capital management on the profitability of the organizations. After that researcher evolve a number of approaches by using Nadiri's model.

There is extensive literature available on working capital approaches about risk and return of the same (Pinches, 1991; Brigham and Ehrhardt, 2004; Gitman, 2005 and Moyer et al., 2005). Aggressive working capital policies associated with minimum investment in current assets. Resultantly characterized with high risk and high return characteristics. Conservative working capital policies are associated with huge investment in current assets as compared to aggressive policies hence, characteristics with low return and low risk (Van Horne and Wachowicz, 2004).

Jose, Lancaster, and Stevens (1996) suggest that the cash conversion cycle is the most appropriate measure of working capital management. CCC measures the period between cash paid for acquiring inputs and cash received from regular sales (Knauer & Wohrmann, 2013). CCC is the period acquiring the inputs and then the collection of cash from the sale of goods (Charitou et al., 2010; Deloof, 2003); Afza and Nazir (2009) claim that shorter the CCC leads to an increase in the profitability of the company.

Researchers claims that there is an inverted U-shaped relationship exists between firm performance and working capital management that means an optimal level of investment in current asset differ between firms according to the level of financial constraints they face. This U-shaped relationship exists because working capital is linked with profitability positively at the minimum level of working capital and inversely associated with the high level of working capital requirement.

Modigliani and Miller (1958) claim that companies' availability of external finance is not a problem especially in a frictionless world; hence investment does not depend on the availability of internal funds. In an imperfect market, external funds prove to be costly as compared to internal resources. Fazzari et al., (1988) claim that firms' placement of funds in current assets depends upon various financial factors like availability of internal finance, cost of external funds, and access to the financial market. Filbeck and Krueger (2005) study the working capital management policies of 32 non-financial industries of the US to analyze the impact of the same on the profitability of the organization. They concluded that working capital policies significantly differ among industries over time. These policies also change from time to time among firms.

Shin and Soenen (1998) collect the data of 58,985 firms from 1975 to 1994 to empirically test the possible association between net trade cycle and profitability of sample firms. They conclude that there exists a strong association between net trade cycle and profitability and suggested in order the increase profitability firm should reduce the net trade cycle. Rehan and Nasir (2007) analyze the possible association between working capital and profitability by using the data of 94 Pakistani firms. They use CCC as a working capital measure to measure the impact of the same on firms profitably. They concluded that CCC is negatively associated with profitably.

Ghosh and Maji (2003) empirically test the working capital management performance of the comment industry by using the data of 1992-1993 and 2001-2002. They calculated the indices instead of traditional working capital measures to analyze the efficiency of targeted firms. They found Indian Cement industry performance not satisfactory during the studied period. Gill et al. (2010) analyzed the impact of working capital management on a firm's profitability. They collect the data of 88 US firms from the period 2005 to 2007. They used a generalized least square regression model and concluded that there is a significant relationship between CCC and profitability.

Mohammad (2011) analyzed the relationship between profitability and working capital management in Iranian firms by using the data from 2001 to 2006. The cash conversion cycle is used as a measure of working capital efficiency. He concluded that the average collection period is inversely associated with profitability and inventory Turnover days were found significantly associated with profitability. They suggested that the firm should decrease the CCC to increase the firm profitability.

Mona (2012) studied the working capital policies (conservative, Aggressive) of Jordanian firms from the period 2001 to 2009.

Conservative working capital policy, as a relatively large investment in current assets, measuring current assets to total assets. He found by using a regressive method that conservative working capital policy is positively associated with profitability and the value of the firm. Aggressive working capital policy on the other land is negatively associated with firm profitability and value.

Mosa et al., (2012) investigate the working capital management and profitability relationship of food companies of Tehran by collecting the data from 2006 to 2011. They take debt rate and log sales as control variables and conclude that debt payment period. Inventory turnover and CCC are negatively associated with profitability. So, the manager should behave accordingly to enhance firms' value.

3. Methodology

3.1. Sample

This study uses data of non-financial firms listed on the Pakistan Stock Exchange. A firm must meet the following acceptance criteria in order to be a part of the study i.e. (Tables 1 & 2).

- The firm does not discontinue its business in any way during the study period.
- The firm should never delist during the study period.
- The firm has complete data of study period.

The data of sample firms were collected from their respective income statement and balance sheet. Finally, as per selection criteria 41 KSE listed firms were selected which comprises 11 firms from the Automobile sector, 7 firms from the pharmaceutical sector, 15 firms from the chemical sector, and 8 firms from the food sector. We take financial statements of sample firms from their respective websites and data regarding the market price of shares collected from daily quotations of KSE.

Table 3 describe descriptive statistics of 41 sample firms of the Automobile, Chemical, food, and pharmaceutical sector of Pakistan for the period from 2010 to 2015. In part A of the table, we present Industry-wise descriptive statistics. Results show that the cash conversion cycle of the chemical sector is about 14 days while the mean value of the cash conversion cycle of the automobile, food, and pharmaceutical sectors is 37 days, 35 days, and 61 days respectively.

The net trade cycle of the chemical sector is 21 days which is the lowest as compared to other sectors. The net trade cycle of the automobile, food, and pharmaceutical sectors are 57 days, 30 days, and 76 days respectively.

In the automobile sector, there is a difference between the net trade cycle and cash conversion cycle. Results show that the net trade cycle of the automobile sector is about 20 days more as compared to the Cash conversion cycle.

Other sectors have almost the same net trade cycle and cash conversion cycle. Hence based on descriptive results we conclude that the chemical sector manages its working capital more efficiently as compared to other sectors of study.

The average return on assets of sample firms is 12.48 % and the mean value of return on equity is 27.22%. The average net trade cycle of studied firms is 42 days and the average cash conversion cycle is 32 days.

3.2. Variables of Study

3.2.1. Dependent Variables

To quantify the role of working capital management on corporate profitability, we used Return on Equity (ROE), and Return on Asset (ROA) as dependent variables. Following Shin and Soenen, 1998; Afza and Nazir, 2008;

Nazir and Afza, 2009; Reheman et al., 2010 in their seminal work used ROE as a measure of corporate profitability.

It depicts how efficiently shareholders' investment is used to generate profit. On the other hand, there are several researchers like Jose et al., (1996); Wang, (2002); Garcia-Teruel & Martinez-Solano (2007) used return on asset (ROA) as a proxy to measure a firm's profitability.

3.2.2. Independent Variable

Net Trade Cycle (NTC) and Cash Conversion Cycle (CCC) were used as a variable to judge the working capital management efficiency of the sample firms. CCC is a widely used proxy to measure working capital management (Deloof, 2003; Gill et al., 2010).

It measures the time span between cash outflow in order to acquire the resources and then eventually cash inflow by way of sales. Following Shin and Soenen NTC is an efficient proxy to measure the working capital management.

So, we used both widely used working capital management proxies to testify the impact of both on profitability. Following previous literature Firm size, liquidity, firm's financial leverage, and growth opportunities were used as control variables in the present study (Table 4).

Table 1. Variables and their measurements

Variables of Study		
Variables	**Symbol**	**Desciption**
Dependent Variales		
Return on Asset	ROA	Ratio of Net Income to Total Assets
Return on Equity	ROE	Ratio of Net Income to Shareholder's Equity
Independent Variables		
Cash Conversion Cycl	CCC	Days A/R +Days Inventory-Days A/P
		A/R /Sales *365+ Inventory/CGS*365 - A/P/CGS*365
Net Trade Cycle	NTC	(Accounts Receivables / Sales)* 365 + (Inventories / Sales) *365 -
		(Accounts Payalbe /Sales)* 365
Control Variables		
Firm Size	FS	Natural Logrithm of Total Assets
Financial Leverage	LEV	Debt/ Total Assets
Liquidity	LIQ	Current Assets / Current Liabilities
Growth Opportunities	GRO	Current Sale - Previous Sale/ Previous Sale

Table 2. Descriptive Statistics

Industry wise Descriptive Statistics						
Industries	**Firms**	-	**NTC**	**CCC**	**ROA**	**ROE**
Automobile	11	Mean	57.6365	37.031	0.1216	0.213
		Std.dev	60.702	62.8732	0.101	0.1302
Chemical	15	Mean	21.5551	14.019	0.1135	0.20428
		Std.dev	57.3644	75.3261	0.1377	0.288
Food	8	Mean	30.81	35.3261	0.1627	0.5589
		Std.dev	77.479	81.2728	0.111	0.5753
Pharma	7	Mean	76.119	61.937	0.11	0.1833
		Std.dev	25.03	40.451	0.747	0.098
Panel C: Statistics on Variables						
			N	Mean		Std.dev
Firm Characteristics						
Firm Size			246	9.7966		0.6318
Financial Leverage			246	0.27		0.362
Growth Opportunities			246	0.7637		0.9322
Liquidity			246	2.0033		1.6922
Firm performance Variables						
Return on Assets			246	0.1248		0.1151
Return on Equity			246	0.2722		0.3461
Main Explanatory Variables						
Net Trade Cycle			246	42.7654		61.8967
Cash Conversion Cycle			246	32.5891		70.2299

Table 3. Correlation Matrix

-	ROE	ROA	CCC	NTC	FS	LIQ	LEV	GRO
ROE	1							
ROA	.669** (.000)	1						
CCC	-.385** (.000)	-.220** (.001)	1					
NTC	-.425** (.000)	-.195** (.002)	.789** (.000)	1				
FS	.094 (.142)	.019 (.0763)	-.483** (.000)	-.427** (.000)	1			
LIQ	-.131* (.039)	.197** (.002)	.291** (.000)	.332** (.000)	-.232** (.000)	1		
LEV	-.195** (.002)	-.310** (.000)	.017 (.794)	.073** (.256)	.175** (.006)	-.397**	1	
GRO	.244** (.000)	.195** (.002)	-.032 (.620)	.008 (.890)	.081 (.205)	-.050	-.038 (.594)	1

** Correlation is significant at the 0.01 level (2-tailed); *correlation is significant at the 0.05 level (2-tailed)

3.3. Correlation Analysis

Table 5 presents the correlation results among studied variables. Correlation measures that how variables are associated with each other. Results show cash conversion cycles are highly negatively correlated with return on equity and return on assets. Net Trade Cycle too negatively correlated with return on equity and return on equity. Firm size and Growth opportunities are positively associated with return on equity and return on assets. Liquidity and a Firm's financial leverage are negatively associated with return on assets and return on equity.

3.4. Models

OLS is a widely accepted technique used by the majority of researchers to empirically test the impact of working capital management policies on firms' profitability and shareholders' wealth maximization. (See for example; Deloof, 2003; Afza and Nazir (2009); and Lazaridis and Tryfonidis (2006). To analyze the impact of firm working capital policies on its profitability, we used the following model by applying panel data methodology.

$$ROAit = \beta0+\beta1CCCit+\beta2FSQit+\beta3LEVit+\beta4LIQit+\beta5GROit+ei \quad \ldots\ldots\ldots\ldots\ldots (1)$$

$$ROAit = \beta0+\beta1NTCit+\beta2FSQit+\beta3LEVit+\beta4LIQit+\beta5GROit+ei \quad \ldots\ldots\ldots\ldots\ldots (2)$$

$$ROEit = \beta0+\beta1CCCit+\beta2FSQit+\beta3LEVit+\beta4LIQit+\beta5GROit+ei \quad \ldots\ldots\ldots\ldots\ldots (3)$$

$$ROEit = \beta0+\beta1NTCit+\beta2FSQit+\beta3LEVit+\beta4LIQit+\beta5GROit+ei \quad \ldots\ldots\ldots\ldots\ldots (4)$$

Where ROA represents Return on Asset, ROE represents Return on Equity, CCC represents Cash Conversion Cycle, NTC represents Net Trade Cycle, FS represents Firm Size, LEV represents firm's financial leverage, LIQ represents Liquidity, and GRO represents Growth Opportunities.

Table 4. Regression results on Return on assets as dependent variable and Net Trade Cycle as an independent variable along with control variables

Return on Asset	Panel Data Analysis				
	Full Sample	**Automobile**	**Chemical**	**Food**	**Pharma**
Net Trade Cycle	-0.001	0.000	0.000	-0.001	-0.001
p-value	0.000	0.079	0.457	0.003	0.17
Firm Size	-0.006	0.018	0.003	-0.028	0.079
p-value	0.616	0.575	0.902	0.211	0.013
Financial Leverage	-0.076	-0.044	-0.038	-0.128	-0.094
p-value	0.000	0.693	0.204	0.017	0.032
Growth Opportunities	0.024	-0.033	0.066	0.01	0.007
p-value	0.001	0.18	0.000	0.306	0.443
Liquidity	0.014	0.01	0.051	0.017	-0.009
p-value	0.003	0.131	0.000	0.494	0.477
Year Fixed Effect	Yes	Yes	Yes	Yes	Yes
R-square	0.208	0.138	0.372	0.61	0.346
N	246	66	90	48	42

Table 5. Regression results on Return on assets as independent variables while Cash conversion cycle used as an independent variable along with control variable

Return on Asset	Panel Data Analysis				
	Full Sample	Automobile	Chemical	Food	Pharma
Cash Conversion Cycle	0.000	-0.001	0.000	0.000	0.000
p-value	0.000	0.063	0.081	0.175	0.693
Firm Size	-0.010	0.008	-0.005	-0.012	0.099
p-value	0.403	0.817	0.797	0.597	0.02
Financial Leverages	-0.067	0.02	-0.034	-0.201	-0.118
p-value	0.001	0.871	0.239	0.000	0.019
Growth Opportunities	0.024	-0.031	0.06	0.011	0.009
p-value	0.001	0.216	0.001	0.291	0.387
Liquidity	0.013	0.014	0.051	-0.013	-0.014
p-value	0.003	0.071	0.000	0.593	0.367
Year Fixed Effect	Yes	Yes	Yes	Yes	Yes
R-square	0.205	0.147	0.391	0.538	0.313
N	246	66	90	48	42

Table 6. Regression results on return on equity as a dependent variable while NTC taken as independent variable along with control variable

Return on Equity	Panel Data Analysis				
	Full Sample	Automobile	Chemical	Food	Pharma
Net Trade Cycle	-0.003	-0.001	-0.001	-0.004	-0.001
p-value	0.000	0.005	0.094	0	0.033
Firm Size	-0.053	0.023	0.018	-0.205	0.033
p-value	0.111	0.581	0.706	0.069	0.43
Financial Leverage	-0.225	0.057	-0.161	-0.313	-106
p-value	0.000	0.685	0.018	0.228	0.075
Growth Opportunities	0.087	0.013	0.161	0.041	0.014
p-value	0.000	0.681	0	0.375	0.301
Liquidity	-0.017	-0.001	0.030	-0.181	-0.019
p-value	0.176	0.943	0.206	0.142	0.304
Year Fixed Effect	Yes	Yes	Yes	Yes	Yes
R-square	0.298	0.187	0.296	0.644	0.283
N	246	66	90	48	42

4. Results and Discussion

This section describes the regression results to conclude the findings. We analyze the impact of working capital policies in two perspectives (I) impact on firm performance and II impacts on shareholder's return. with two measures of profitability Return on Asset and Return on Equity. Working capital management to measure with two proxies i.e., Net trade cycle and Cash conversion cycle. Firm size, financial leverage, liquidity, and growth opportunities were used as control variables to conclude the findings.

4.1. Working Capital Policies and Firm's Performance

Table 5 and 6 presents the regression results, in which net trade cycle and cash conversion cycle are used respectively as working capital management proxies to analyze the possible impact of the same on a firm's performance. Firstly, we conclude the findings by taking variable data as a whole and after that industry-wise analysis is conducted. Results show that the net trade cycle has a negative impact on a firm's profitability but this impact is insignificant.

We can predict that by squeezing the net trade cycle firm can increase their profitability. While in industry-wise analysis all the sectors have not on one page. In Food and Pharma sector, the net trade cycle is insignificantly negatively associated with a firm's performance and the automobile and chemical sector net trade cycle found irrelevant regarding the firm's performance point of view.

A firm's size and financial leverage are too negatively associated with corporate profitability. As the firms grow and insert more debt into their capital structure, firm performance will move downward. These findings quite match with the second equation in which the cash conversion cycle is used as a working capital management proxy.

As per findings, the cash conversion cycle was found to be irrelevant regarding the firm's performance. Whatever policy regarding managing the cash conversion cycle adopted by the organization, has not any impact on the firm's profitability.

In industry-wise analysis, cash conversion cycle too found irrelevant except automobile sector in which CCC found insignificant negative relationship with firm's performance. These findings quite mismatch with earlier conclusions made by different researchers. (Ben Ukaegbu, 2014; Kieschnice et al. 2013) concluded in his study that the cash conversion cycle put a negative impact on profitability.

They argued that to increase investment in working capital, firms need additional financing that ultimately has a certain cost and increases the probability of bankruptcy as well. Hence lowering the profitability of the organizations. Control variables too, interact differently on a firm's profitability as per findings. A firm's size, financial leverage is found to be negatively associated while liquidity and growth opportunities were found to be positively associated with the firm's earnings.

4.2. Working capital policies and shareholders wealth maximization

Tables 6 and 7 presents the regression results, in which working capital management proxies are used to analyze the possible impact of the same on shareholders' wealth maximization. Findings are concluded in different steps as at first take data of entire variable as a whole to see the impact and then industry-wise results compiled to further narrow down our conclusions. It has been found that working capital policies act differently on shareholders' wealth maximization as compared to its impact on a firm's performance. Results show that the net trade cycle has a negative impact on a firm's profitability but this impact is very minimal.

A financial manager can improve shareholders' earnings after designing a carefully working capital management policy. Cash conversion cycle to have the same direction as net trade cycle has regarding the impact on return on equity. In industry-wise analysis too result is not much surprising as sector-wise too both working capital management proxies are negatively associated with shareholders' wealth maximization.

Literature too proves that the cash conversion cycle is negatively associated with profitability (Deloof (2003),

Wang (2002), Lazaridis and Try fonidis (2006), Gil et al (2010) in their studies prove a negative relationship of cash conversion cycle towards profitability. Firm size, financial leverage, and liquidity are negatively associated with return on equity.

Surprisingly, liquidity is negatively associated with return on equity but the same was not the case regarding a firm's performance as liquidity positively linked with the firm's return on assets. Growth opportunities as earlier findings negatively associated with shareholders' wealth maximization.

Table 7. Regression results on Return on equity as a dependent variable and CCC is the main independent variable along with control variables

Return on Equity	Panel Data Analysis				
	Full Sample	Automobile	Chemical	Food	Pharma
Cash Conversion Cycle	-0.002	-0.001	-0.001	-0.003	0.001
p-value	0.000	0	0.002	0.015	0.249
Firm Size	-0.057	-0.009	0.001	-0.108	0.099
p-value	0.114	0.825	0.985	0.367	0.095
Financial Leverages	-0.197	0.257	-0.137	-0.675	-0.177
p-value	0.001	0.088	0.029	0.011	0.012
Growth Opportunities	0.084	0.015	0.133	0.066	0.017
p-value	0.000	0.615	0.001	0.226	0.231
Liquidity	-0.023	0.011	0.033	-0.33	-0.035
p-value	0.084	0.235	0.148	0.011	0.115
Year Fixed Effect	Yes	Yes	Yes	Yes	Yes
R-square	0.251	0.279	0.351	0.562	0.215
N	246	66	90	48	42

5. Conclusion

The present study aims to study the role of working capital policies in the perspective of a firm's performance and shareholder's return by keeping studying different industrial sectors namely the automobile sector, chemical sector, food sector, and pharmaceutical sector of Pakistan.

Sample data of 41 firms from four different industrial sectors have been collected for the period of six years ranging from 2010 to 2015. Working capital policies are measured through two proxies i.e., Net Trade Cycle and Cash Conversion Cycle.

The impact of working capital policies can be analyzed in two perspectives i.e., regarding firm performance and shareholder's wealth maximization.

Firm size, liquidity, financial leverage, and growth opportunities are taken as control variables. It has been found that working capital policies impact differently on a firm's performance and shareholder's wealth maximization.

Results suggested that working capital policies have no impact on a firm's performance as a whole and in industry-wise analysis too. This means firm's performance is irrelevant with the policies of working

capital adopted by the management. On the other hand, working capital policies are negatively associated with return on equity.

There is an inverse relationship between working capital and shareholder's return. Lower the trade cycle and cash conversion cycle higher will be the return to the shareholders. Firm size, financial leverage, and liquidity too have an inverse relationship with return on equity. Overall results are not matched with earlier findings of different researchers. This may be because of the inconsistent and volatile economic conditions of the country. There may be a need to further explore the reasons in future research.

References

Afza, T., & Nazir, M. S. (2007). Working Capital Management Practices of Firms: Empirical Evidence from Pakistan. 9th South Asian (SAMF) held on Feb. 24-25. *University, Dhaka*, Bangladesh, 334-343.

Brigham, E.F. and Ehrhardt, M.C. (2004). Financial Management: Theory and Practice. 11th Edition, *South-Western College Publishing, New York*.

Charitou, M. S., & Lois, P. (2010). The effect of working capital management. *Journal of Business and Economics research*, 8(12), 63-68.

Deloof, M. (2003). Does working capital management affect profitability of Belgian firms? *J. of Business Finance and Accounting*, 30, (3/4), 573–587.

Filbeck, G., Krueger, T. (2005). Industry related differences in working capital management. *Mid-American Journal of Business*, 20 (2), 11–18.

Fazzari, S.M., Hubbard, R. G., & Petersen, B. C. (1988). Financing constraints and corporate investment. *Brookings Papers on Economic Activity*, 1,141–195.

Fazzari, S.M., Petersen, B.C. (1993). Working capital and fixed investment: new evidence on financing constraints. *RAND J. Econ*., 24, 328–342.

Ghosh, S. K. and Maji, S. G. (2004). Working Capital Management Efficiency: A Study on the Indian Cement Industry. *Management Accountant*, Vol. 39, No. 5, pp. 363-372.

Gill, A., Bigger, N., Mathur, N. (2010). The relationship between working capital management and profitability: evidence from the United States. *Business and Economics Journal*, 2, 1–9.

Gill, A., Bigger, N., Mathur, N. (2010). The relationship between working capital management and profitability: evidence from the United States. *Business and Economics Journal*, 2, 1–9.

Gitman, L. A. (2005). Principles of Managerial Finance. 11th Edition, *Addison Wesley Publishers, New York*.

Haq, I., Sohail, M., Zaman, K., Alam, Z. (2011). The relationship between working capital management and profitability: a case study of cement industry in Pakistan. *Mediterranean J. of S.S*, 2 (2), 365–372.

Jose, M.L., Lancaster, C. and Stevens, J. L. (1996). Corporate Returns and Cash Conversion Cycle, *Journal of Economics and Finance*, Vol. 20, No. 1, pp. 33-46.

García-Teruel, P.J., Martínez-Solano, P. (2007). Effects of working capital management on SME profitability. *Int. J. Manag. Finance*. 3 (2), 164–177.

Knauer, T., & Wöhrmann, A. (2013). Working capital management and firm profitability. *Journal of Management Control*, 24(1), 77-87.

Kieschnick, R., Laplante, M., Moussawi, R., (2013). Working capital management and shareholders' wealth. *Rev. Finance*, 17, 1827–1852.

Lazaridis, I., Tryfonidis, D. (2006). Relationship between working capital management and profitability of listed companies on the Athens Stock Exchange. *J. Financial Management Anal*., 19 (1), 26–35.

Miller, M. H., & Modigliani, F. (1961). Dividend Policy, Growth, and The Valuation of Shares. *The Journal of Business*, XXXIV (4), 411-433.

Mohammad, A. (2011). Working capital management and corporate profitability: Evidence from Iran. *World Applied Sciences Journal*, 12 (7), 1093–1099.

Moyer, R. C., McGuigan, J. R. and Kretlow, W. J. (2005). Contemporary Financial Management. 10th Edition, *South-Western College Publishing, New York.*

Pinches, G. E. (1992). Essentials of Financial Management. 4th Edition, *HarperCollins College Publishers, New York.*

Mona, A. (2012). The impact of working capital management policies on firm's profitability and value: the case of Jordan. *International Research Journal of Finance and Economics*, (85), 147–153.

Mosa, A., Iraj, S.A., Maryam, G. (2012). Studying the relationship between working capital management and profitability at Tehran stock exchange: a case study of food industry. *Research Journal of Applied Sciences, Engg. and Technology*, 4 (13), 1868–1874.

Raheman, A., Nasr, M. (2007). Working capital management and profitability – case of Pakistani firms. *Int. Review of Business Res. P.*, 3 (1), 279–300.

Raheman, A., Nasr, M. (2007). Working capital management and profitability – case of Pakistani firms. *Int. Rev. Bus. Res. Pap*., 3 (1), 279–300.

Shin, H. H., Soenen, L. (1998). Efficiency of working capital management and corporate profitability. *Financial Practice and Education*, 8, 37–45.

Van-Horne, J. C., Wachowicz, J. M. (2004). Fundamental of Financial Management. 12th Ed. *Prentice Hall, New York*.

Wang, Y. J. (2002). Liquidity management, operating performance, and corporate value: evidence from Japan and Taiwan. *J. Multinatl. Finance. Manag*., 12 (2),159–169.

Southern Journal of Research Vol. 3(1), 2023

Learning English Language through Literature at BS level: A Case Study at The Institute of Southern Punjab Multan

Aamir Zahoor[1], Sadia Parveen[1], Masroor Sibtain[2]

[1] Department of English, Institute of Southern Punjab, Multan, Punjab, Pakistan

[2] Professor of English, Government Graduate College of Science, Multan, Punjab, Pakistan

Abstract. Literature plays a vital role in our society. It advocates and reflects the different aspects of our society. Literary studies as an independent discipline are providing different academic and professional opportunities to the students and academia in its own right. In linguistics, literature is seen as a tool for language teaching as literary works involve real-life language. Literature provides an exciting and interesting platform for learners. The current study is intended to examine the opinions and attitudes of university students about the usefulness of literature to learn the English language at the Institute of Southern Punjab, Multan. It is a small-scale quantitative study comprising a population of 20 students in the BS English program. The data was collected through convenient sampling from the students. The structured interviews were conducted to collect data. Close-ended questions were developed to obtain views and opinions of the university students about the effectiveness of using literature to teach the different segments of language. The findings of the present research suggest that most of the students have positive perceptions of the usage of literature for learning English. The findings also suggest that integrating literature can contribute to the development of the particular language of the learners of the English language if it is implemented and planned properly.

Keywords: Language teaching, Language learning, Literature as a Learning tool, Teaching methods

Email: aamirzahoorisp@gmail.com,

1. Introduction

Learning a foreign or second language formally is a highly complex and sensitive enterprise that requires all the relevant elements to be in place appropriately to obtain positive results at an optimal level. The elements per se include an ideal sociolinguistic milieu e.g., the language classroom fitted with all the modern gadgets to teach the language with all the relevant audio-visual aids; (2) teacher trained in the teaching of foreign language efficiently but the most important of all in the entire enterprise is the selection of teaching material to be used as a syllabus for the teaching of the foreign language.

The present study which of course is a pilot work was carried out at ISP with a selected number of students to gain initial information on learning English as a foreign language at the BS level via literature. The study as such involved 40 students. The data from collected through structured interviews using the qualitative method for the study.

2. Scope of the Study

The study as such is perceived as highly useful in the sense that students are expected to find this approach useful because they are already familiar with the study of literature in previous stages of learning. Learning a language from a new perspective can be more exciting for the students and relatively easier for the teacher to handle the intricacies of the language. Learnability of the

students can further be facilitated by using literature. They will become familiar with content and context.

3. Objectives of the Study

The current pilot study has the following objectives:

- To examine the beliefs and opinions of the university students about the usefulness of literature to learn the English language.
- To interpret the beliefs and opinions of the university students about the application of literary texts to learn the English language at the BS level.

4. Literature Review

Studies of this kind have already been undertaken in countries like India, and Malaysia with useful results even in Pakistan. This pilot study as such showed an appreciable potential for extrapolation into a full-fledged study which of course will require an increase in statistics regarding data on student responses as well as that of teachers.

According to Obediat (1997), literature aids students to obtain a native-like aptitude in English, expressing their thoughts in a good way, acquiring the features of updated and valid English rules, learning how language structure is done for communication, perceiving how colloquial expressions can be used, speaks clearly, exactly and briefly, and turn out to be more skillful in the target language, as well as turn out to be inventive, critical, and logical learners.

Literature encompasses the whole life. In English language teaching literature plays a pivotal role in inculcating students with different spheres of life. Teaching English through literature is teaching students the whole culture of English speaking and in some cases the colonial world. The teaching of literature is essentially the way of transmitting the ample treasure of the culture of antiquity.

It is also a source of students' overall awareness about culture, economy, language, religion, and more importantly life itself. Literature carries the emotive and aesthetic aspects to appeal to its audience. Literature appeals to the intellect and emotions of people through its imaginative power. Literature is an art that used words and captivates readers to judge and appreciate the beauty of language. Literature molds the perspectives of people through its aesthetic dimension to look into their matters with a literary and aesthetic lens.

Kelly (1995) described enjoyment, information, cognition, understanding, imagination, and language itself as the core values of literature. The choice of text for the course is of vital importance because it can arise something in students to relate it with their life and kindle their interest in the course. It can also be helpful to lead students to healthy discussions on various aspects of their interests.

The process of learning seeks motivation to get itself completed. Literature is an essential source to develop a sense of motivation and involvement among students as literature is capable to bewitch its reader. Literature in this way strengthens both learners and the learning process. Literature also develops an emotional attachment and pleasure among learners. According to Hill (1988), literature constructs an apparatus for instructors to involve pupils in education by monitoring and regulating their emotions.

Literature gives us a language teaching model. It plays a model role in language teaching. In the thinking process, cognition and language are interrelated.

This is a determined kind of language that is exposed to learners. Comparatively to the conversation as an author,

literature seldom finishes a richer model of language. It is frequently used to elaborate sentences and sumptuous words as well. At the same time speakers focus on employing the same words over and over in conversation.

5. Research Gap and the Rational of the Study

The current research highlights the role of literature in language teaching in Pakistan. In Pakistan, literature is used as a tool for language teaching. Apart from O-Levels and A-Levels teaching systems, literature is being used as a core tool to teach the language from grade one to higher secondary level. English till the higher secondary level is taught as a subject.

The students are familiar with language learning through literature. Literary texts of different genres like poems, short stories and novellas are incorporated into the syllabus of English subjects. These genres are used to make students familiar with the main components of the language.

These components include grammar rules i.e., tense rules, parts of speech, punctuation, translation from English to Urdu, use of articles etc. The teaching of English through literature till the higher secondary level mainly focuses on the development of reading and writing skills only; it does not train students to have a good command of listening and speaking. As the students are very well aware of the use of literature to learn the language, the same strategy can be used at the BS level to enhance second language learning.

The syllabus of BS programs includes different literary genres which can enable the students to learn a language effectively. The current study is aimed to highlight the importance and usefulness of literature in Pakistani classrooms to teach language at the BS level at the Institute of Southern Punjab, Multan.

This study is intended to describe the beliefs and opinions of the university students about the current syllabus having particular literary texts to learn the different components of language in Pakistani classrooms.

6. Methodology

The current study is a pilot work that is intended to examine the beliefs and opinions of university students about the usefulness of literature to learn the English language at the Institute of Southern Punjab, Multan. It is a small-scale quantitative study. The researcher himself is an instructor at the Institute of Southern Punjab, Multan. It was convenient for the researcher to collect data from his institute.

Therefore, a convenient sampling technique was used to obtain the data. The population for this study comprises the respondents from the researcher's institute. Specifically, the data is collected from the 20 students in the BS English program studying in the final semester. The structured interviews were conducted to collect data. Close-ended questions were developed to obtain views and opinions of the university students about the effectiveness of using literature to teach the different segments of language.

7. Findings and Discussion

In analysis, findings are attained through close-ended questions. The question first was Is literature beneficial for English language learning?

Results drawn through responses indicate a higher frequency (90 %) of those who think that literature is useful in English language teaching while only 4 students hold contrary views.

It highly indicates that plenty of participants recognized the importance of teaching literature in English language teaching.

Table 1. Q No. 1 Is literature beneficial for English language learning?

Response	Frequency	Percentage
Agreed	36	90 %
Not Agreed	4	10 %
Total	40	100

If we talk about the second closed-ended question which tries to explore the use of literature in English language teaching classes, most of the participants talk about the texts they used to analyze in their class. Here look at the comment made by a respondent: Classics, as well as modern texts prepared for the level of students accordingly, will draw the attention of the audience. Some participants also shared their views that short stories and poems also could be used for the said purpose. Read the following remarks of a participant: Poems with rhymes and short stories with interesting themes are interesting to read and easy to learn a language.

Drama activities are also proved useful in an extraordinary way to captivate the audience's attention. It made the course easy and interesting. After evaluating the responses of participants it's highly assumed that cultural aspects must be taken into account to make students more aware of the cultural aspects of a language.

Table 2. Q No. 2 How literature can be used for English language learning?

Parameters	Frequency	Percentage
Reading and analyzing literary texts i.e., Drama and Novel	13	32.5 %
Extracting information about the renowned literary figures	09	22.5 %
By adding poems and short stories in the classroom	10	25 %
By promoting cultural awareness	08	20 %
Total	40	100

Table 3 illustrated the reaction to the third close-ended query which asked whether the candidates get help from literature in learning.

A profuse of partaker (67.5 %) states that they get help from literature in English language learning which is to a greatly extended in the line with the reaction to the first closed-ended query.

Table 3. Q No.3 Does literature help in your English language learning?

-	Frequency	Percentage
Agreed	67	67.5 %
Not agreed	13	32.5 %
Total	40	100

The fourth close-ended query was asked to see whether the partaker work educational Background work has affected their basic use of "literature subjects in English language learning".

Table no 4, brought out that the education system level of the candidate has been a greatly significant effect on their fondness for using "literature subjects in English language learning".

Table 4. Q No. 4 Are the literature subjects included in B.S English degree very effective for language learning?

-	Frequency	Percentage
Effective	22	55 %

Modest	07	17.5 %
A bit	08	20 %
Not at all	03	7.5 %
Total	40	100

The fifth close-ended query was asked to see the proper ways of literature used by the teachers. According to Table 5, 16 participants states that their teachers used a few types of "literary texts" accurately to improve their proficiency level. 17 students said that their teachers use literature to improve their learning i.e., novels, short stories and poems.

Five participants illustrated movies adapted from literary works as resources used by their teachers. Participants stated that novels, short stories and poems are used by teachers to emphasize the fact that these literary devices used in these genres enhance the learning in the classrooms as they make the lesson more interesting and effective.

Only 2 students stated that their teachers do not use any text in class for improving English language proficiency.

Table 5. Q No. 5 Do your teachers use literary texts for your language learning specifically?

-	Frequency	Percentage
Use of literary texts by teachers	16	40 %
Use of novels, shorts stories and poems by teachers	17	42.5 %
Use of movies	05	12.5 %
No use at all	02	05 %
Total	40	100

The result in the last close-ended question about the possible contribution of literature regarding English language learning indicates that 25 respondents stated that literature helps to improve their skills of language like reading, grammar, writing, and vocabulary.

It is also derived from the 07 respondents that through the literature students become aware of gaining cultural awareness and target culture.

Five of the respondents also responded that the literature enables students to gain the ability to analyze, think, and evaluate thereby making imagination.

Table 6. Q No. 6 On what level, do literature contributes to your English language learning?

-	Frequency	Percentage
Literature helps to improve all skills.	25	62.5 %
Only helps in vocabulary and reading	03	7.5 %
Only gives cultural awareness.	07	17.5 %
Helps in critical thinking.	05	12.5 %
Total	40	100

In crux, the study and its overall results said that the overwhelming number of respondents believe that the use of literature in language learning has positive impacts. They further believe that the literature would be benefited language teaching literature.

Based on the remarks of respondents, using poems, novels, and short stories in the classes of language can

contribute more to enhancing the language proficiency of students.

It increases the ability to increase the grip over vocabulary learning, and the accuracy of grammar. Furthermore, it always contributes more to broadening the horizon of students and making them more intelligent.

It increases awareness about the target culture. In the same way, a few numbers of respondents argued that literature does not affect students' language proficiency.

There are many negative perceptions rising day by day and these negative perceptions have arisen from several reasons likewise, including the dearth of the adequate educational record of mentors, instructors, trainers, and teachers on how to use literature for teaching language.

The content that is used by teachers and trainers is the perceptions of their students toward literature and language teaching.

8. Conclusions

The current study highlights the exertion of literature to teach language effectively at the BS level at the Institute of Southern Punjab, Multan.

This particular pilot study was being conducted to get insights into the views of students concerning the roles of literary texts in English language learning.

The results of the present research demonstrate that the majority of the participants strongly agree that literature must be a component of English language learning and most of them said their teacher utilizes literature in the teaching of the English language.

The majority of them also agree that the literature subjects included in their B.S degree have a positive impact on their learning and they consider the role of literature as good for language learning purposes.

It is clear from the results of this research, that the majority of participants think about literature use helpful in different ways like improving vocabulary knowledge, increasing cultural consciousness, and building the language abilities of learners, especially in writing and reading.

Additionally, they have different views on how you can make use of literature within English language learning like examining classical literature works, using stories and poems that are short and presenting information regarding the key figures in the literature.

Collectively, the results of the current analysis seem to be a bit of proof that most of the students belonging to the present research have good perceptions of the usage of literature for the teaching of the English language reasons.

Nevertheless, the results of the present research should be interpreted with extreme caution because they just reveal the participants' good perceptions of the usage of literature wearing English language learning.

Almost two-thirds of the individuals highlight the advantages of genuine works and texts of classical literature.

Producing cultural awareness is extremely uncommon. Getting knowledge regarding literary texts is also seen to become very rare. Almost three-fourths highlight the effective consequences of their responses that belong to their background of formal education.

The researcher is of the view that integrating literature can contribute to the development of the particular language of the learners of the English language, but this is challenging and demands serious things to consider of a selection of elements coming directly into play if the likely advantages in the addition of literature to their lessons are to become accomplished within the process.

These elements include thorough planning consistent with the training goals, well-chosen literature depending on the requirements, passions, and language level of the learners, and well-designed activities.

Without considering these kinds of aspects in the beginning, literature usage for language teaching might risk time as well as energy spent and also fall short of reaching anticipated and desired final result regardless of the positive perceptions of instructors and language teachers towards using literature in their language classes. A paradigm shift is essential to accomplish it effectively.

References

Arikan, A. (2005). An Evaluation of Literature Component of Hacettepe University English Language Teaching Department. *Hacettepe University Journal of Education*, 29, 27-33.

Hill, J. (1988). Using literature in language teaching. *Janus Book Pub Alemany Press*.

Kelly, L. P. (1995). Processing of bottom-up and top-down information by skilled and average deaf readers and implications for whole language instruction. *Exceptional children*, 61(4), 318-334.

Obeidat, M. (1997). Language vs. literature. *Language*, 35(1).

Robson, A. E. (1989). The use of literature in ESL and culture-learning courses in US colleges. *TESOL Newsletter*, 23(4), 25-27.

Vaughn-Roberson, C., & Hill, B. (1989). The Brownies' book and Ebony Jr.! Literature as a mirror of the Afro-American experience. *The Journal of Negro Education*, 58(4), 494-510.

Zaker, A. (2016). Literature and Creativity in an ELT context. *ASIAN TEFL*, 1(2).

A Blockchain Model (BCM) study of the Syntactic and Semantic grid in Urban History and its origin from the Indus Script Pictorial Form

Esther Park[1]*, Javeria Manzoor Shaikh[2]

[1]* Illhyang Korea Art history Research Institution

[2] Department of Architecture, School of Art and Design, Aror University, Sindh, Pakistan

Abstract. The geographical dimension used pattern of the grid has a long history of the spatial framework in terms of evolution, the semantic position and precision of orientation in the urban grid used today in City occurred by the sequential overlap of hierarchical transformations spanning over time. There are multiple factors of the framework which positions the present shape of the modern Mooltan Planning grid. The grid has spatial syntactic dimensions overlapped with spiritual historical varying from micro-level of Indus script which was intellectually fashioned based on logic and effort for designing anthropomorphic symbols. On the other hand, at the macro level geographical dimension and positioning of the semantic space division; e.g., navigational instinctive system of moving forward or backward, or left and right. Natural fringes which were the Punjab Rivers in this case along with the phonetic signs and their pictorial forms. The study is linked by application of Block-chain model with research gap in light of works from other countries compared with that of Pakistan- Mooltan Planning. The discussion section, elaborated on this Manuscript emphasized the policy discussion to cater to the issues of such interconnections with land use and morphological interventions.

Keywords: Indus Script; Pictorial Form; Spatial Syntactic; Dimensions Blockchain Quasi-model; Pseudo-randomly Model.

Email: estherpk@hanmail.net

1. Introduction

The objective of the research is to develop a methodology for making quasi-block-chain analysis from city Planning heritage especially the fringes of monuments using morphology policy applicable internationally. The author aims to simulate the planning, monuments, and nodes from City. This section covered the overall background and description of the study, narrow down to research objectives of finding the roots for the planning of city Planning, motivation of the topic which is the symbols, importance, and significance of the semantic written language pattern and impact on the planning of Central Mooltan of Pakistan city Planning. The process is deciphering the linkages between the symbols of Indus Script and its alignment with the fringes and planning bases for the urban plan by applying the Markov model along with the Agent-based Model. One of sequential analysis of emerging, which can be defined as "the whole which is considered as the grid for the urban planning to be greater than the sum of its parts which could refer here as the symbols from the ancient Indus script as a metaphor". In other words, spider pattern grid and winding roads higher-level system properties emerge from the interactions of lower-level subsystems modeled here as the Indus script symbols. Or, macro-scale state changes emerge from micro-scale agent behaviors of the earlier script. Or, simple behaviors (meaning rules

followed by agents) generate complex behaviors (meaning state changes at the whole system level of the semantic space).

2. Literature Review

This section critically describes the use of grid and its roots been simulated Baran, et al., (2008) and Biagi and Cremaschi, (1991) by the symbols and evaluate literature relevant to research problem stated, by Bignami, (2014) described in the territorial and historical framework of city Planning which described Mooltan Planning as a prosperous land of the era from prehistory and he argued that the inspiring heritage of the grid presented as a past leading to new progress of urban planning as a Sustainable Social ground for the grid along with the economic and evolution of the grid could be traced back to the environmental revitalization in Mooltan Planning city grid. This section establishes context, as presented by Hussain et al., (2020) who studied the land covered and comparison with the land use along with the temporal changes and applied the GIS mapping strategies as a case for Mooltan Planning described as a district in Pakistan considering the environment as a precedence for the grid plan and monitoring and assessing the evolution of the grid planning Bokil (2009), Brass (2004), Burton (2000), Burns (1976), Brown (2001). They compared and contrasted the most recent developments in the history of Mooltan Planning from literature and planning trends. In this section we Searched gaps as Faiz (2021) described the building language after concentrating building province on thought leaders' work of civil society and ethnic nationalism and linking the research with relevant theories in Pakistan.

Kepaptsoglou et al., (2020) compared grid as a system to be evidence-based design from Mooltan city Planning, they said that the Grid origin is before gridiron phenomena, the aim here for this paper is to trace the semantic space based on symbols and script features as a prototype and origin of the grid which is been hypothetically argued in the paper for the grid philosophy in Planning. Duany (2000), Childe (1950), Corbusier, (1929), Conzen (2004), Drennan (2010), De Vorsey, Luis. (2012), Fairservis (1971) Fox (2000). This has occurred as early as cave dwellings flanking the Indus Civilization in the region of Mooltan Planning which is the midpoint of Mohen-jo-Daro and Harappa civilization. The City Planning spiderweb grid made more than a few unintentional comebacks, the inherent grid history complexed the traditionally narrated phenomena of the grid, reinforced current modernist trends to materialize the present grid, and re-own the history of the grid plan.

There is a vacuum in the investigation and examination of the function of the grid following the river as a topographical restraint; from the time when the spider grid was used in City Planning. The spider grid facilitated the variety of spacious agricultural and industrial spaces for all the classes or congregational meetings in the historical era as Del-Bo (2014) introduced this approach of the grid as sharing culture and knowledge of the Core as Indus script of City Planning. The literature review suggests that there is a vacuum in the temporal models as stated by Stanslawski (1994) which deciphered the grid plan up to Mohenjo Daro (2500 B.C.). The analysis of (Gangal et al., 2010) on City Planning (7000 B.C.) for tracing the Indus urbanization consider the prototypes which existed earlier than Multan, thus this research further expands earlier providing evidence for the grid patterns from pre-historic times as the Indus Script symbols. Annexure 1,2.

The origin of the motivation behind this paper is to retrogressively trace the motives of the prototypical grid form. It is inferred that the spider grid originated before Oglethorpe's Utopian intelligently grided Savannah's plan an American planned city, earlier of Hippodamus of Miletus, 498- 408 BC before this era Indus Valley 2600–

1900 BC had planned on-grid form, which had precedence of Çatalhöyük 7500 BC to 5700 BC as mature operational grid Pateman (1987), Fait (2021), Ahearn (2021), Martinich (2009) Mair (2021), Pettersson (2016) and Luo et al., (2021).

3. Experimental Program Simulation Procedure

The methodology follows a sequence of activities to achieve the desired objectives. At first, the Mooltan planning simulated were designed, and then quasi- block-chain tests were performed on it, Annexure 3 and 4 (Table 1).

Table 1. Comparative analysis of Mooltan planning

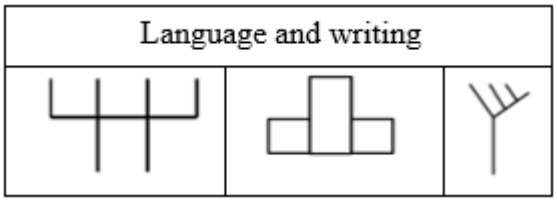

Writing and language evaluation and its alignment with the grid formation for urban planning is the intellectual creativity of civilization at Multan. This analysis reveals that people who designed the Indus script were intellectually creative and considerable time and effort went into designing the cities from the micro level to macro level, Annexure 2 and 4.

4. Section title: Symbols from Mooltan

The micro-level phenomenology for the grid is driven from the human and ergonomic instinctive constraint of nature as a human being anthropologically direction-finding of forward and backward and right and left navigation orientation. The understanding is applied for the mapping and reading along with the route planner on syntax and axial move, eye connecting tool for grid design, and communication ease. The understanding and simply Mooltan of the grid as a place. The gird universality is marked by its easy to occupy, rent, demarcate, and premises limits. Fox (2000) defined the grid as geography shaping our brain and converting terrain into the territory, the geometric shape patterns are manmade. The human brain is continuously been trained to measure, by images of lines and human vision, when human visits a new place he wants to know his current GPRS and position, according to the two-dimensional mapping derived in the mind, he would unconsciously measure in his surrounding concerning another side of his vision. Therefore, is in the innate human psyche to use the grid from simple signs in Table 2 as a beginning of a settlement.

Table 2. Analysis of the Written Symbols

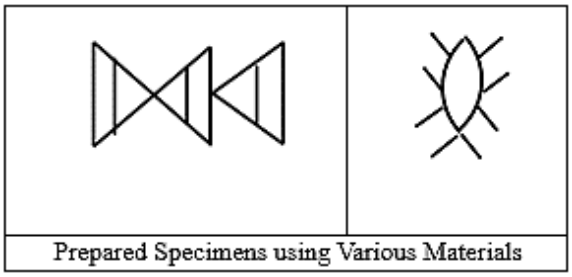

The second instinct of expandability is the primary grid motivation when compared to other towns e.g., circular plan of Baghdad (al- Mansur AD 762-7) and Multan which does not allow orthogonal spread out but rather a winding road pattern or spider pattern grid and serpentine style plot size which wedge shape as the early writing suggested from Mesopotamia. Spaces wrapped around the central bazaar with limit the opportunity for expandability. Brick was a unit for the orthogonal planning and other constructional constraints also defining out the division for grid planning. Hillier (1996), Gangal (2010), Grant (2001), Gnisci (2011), and Higgins (2009).

a. Blockchain Analysis

In Fig. 3 the Indus script in the above figure presents a logo-syllabic shape, it mainly constitutes a system of graphemes which are single-valued and syllabic scripts, which could be cracked as artificial intelligence. Individual signs may be interpreted one by one as an agent-based model which is a semantic grid study of the

semantic module in Multan urban history. Many of the graphemes may remain eternal mysteries, though its evolution from the Indus script pictorial forms a Semantic sequential for the Geographical Dimensions of Multan Bazar compared with the Spatial Framework of Sufi Shrines could be deciphered in the upcoming research. Multan has undergone a radical transformation and aesthetic growth. The Mythologies of the Grid, this paper documents the downtown providence plan of Multan, secondly it creates an accurate plan of Mooltan center by modifying an AutoCAD base map interpretive analysis on micro-level with that of the Indus Script. The Collected Lime from Multan Fertilizer is brought to the site and plant of the Sothern University of Punjab. The Lime from Multan Fertilizer, fly ash from Sanawa power plant and pumice from Chaghi (Baluchistan) are taken in proportion by weight and Fly Ash is added and mixed thoroughly using rod and trowel before it hardens.

i. Fly Ash

The mixture is then homogeneously poured into the cylindrical mold and then is compacted with the aid of a steel rod and the surface is finished using the trowel. Before pouring the mix into the mold, the walls of the mold are oiled for smooth removal afterward, Gupta (2021), as shown in Table 3. The urban morphology for early man depended upon his way of vocation earlier then agriculture native was making tools to symbols, this is the pivotal point in history where he has the tool to construct therefore, he planned dwelling towns according to the symbols based on the river pattern Lambrick, (1973); Hall (2002); Jacobs (1993); Kenoyer (2001); Johnson (2001); Kostof (2009); Levinson (2005); Lynch (1984); Mackay (1938). These towns were based on well-calculated orientation and the understanding of Homo for geometrical and ergonomically proportional features represents the intellect and precision of urban morphological decisions. Moreover, the 1:2 rectangular proportions for the grid and the 45-degree angle overlapped shift which is parallel to north qualifies Homo as an urban designer for this earliest city. He also understood the spider web pattern and serpentine growth, Annexure 1 to 4.

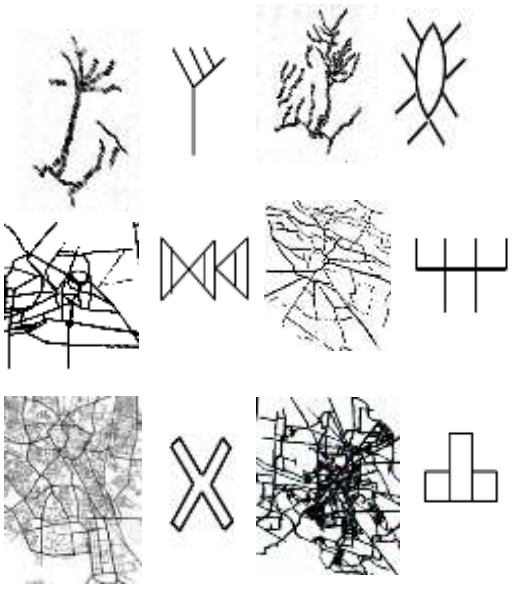

Table 3. Model Output Training Data for the Comparative Analysis of Five P-theory

5. Conclusions

The goal of triggering a historical core of an ancient city: Multan the oldest city of central southerly Asia. A comprehensive territorial condition of human community growth. To study the multilayered site of Multan, technical actions were devised based on the cultural identity. This section described the statistical techniques applied to the collected grid data sets with the explanation of the construction of hypotheses that the symbols of Indus Script and the river fringe is been used as semantic and syntactic equations for the statistical tool and justification for the grid in this case, quantitative analysis for the map of Multan while for qualitative analysis of the typo-morphology of the phonics and symbols, methodology of the research based on Markov Model is mentioned. A list of variables of symbols of Indus script is described in this part of the section.

1. The section covered in-depth interpretation through applying higher-order thinking skill input data in the program sequences of languages: ancient Indus script, then we gave it samples of four non-spoken communication systems: node, street sequences, and an artificial language. The program calculated the level of order present in each language. Urban planning fringes as the orientation of the language fell in the middle of analysis and the research developed a novel argument which is based on the significance of statistics relations of grid to symbol. Establish interconnections pattern-analyzing software of space syntax at the micro-level, and GIS running what's known as an SVM (Support Vector Machine) Hidden Markov model, a computational tool used to map system among and within variables. Testing hypotheses and comparing with the literature of part two. The program was seeded with fragments of Indus script, it returned with geometrical rules based on patterns of symbol arrangement. These proved to be moderately ordered, similar to the spider web pattern grid of current Multan in 2022 grid coded language. Theoretically, the argument fills the vacuum between the retrogressive spatial-temporal models by presenting the model for agricultural society at Multan preceded by nomadic settlements. Morphologically this paper bridged the gap of the grid form which is bee traced to the grid plan. While our research expands further the original prototype by suggesting urban morphologies earlier than Multan. Case studies of evidence-based grid planed morphologies are presented up to hundred years. We have conducted field surveys to infer urban grid patterns in the vicinity of Multan.

Annexure 1. Research on the City Planning from the Material

Annexure 2. The City Planning and the Micro-level Block

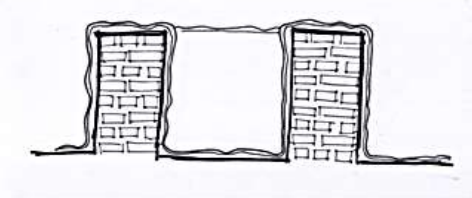

The successful use of the geo membrane, whose life is almost 100 years, this process is successfully used on the stupa area, where it has been, membrane and then mud puklta is applied.

When water accumulated into the pours of the bricks, and due to temperature, expends an contracts constantly, that is in the summer night contracts and summer day expends, and in monsoon, water is accumulated then in the winter, when temperature falls at night, below zero, then the crystal is formed inside these pours inside the bricks. The porosity level also varies, some bricks parts are highly porous some are lesser dense. This constant contraction and expansion over the seasons and over the night and day, has made this wall tired and the bricks are completely exhausted, and as a result the bricks crumble in the form of powder.

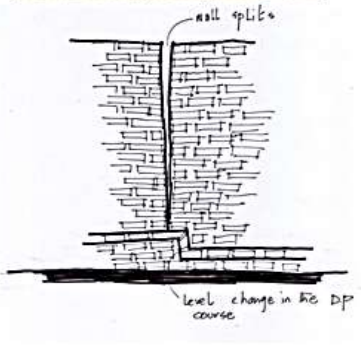

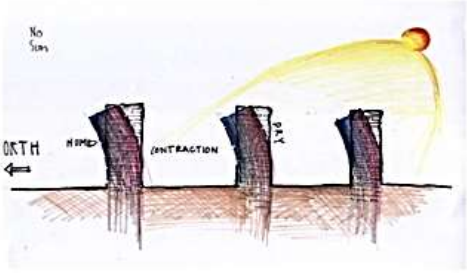

Some salts are associated with the mortar type only, and very often these salts are produces as a reaction product with other brick material Several chemical species come to being, though the more frequent in buildings are the 7 and 6 hydrated forms

Decay by salts

What is a "salt"? Chemistry: a product obtained through the reaction between an alkali and an acid.
Heritage science: a soluble chemical compound that crystallizes on or inside any material.

Being soluble, the salt coupled with the presence of water mobilizes salt in solution. When crystallization occurs inside a pore produces a pressure (crystallization Pressure) that presses against the pore walls that can break. When water evaporates, salts crystallize inside the porous of the brick or mortar or in the surface cracks.

Annexure 3. The Figure for City Planning

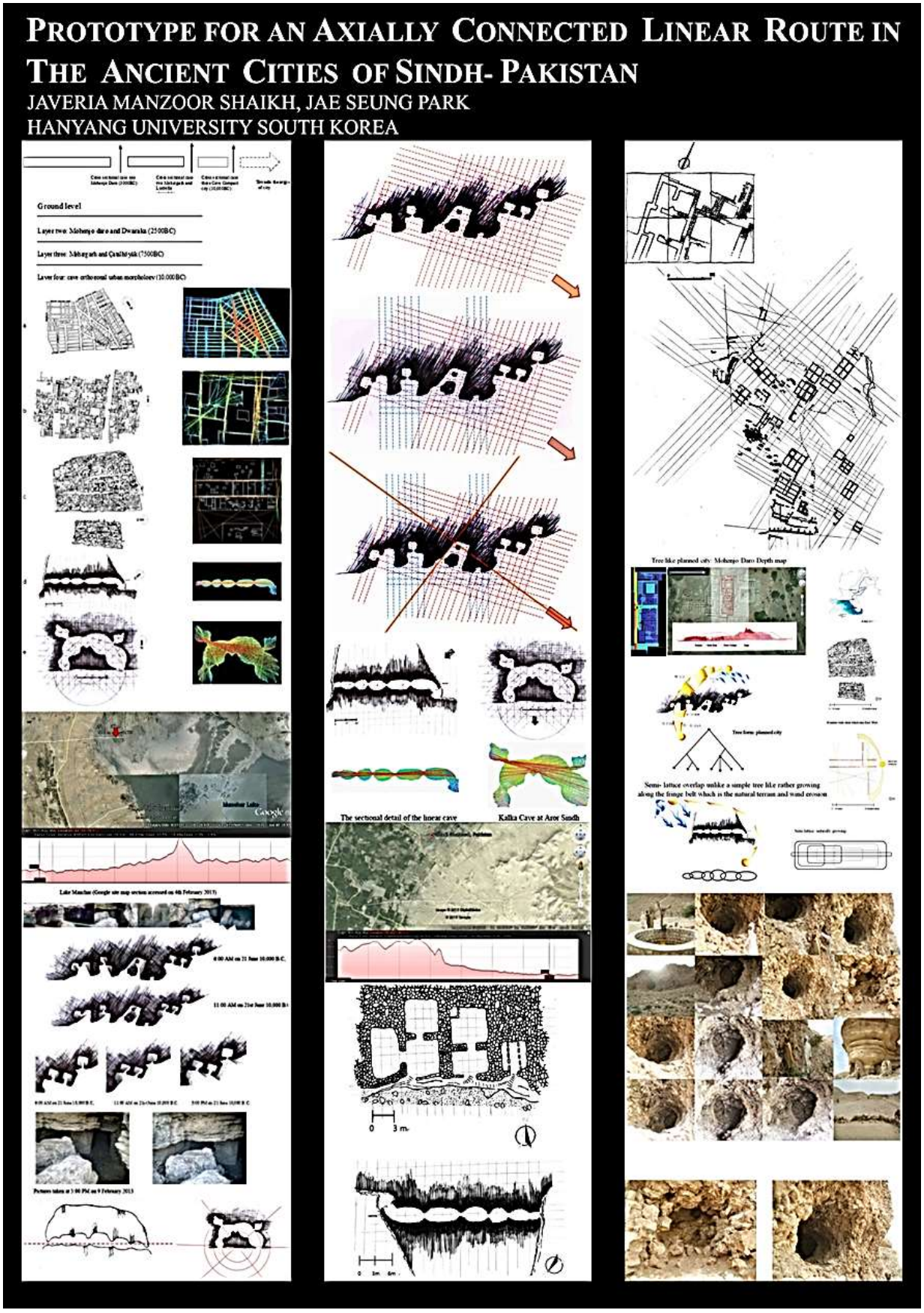

Annexure 4. City Planning and its History

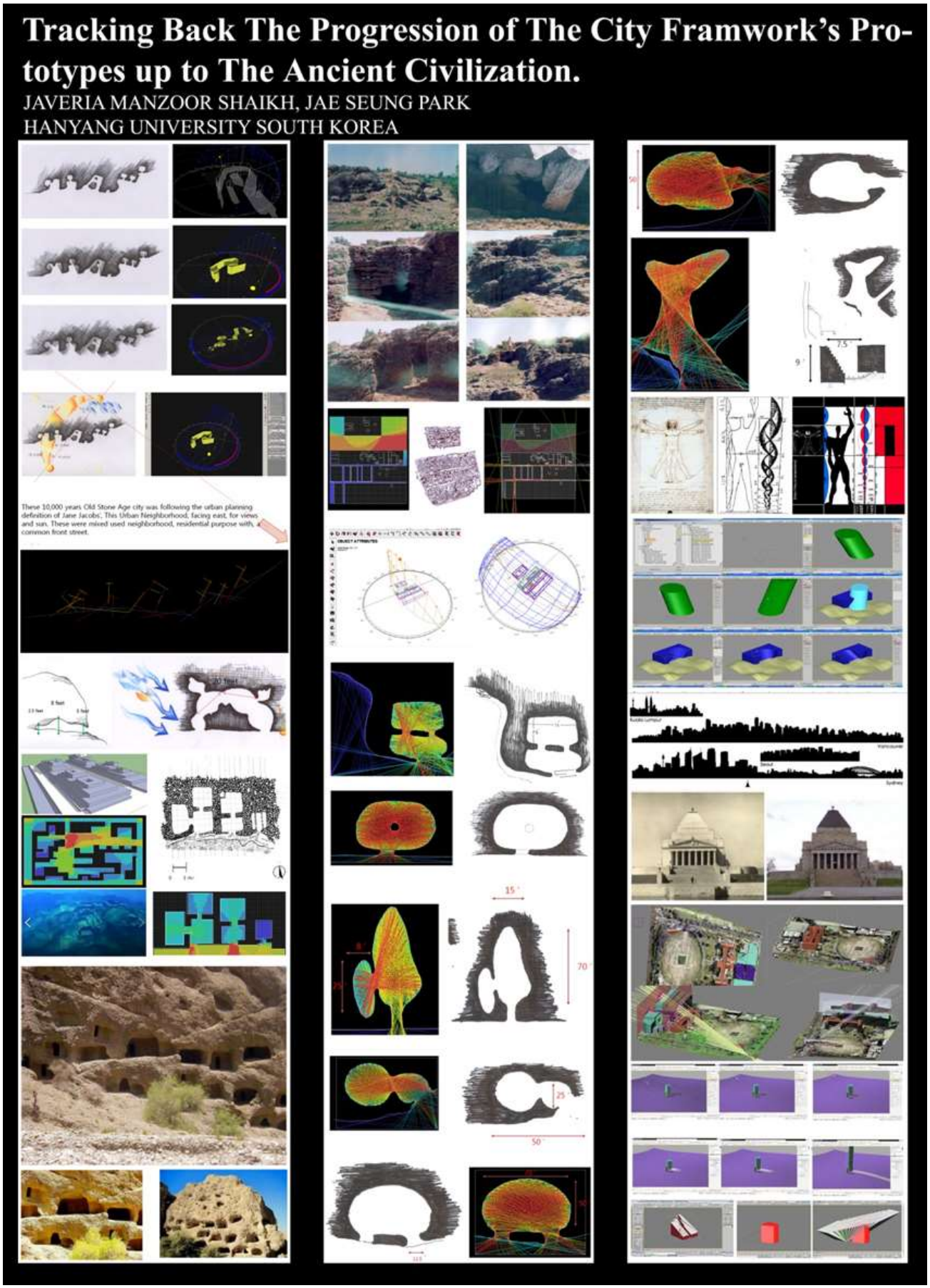

References

Baran, P. K., Rodríguez, D. A., & Khattak, A. J. (2008). Space syntax and walking in new urbanist and suburban neighborhoods. *Journal of Urban Design*, 13(1), 5-28.

Biagi, P. and Cremaschi, M. (1991). The Harappan flint quarries of the Rohri Hills' Antiquity 246: 97-102.

Bokil, P. (2009). Functions of Grid, a key for flexibility in the framework. *Des Thoughts*, 2, 42-48.

Brass, M. (2004). The nature of urbanism in Ancient Egypt (Doctoral dissertation, Essay for Degree: MA in Archaeology, *Uni. College London* (2003-4): 2).

Burton, E. (2000). The compact city: Just or just compact? A preliminary analysis. *Urban Studies* 37 (11): 1969-2001.

Burns, A. (1976). Hippodamus and the planned city." *Historia: Zeitschrift fur Alte Geschichte*: 414-428.

Brown, K. (2001). Gridded lives: Why Kazakhstan and Montana are nearly the same places. *American Historical Review*, 17-48.

Duany, A. (2000). The rise of sprawl suburban and the decline of the nation the American dream *New York: North Point Press*: 37

Childe, V. G. (1950). 'The urban revolution' Town *Planning Review-Journal*, 21: 3-17.

Corbusier, L. (1929). The Mooltan of Tomorrow and its Planning *(New York: Dover Publications).*

Conzen, M.P. and Conzen, M.R.G. (2004). Thinking about Urban Form: Papers on Urban Morphology, 1932-1998 *(Lang Publishing, Incorporated Oxford*).

Conzen, M.P. (2001). The study of urban form in the United States. *Urban Morphology*, 5, 3-14.

Drennan, M. E. (2010). Architecture in archaeology: an examination of domestic space in Bronze Age *Mesopotamia*.

De-Vorsey, L. (2012). The Origin and Appreciation of Savannah, Georgia's Historic Mooltan Squares. *Southeastern Geographer*, 52(1), 90-99.

Fairservis, W. (1971). The Roots of Ancient India *(New York: The Macmillan Company)*.

Fox, W.L. (2000). "The grid, the City and the Mind". In the Void, the Grid, & the Sign, 9-19, *Traversing the Great Basin. Salt Lake City: University of Utah Press*.

Hillier, B. (1996). Space is the machine (*Cambridge University Press, Cambridge)*.

Gangal, K.V.M. and Adhikari, R. (2010). Spatio-temporal analysis of the Indus urbanization. *Current Science Academic Journal*, 98: 846 -852

Grant, J. (2001). The dark side of the grid: power and urban design. *Planning perspectives*, 16:219-241.

Gnisci, A. (2011). "Designer Cities, Next Decade" Projects Today: 47-49 accessed on May 17, 2013, http://www.projectstoday.com/PTSpecialFeatures/PDFData/PT_KGFT_oct11.pdf.

Higgins, B.H. (2009). "Gridiron 2670 BCE." In the Grid Book *(The MIT Press Cambridge: England)*.

Lambrick, H.T. (1973). Sindh, History of Sindh, vol-II, *Before the Muslim Conquest 1st Edition*
second Edition 1996, Tilak Incline, Hyderabad, Sindh, Pakistan.

Hall, P. (2002). Cities of Tomorrow: An Intellectual History of Urban Planning and Design in the Twentieth Century. *Oxford, UK: Blackwell Publishers.*

Jacobs, J. (1993). The death and life of great American cities. *New York: Random House (originally published in 1961).*

Jonathan. M.K. (2001). Urban Process in the Indus Tradition: A Preliminary Model from Harappa, Excavations on two of the major mounds at Harappa

have revealed traces of an early settlement, a transitional phase of development, and several phases of full urban and post-urban occupation. http://harappa.drupalgardens.com/category/articles/pdf?page=1.

Johnson, M. (2001). Environmental impacts of urban sprawl: A survey of the literature and proposed research agenda. *Environment and Planning A*, 33, 4: 717-35.

Kostof, K.S. (2009). The city shaped: urban patterns and meanings through history *(New York: Bulfinch Press, Boston)*.

Levinson, D. M., & Yerra, B. (2005). How Land Use Shapes the Evolution of Road Networks. *Available at SSRN 1736160*.

Lynch, K. (1984). Good City Form, *(London: MIT Press)*.

Mackay, E.J.H. (1938). Further Excavations at Mohen-jo-Daro *(New Delhi: Government of India)*.

Morris, A. E. J. (1976). History of Urban Form: Before the Industrial Revolution (2nd edition). *Prentice-Hall*.

Nelson, G. (2009). Grid and Anti-Grid. A landscape dialectic of socioenvironmental ideals. Rafi, U.S. (2000). 'Ancient Indus Civilization', Published by *Royal Book company*, BG-5

Soja, E.W. (2000). Postmetropolis: Critical Studies of Cities and Regions. (*Malden: Blackwell Publishers).*

Bignami, D.F. (2014). Territorial and Historical Framework of Multan: A Prosperous Land and an Inspiring Past Leading to a New Progress. In *Sustainable Social, Economic and Environmental Revitalization in Multan City (pp. 33-41). Springer, Cham.*

Hussain, S., Mubeen, M., Akram, W., Ahmad, A., Habib-ur-Rahman, M., Ghaffar, A., and Nasim, W. (2020). Study of land cover/land use changes using RS and GIS: a case study of Multan district, Pakistan. *Environmental monitoring and assessment*, 192(1), 1-15.

Faiz, A. (2021). Building language, building province: Civil society and ethnic nationalism in Pakistan. *Journal of Civil Society*, 1-19.

Kepaptsoglou, K., Milioti, C., Spyropoulou, D., Haider, F., & Karlaftis, A. G. (2020). Comparing traveler preferences for BRT and LRT systems in developing countries: Evidence from Multan, Pakistan. *J. of Traffic & Trans. Engg.*, 7(3), 384-393.

Del-Bo, A. (2014). Introduction and Approach: Sharing Culture and Knowledge of the Core of Multan. In Sustainable Social, Economic and Environmental Revitalization in Multan City (pp. 3-15). *Springer*.

Pateman, T. (1987). Language in mind and language in society: *Studies in linguistic reproduction*.

Fait, P. (2021). Mario Mignucci, Ancient Logic, *Language, and Metaphysics*: *Selected Essays*.

Ahearn, L. M. (2021). Living language: An introduction to linguistic anthropology. *John Wiley & Sons*.

Martinich, A. P. (2009). Philosophy of language.

Mair, V. H. (2021). The cultures of ancient Xinjiang, Western China: crossroads of the silk roads: edited by Alison Betts, Marika Vicziany, Peter Weiming Jia and Angelo Andrea di-Castro, *Oxford, Archaeo-press*, 2019, 218.

Pettersson, A. (2016). Language, Truth, and Literature: A Defense of Literary Humanism by Richard Gaskin. Oxford: *Oxford University Press*, 2013, 376 pp. ISBN 978-0-19-965790-2.

Luo, J., Hartmann, F., Santus, E., Barzilay, R., & Cao, Y. (2021). Deciphering Under segmented Ancient Scripts Using Phonetic Prior. *Transactions of the Association for Computational Linguistics*, 9, 69-81.

Reduction by Hydrogen of the Waste Rock Minerals Constituents of a Vanadium Ore

Túlio Simplício Ferreira[1], Isabel Cristina Braga Rodrigues[2], Adilson Lago Leite[3], Victor de Andrade Alvarenga Oliveira[*1]

[1]Thermal Analysis and Non-Ferrous Extractive Metallurgy Laboratory – Department of Metallurgical and Materials Engineering, Universidade Federal de Ouro Preto – Ouro Preto - Minas Gerais – Brazil – CEP 35400-000.

[2]Department of Chemistry, Biochemistry and Bioprocess Engineering - Universidade Federal de São João del-Rey, Ouro Branco, Minas Gerais, CEP 36497-899 – (ORCID 0000-0002-5474-6225).

[3]Geochemistry Laboratory – Department of Civil Engineering – Universidade Federal de Ouro Preto, Ouro Preto, Minas Gerais, CEP 35400-000, Brazil.

Abstract

A sample of vanadium ore has been characterized by X-ray diffractometry (XRD), scanning electron microscopy coupled with dispersive energy spectrometry (SEM-EDS) and thermogravimetric analysis (TG). The mineral composition was determined by the Rietveld method and the results showed that the major mineral constituents are maghemite (52.32%) and magnetite (15.73%). The SEM-EDS images showed that the vanadium is diffused over the crystal structure of almost all the minerals. Hydrogen reduction was assessed by thermogravimetry (TG), where three thermal events has been identified in the TG curves. The first event was probably related to two chemical reactions: (i) the oxidation of the mineral ulvospinel by different vanadium oxides, followed by the reduction of the products of this redox reaction by the hydrogen, and (ii) the reduction of the mineral magnesioferrite by the hydrogen. The other two events were attributed to the dehydroxylation of the phyllosilicates (greenalite, cronstedtite and sudoite) and the reduction of maghemite, magnetite, titanium oxides and vanadium oxides. Finally, the integration isoconversional method was used to determine the apparent activation energy (E_a), which ranged from 44.28kJ.mol^{-1} to 82.47 kJ.mol^{-1} for the Kissinger-Akahira-Sunose method (KAS), and from 33.44kJ.mol^{-1} to 65.54kJ.mol^{-1} for the Ozawa-Flynn-Wall method (OFW). These values imply that the reduction is controlled by mixed process for low conversion values (diffusion and chemical reaction are the controlling steps) and by chemical reaction for high conversion values.

Keyword: Isoconversional method; vanadium ore; reduction by hydrogen; kinetics

[*]Corresponding author: victor@ufop.edu.br

1. Introduction

The main application of vanadium is as an alloying additive to the steel-making process and the consumption of this element by this metallurgical sector corresponds to 85% of the worldwide production (Zhang et al., 2019; Gilligan and Nikoloski, 2020; Gasik, 2013; Moskalyk and Alfantazi, 2003). Minor amounts of vanadium (0.05-0.2%) reduces the particle grain size, increases hardenability, and improve the overall wear resistance. In addition, this element is also an important stabilizer for titanium and other special alloys (Zhang et al., 2019; Gilligan and Nikoloski, 2020; Gasik, 2013).

Vanadium is mostly commercially available as oxide (> 98% V_2O_5) (Zhang et a., 2019) or in ferrovanadium

alloys (40%, 60% or 80% of vanadium) (Moskalyk and Alfantazi, 2003). The primary sources of vanadium have a complex mineralogy (Liu et al., 2014; Sui et al., 2017) and substantial amounts of other metallic elements (e.g., Ti, Cr and Fe). It is worth to point out that a high chromium content in the ore leads to environmental and economical disadvantages, considering the fact that the presence of this element in the metallurgical waste increases the cost and restricts the possibilities of waste disposal (Peng, 2019; Wang et al., 2017). On the other hand, chromium and titanium can be recovered through the metallurgical process, to be sold as a by-product (Wang et al., 2017). Therefore, becomes imperative the development of alternatives for the vanadium extraction process aimed at the recovery of vanadium and other metallic elements.

Among many sources, it can be distinguished the vanadium titanomagnetite (VTM) as the primary source, metallurgical slags (containing 12-24 wt.% of V_2O_5) (Xiang et al, 2018; Wang et al., 2018; Zhang et al., 2019) and petroleum residues (Zhang et al., 2019; Xio et al., 2010). Most of the vanadium is now produced from the steel slag and many studies deals with the extraction of this element using direct leaching procedures, carbothermic reduction followed by magnetic separation and pyrometallurgical operations such as reduction, calcination and roasting followed by leaching with different chemical solutions (Wang et al., 2018).

Primary vanadium sources usually are submitted to a pyrometallurgical reduction step. The reduction of VTM concentrate is an essential step for the Blast Furnace (BF) process, reduction roasting magnetic separation and pre-reduction electric furnace melting process (Liu et al., 2014; Sui et al., 2017). Thus, the understanding of the reduction kinetics and reduction mechanisms of these ores is essential for developing new processes and techniques that promote a better use of these mineral resources.

In this research, the reduction of a vanadium ore sample was performed under low temperature (< 950 °C) in order to convert oxidized iron mineral phases into elemental iron (Fe^o), as a preparation for the subsequent hydrometallurgical acid leaching procedure. It is well known that the Fe^0 leaching is greatly faster and involves less aggressive conditions than those used for oxidized minerals iron phase.

2. Material And Methods

The vanadium ore sample has 100% particle size less than 75µm, and was oven dried for 24h at 105°C before being submitted to the experimental procedures. The sample was provided by the company Largo Resources and was obtained from a Brazilian mine located in the state of Bahia.

3. Chemical Composition

The major chemicals were determined on a solid blend composed of 0.2 g of ore and 4.0 g of a 1:1 mix of sodium carbonate (FMaia – 99.5%) and sodium tetraborate (Synth -99.5%). This mixture was then homogenized and melted in platinum crucible at 950°C for 30 minutes. After cooling in a desiccator, this mixture was completely dissolved using hydrochloric acid solution (≈16%). The major chemicals of the ore were then determined using inductively coupled plasma-optical emission spectrometry (ICP-OES – Varian 725-ES).

4. Mineral Composition

The mineral composition was determined using the x-ray diffraction (XRD) D2 Phaser (Bruker). The XRD patterns were compared with the ICSD standard incorporated into the Diffract. EVA software. The

Rietveld refinement method was carried out using the software TOPAS 5.0. The instrument settings, parameters, and references for the XRD analysis are shown in tables 1, 2 and 3, respectively.

Table 1. Instrument settings for XRD.

Diffractometer	Bruker D2 Phaser
Goniometer	Θ-2Θ, radius 141.1
Source	CuK_α (λ = 1.54184 Å)
Generator	30kV, 10mA
Sample	
Surface diameter (mm)	25
Spinning rate (rpm)	8
Preparation	Block loading
Incident optics	
Fixed divergence slit	0.6 mm
Receiving optics	
Soller slit	2.5
Detector	Lynxeye
Scan Info	
Angular range (2Θ)	15-70°
Step (2Θ)	0.18189
Length linear detector (2Θ)	5.002106
Time per step (s)	1.000
Measurement time (s)	3299

Table 2. Parameters used for quantitative analyses of XRD data.

Background	
Chebychev coefficients	6
1/x	Fitted for all
Profile function	Fundamental parameters
Cell parameters	Fitted for all phases
Crystallite size for each phase	Fitted the crystallite
Number of fitted parameters	~34

Table 3. References of the phase structures used for Rietveld analysis.

Phases	**COD – ID**	**Ref.**
Anatase	5000223	Horn et al., 1972
	7206075	Rezae et al., 2011
Clinopyroxene	9003349	Redhammer et al., 2004
Cronstedtite	9000019	Hendricks (1939)
Fayalite	9000559	Hazen (1977)
Greenalite	9000132	Shiruzu & Bailey, (1965)
Hematite	641734	TSV (1988)
Karelianite	9008083	Newnhen & Haan (1926)
Ilmenite	9008035	Barth (1934)
Indialite	9006271	Swartz (1994)
Iron	631734	Kim (1969)
Magnesioferrite	1011241 1011245	Barth (1932); Passereni, (1930)
Maghemite	9006317	Pecharromán (1995)
Magnetite	65339	Fleet (1986)
Melanovanadite	9010026	Konert & Evans (1987)
Pyrope	9001527	Ganguli & Cheng, (1994)
Rutile	9004144	Meager & Lager, (1979)
Spinel	9015716	Princivalle et al., (2012)
Sudoite	9000151	Eggleton & Bailey (1967)
Ti_7O_{13}	1008196	Page (1982)
Tistarite	9008082	Newnham, (19820
Tricalcium Silicate	9015421	GN (1975)
Ulvospinel	9013538 9013536	Bosi et al., (2009)

5. Thermogravimetric Analysis (Tg)

Approximately 75 mg of ore sample was submitted to thermogravimetric (TG) analyses using a Mettler Toledo apparatus (model Star System). High purity hydrogen (99.9990%) was applied as the reducing gas at a flow rate of 100 $mL.min^{-1}$. These quantities were chosen according to preliminary tests, which also demonstrated that under the experimental conditions, these variables have no influence on the TG curve pattern. The TG heating rates were 2.5°$C.min^{-1}$,

5°C.min^{-1}, 10°C.min^{-1}, 15°C.min^{-1} and 20°C.min^{-1} in the temperature range of 50°C to 950°C. All the gases used in the TG determinations were supplied by White Martins.

Scanning electron microscopy (sem) and energy dispersive spectroscopy (eds). Scanning Electron Microscopy (SEM) including Energy Dispersive Spectroscopy (EDS) were performed using a Tescan equipment, model VEGA 3 LMH, coupled to an EDS INCA x-act, model 51-ADD0007. All the ore samples were embossed using a commercial polyester resin, to be after polished using sandpaper of different grit sizes. The polishing finishing was done using 1.0 μm alumina paste. Subsequently the samples were covered with gold by sputtering techniques.

6. Reduction Tests

Reduction tests were performed on 5 g ore samples using a rotary kiln (20 rpm). Tests conditions were temperatures of 420°C, 520°C and 950°C; flow rate of 1 L.min^{-1} for 1h. Hydrogen (99.9990%) was used as the reducing gas where the flow rate was fixed using a mass flowmeter. After the reduction tests, the samples were naturally cooled in the oven using N_2 (99.990%) at a flow rate of ≈ 1 L.min^{-1}. After cooling, the sample was kept in a desiccator for the subsequent XRD analysis. All the gases used in the experiments were supplied by White Martins.

7. Isoconversional Kinetics

The isoconversional method is widely applied for understanding the decomposition, oxidation and reduction reactions of many materials of technological interest (Cheng et al., 2015; Zivkovic et al., 1998; Guimarâes et al., 2016; Olzak et al., 1999; Wang et al., 2018; Pourghahramani, 2007; Tomic et al., 2012). It allows the estimation of the activation energy of a thermal process without the prior knowledge of the involved kinetic model (Chilgi et al., 2014). Its basis relies on the kinetics as shown by the Equation (1) (Vyazovkin et al., 1965):

$$\frac{\partial \alpha}{\partial T} = \frac{A}{\beta} exp\left(\frac{-E_a}{RT}\right) f(\alpha) \qquad (1)$$

Where A and E_a are respectively the pre-exponential factor and activation energy, R is the universal gas constant, T is the absolute temperature, $f(\alpha)$ is the conversion function, β is the heating rate and α is the extent of the conversion of reactants to the products. The isoconversional principle establishes that for a constant extent of conversion (α), the reaction rate is only a function of the temperature (T). The Equation (2) is obtained by rearranging and taking the natural log of both sides of the Equation (1). It is the basis of the differential method of Friedman (Vyazovkin et al., 1965).

$$ln\left(\beta \frac{d\alpha}{dT}\right)_\alpha = ln(A_\alpha \mathrm{f}(\alpha)) - \frac{E_\alpha}{RT_\alpha} \qquad (2)$$

This method requires the differentiation of the curves α versus T, and this procedure usually creates some scattering on the E_α values. Numerical differentiation can be avoided by using integration methods. Equation (3) is the result of the integration of Equation (1):

$$g(\alpha) \equiv \frac{A}{\beta} \int_0^{T_\alpha} exp\left(\frac{-E_\alpha}{RT}\right) dt = \frac{A}{\beta} I(E,T) \quad (3)$$

The integral $I(E, T)$ has no closed-form analytical solution and it is solved by using numerical methods. Two expressions are commonly used as approximate solutions to the integral I(E,T): (i) the Ozawa-Flynn-Wall Solution (OFW) (Equation 4) (Ozawa, 1965; Flynn, 1966) and (ii) the Kissinger-Akahira-Sunose Solution (KAS) (Equation 5) (Coats et al., 1964):

$$\ln(\beta) = 1.0516\left(\frac{E_a}{RT_p}\right) - A' \quad (4) \qquad -ln\left(\frac{\beta}{T_p^2}\right) = \frac{E_a}{RT_p} - ln\left(\frac{A''R}{E_a}\right) \quad (5$$

where A´ and A´´ are constants.

Thermodynamic Data

All the thermodynamic data were obtained from HSC Chemistry 6.0 software.

8. Results

8.1. Chemical / Mineral Composition

The element composition of the ore sample is shown on Table 4 (weight %). The vanadium content is considerably higher compared to other similar studies, where the vanadium ore (VTM) and concentrates were also submitted to reduction process (Li et al., 2019; Zhao et al., 2019). It is noteworthy that a high vanadium content implies less energy for heating and/or melting the gangue, which corroborates the choice of pyrometallurgical routes.

Table 4. Chemical composition of the vanadium ore (weight %).

Elements	Content Percentage(%)
Al	0.72
Ca	0.29
Fe	58.2
K	0.17
Mg	0.79
Mn	0.11
Si	1.47
Ti	4.33
V	1.92

As Table 1 shows, the ore sample presents a high iron content, which is a common feature for vanadium ores. Additionally, the titanium content is relatively low, and as will be discussed later, it was not found in the crystalline network of the magnetite.

Finally, the absence of chromium, an element which is also ordinary for vanadium ores, enables the choice of the reduction method for ferrovanadium alloys production, since this element has deleterious effects on the blast furnace process (BF process) and "pre-reduction roasting magnetic separation process" (Sui et al., 2017). The x-ray patterns and interpretation for the ore sample are shown on Table 5 and Figure 1, respectively. The results reveal that the main mineral constituents are maghemite (52.32%) and magnetite (15.73%), and that most of the iron content (85.8%) is found in these mineral phases. The total iron content estimated from its proportions on the mineral phase is 57.6%, which is close to the elemental composition presented on Table 4 (58.2%).

Table 5. Mineral composition of the vanadium ore sample.

Mineral name	Chemical structure	Content (%)
Tricalcium silicate	Ca_3SiO_5	1.85
Clinopyroxene	$Ca_{0.4}Mg_{1.6}Si_2O_6$	4.22
Cronstedtite	$Fe_4SiO_5(OH)_4$	0.75
Fayalite	Fe_2SiO_4	1.8
Ulvospinel	Fe_2TiO_4	5.93
Greenalite	$Fe_{2.8}Si_{2.2}O_5(OH)_{3.3}$	2.07
Ilmenite	$FeTiO_3$	4.18
Indialite	$Mg_2Al_4Si_5O_{18}$	1.12
Magnesioferrite	$MgFe_2O_4$	5.12
Magnetite	Fe_3O_4	15.73
Maghemite	γFe_3O_4	52.32
Melanovanadite	$CaV_4O_{10}*5H_2O$	3.12
Sudoite	$Mg_{1.9}Fe_{0.3}Al_{3.9}Si_3O_{10}(OH)_{7.9}$	1.81

Figure 1. XRD patterns and Rietveld refinement of the vanadium ore sample. (Cr) cronstedtite; (C) clinopyroxene; (F) fayalite; (U) ulvospinel; (Ca) tricalcium silicate; (G) greenalite; (M) magnetite; (Mh) maghemite; (I) Ilmenite; (In) Indialite; (V) melanovanadite; (Mg) magnesioferrite and (S) sudoite.

Figures 2 and 3 show the scanning electron microscopy (SEM) and EDS mapping images of the ore sample. Both figures show that the vanadium element is diffused all over the mineral phases, which leads to difficulties on the vanadium concentration process by conventional unit operation. Some minerals identified by the XRD analysis were highlighted on Figure 3.

As mentioned before, the EDS mapping do not show the presence of titanium in the crystalline network of magnetite and maghemite.

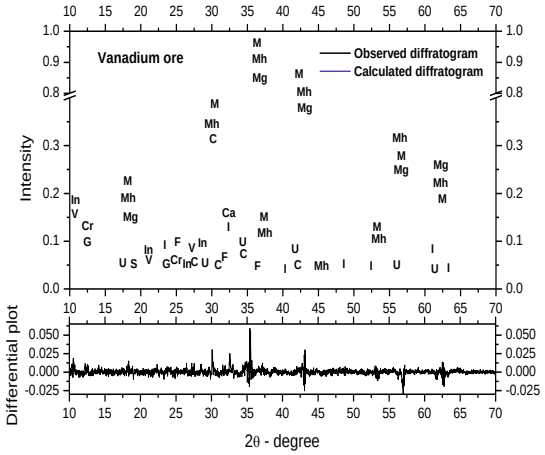

Figure 2. SEM-EDS of the vanadium ore. Left hand side secondary electrons image and right-hand side backscattered electrons image.

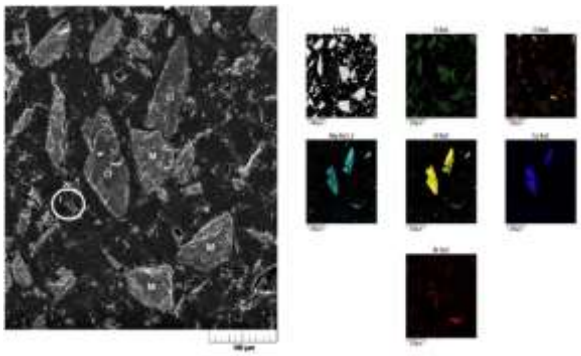

Figure 3. SEM-EDS of the sample. (I) Ilmenite; (Cl) Clinopyroxene and (M) magnetite or maghemite.

8.2. Hydrogen Reduction

The TG and DTG curves of the ore sample submitted to hydrogen reduction are shown on Figure 4. Three thermal events can be identified on these curves, named here as A, B, and C for the TG curve, and A´, B´ and C´ for the DTG curve. After hydrogen reduction, the ore samples were submitted to XRD (Figure 5, 6 and 7) and mineral phases were quantified using the Rietveld method (Table 6).

Figure 4 shows that the thermal event A take place from 350°C to 420ºC, which may be related to the reduction of the thermal decomposition products of the minerals ulvospinel (Fe_2TiO_4) and magnesioferrite ($MgFe_2O_4$). While this thermal decomposition is not thermodynamically favourable at 420°C under an inert atmosphere, as demonstrated by equations (6) and (7), it is favourable for the magnesioferrite when using a reducing atmosphere (Equation 8).

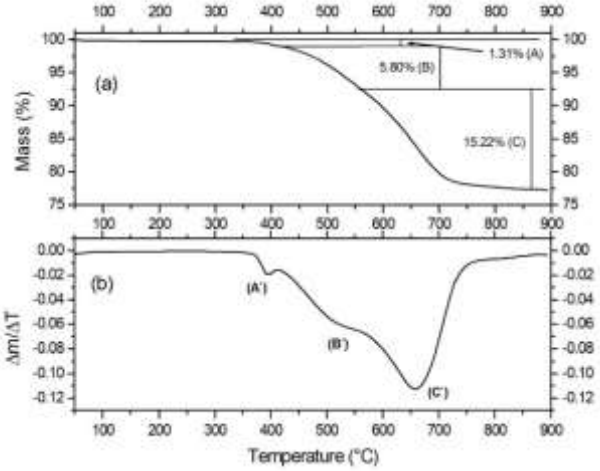

Figure 4. Hydrogen reduction of the ore sample (H_2 = 100ml/min; heating rate = 10°C/min): (a) TG and (b) DTG curves.

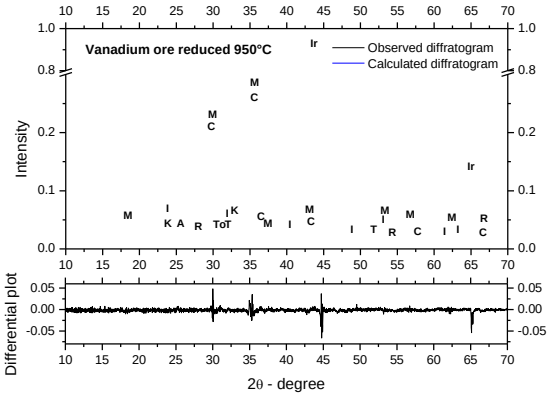

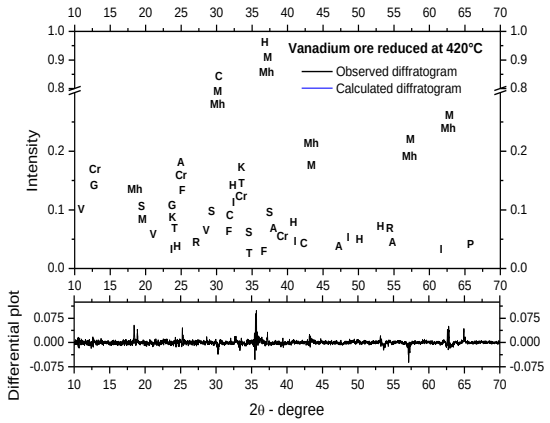

Figure 5. XRD patterns and Rietveld refinement method of the vanadium ore reduced at 420°C. (A) anatase; (C) clinopyroxene; (Cr) cronstedtite; (F) fayalite; (G) greenalite; (H) hematite; (K) karelianite; (I) ilmenite; (M) magnetite; (Mh) maghemite; (V) melanovanadite; (P) pyrope; (R) rutilie; (S) spinel and (T) tristarite.

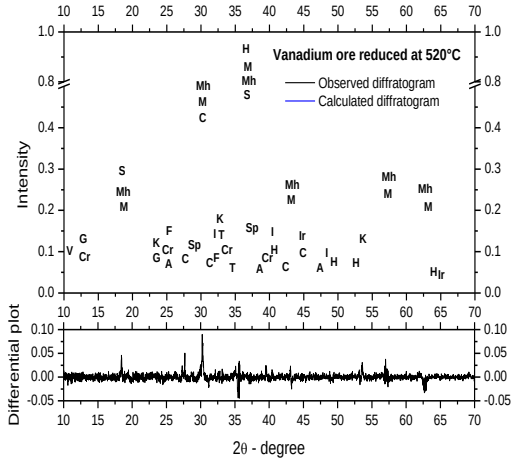

Figure 6. XRD patterns and Rietveld refinement method of the vanadium ore reduced at 520°C. (A) anatase; (C) clinopyroxene; (Cr) cronstedtite; (F) fayalite; (G) greenalite; (H) hematite; (K) karelianite; (I) ilmenite; (Ir) iron; (M) magnetite; (Mh) maghemite; (V) melanovanadite; (Sp) spinel; (S) sudoite and (T) tristarite.

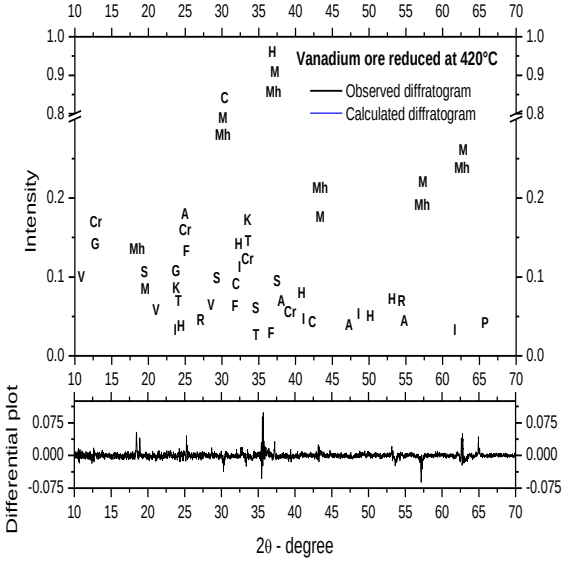

Figure 7. XRD patterns and Rietveld refinement method of the vanadium ore reduced at 950°C. (A) anatase; (C) clinopyroxene; (K) karelianite; (I) ilmenite; (Ir) Iron; (M) Magnetite; (R) Rutile; (To) Ti_7O_{13} and (T) tistarite.

Table 6. Mineral composition of the vanadium ore reduced at different temperatures.

Mineral name	Chemical Structure	Content (%)		
		420° C	520 °C	950° C
Anatase	TiO_2	2.06	0.82	0.61
Clinopyroxene	$Ca_{0.4}Mg_{1.6}Si_2O_6$	3.22	12.51	30.5
Cronstedtite	$Fe_4SiO_5(OH)_4$	1.41	0.54	-
Fayalite	Fe_2SiO_4	1.67	1.35	-
Greenalite	$Fe_{2.8}Si_{2.2}O_5(OH)_{3.3}$	1.85	0.49	-
Hematite	Fe_2O_3	4.36	0.26	-
Karelianite	V_2O_3	2.17	2.86	1.03
Ilmenite	$FeTiO_3$	4.69	4.21	7.47
Iron	Fe	-	1.99	42.26
Magnetite	Fe_3O_4	15.85	16.61	15.34
Maghemite	γFe_3O_4	56.22	38.84	-
Melanovanadite	$CaV_4O_{10}*5H_2O$	3.03	1.46	-
Pyrope	$Mg_3Al_2(SiO_4)_3$	0.3	-	-
Rutile	TiO_2	0.8	-	0.15
Spinel	$Mg(Al,Fe^{3+})_2O_4$	0.58	9.33	-
Sudoite	$Mg_2Al_3(Si_3AlO_{10})(OH)_8$	-	6.16	-
-	Ti_7O_{13}	-	-	1.62
Tistarite	Ti_2O_3	2.05	2.12	1.02

$$MgFe_2O_4 = Fe_2O_3 + MgO$$

$$\Delta G^0 = -0.0164T^2 + 21.04T + 13{,}509 \text{ (J/mol) } (473K < T < 1273K) \quad (6)$$

$$Fe_2TiO_4 = 2FeO + TiO_2$$
$$\Delta G^0 = -2.85T + 38{,}065 \text{ (J/mol) } (473K < T < 1273K) \quad (7)$$

$$3MgFe_2O_4 + H_2(g) = 2Fe_3O_4 + 3MgO + H_2O(g)$$
$$\Delta G^0 = -116.24T + 74{,}562 \text{ (J/mol) } (473K < T < 1273K) \quad (8)$$

It is believed that the thermal decomposition of the ulvospinel occurs as one of the chemical reactions presented from equations (9) through (19). They all represent redox reactions where Fe^{2+} is oxidized to Fe^{3+} by different vanadium oxides.

$$Fe_2TiO_4 + V_2O_5 = Fe_2O_3 + TiO_2 + 2VO_2 \quad (9)$$

$$Fe_2TiO_4 + 2/3V_2O_5 = 2/3Fe_3O_4 + TiO_2 + 4/3VO_2 \quad (10)$$

$$Fe_2TiO_4 + 1/3V_2O_5 = 2/3Fe_3O_4 + TiO_2 + 1/3V_2O_3 \quad (11)$$

$$Fe_2TiO_4 + 3/5V_2O_5 = Fe_2O_3 + TiO_2 + 2/5V_3O_5 \quad (12)$$

$$Fe_2TiO_4 + 1/2V_2O_5 = Fe_2O_3 + TiO_2 + 1/2V_2O_3 \quad (13)$$

$$Fe_2TiO_4 + 3VO_2 = Fe_2O_3 + TiO_2 + V_3O_5 \quad (14)$$

$$Fe_2TiO_4 + 2VO_2 = Fe_2O_3 + TiO_2 + V_2O_3 \quad (15)$$

$$Fe_2TiO_4 + 2VO_2 = 2/3Fe_3O_4 + TiO_2 + 2/3V_3O_5 \quad (16)$$

$$Fe_2TiO_4 + 4/3VO_2 = 2/3Fe_3O_4 + TiO_2 + 2/3V_2O_3 \quad (17)$$

$$Fe_2TiO_4 + 4/3V_3O_5 = 2/3Fe_3O_4 + TiO_2 + 2V_2O_3 \quad (18)$$

$$Fe_2TiO_4 + 2V_3O_5 = Fe_2O_3 + TiO_2 + 3V_2O_3 \quad (19)$$

Figure 8 presents the Ellingham Chart for the reactions (9) through (19), showing that they are thermodynamically favourable at the temperature of the thermal event A. These charts also show that for the same oxidizing agent at the temperature of the event A, with the exception of the oxidation reaction induced by V_3O_5 (equations 18 and 19), the formation of hematite is always more favourable than magnetite. The formation of hematite, in turn, is due to solid reactions among the ore minerals.

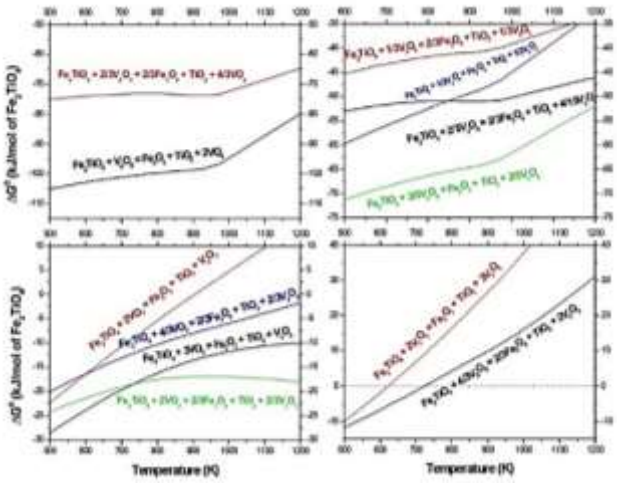

Figure 8. Ellingham chart for decomposition reaction of ulvospinel

The absence of the ulvospinel and magnesioferrite minerals on Table 6 indicates their decomposition induced by reduction, as described by the equations 6 through 19. Consequently, there was an increase in the maghemite content and the formation of hematite, as shown on Table 6 (reduced at 420°C). Table 5 indicates an initial magnesioferrite content of 5.12%, and according to the Equation (8), the expected loss of mass by reduction of this mineral is approximately 0.14% (0.0267 x 5.12%). The mass loss associated with event A is considerably greater than the calculated value and this can be attributed to the partial reduction of the hematite content formed after the decomposition of the ulvospinel.

Finally, Table 6 shows the formation of Tistarite (Ti_2O_3) due to reduction of $FeTiO_3$ or TiO_2, which means that for an atmosphere with $pH_2O/pH_2=10^{-5}$, the reduction of the minerals rutile, anatase and ilmenite is not thermodynamically favourable when the activity of the solid species is 1 (Figure 9). However, the formation of Ti_2O_3 suggests that some solid-state reaction is inducing the reduction of TiO_2 or that the activity of this specie is high enough for the reaction to be spontaneous under the applied experimental conditions. The ilmenite reduction reaction also contributes to the loss mass associated with the event A.

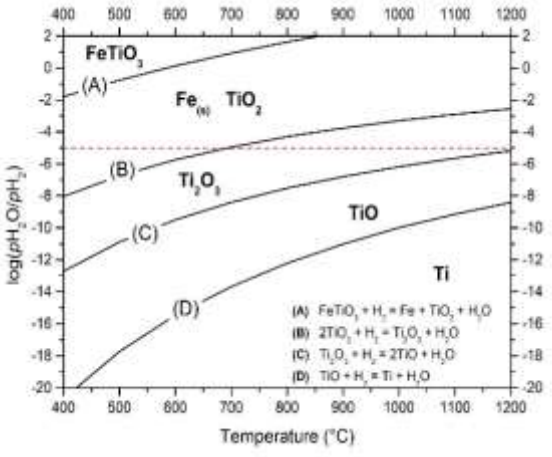

Figure 9. Diagram log(pH_2O/pH_2) vs Temperature for the Fe-Ti-O-H system. The dashed red line represents the experimental conditions of this study

Dehydroxilation of cronstedtite, sudoite and greenalite phyllosilicates occurs in the temperature range of 550°C

to 800°C (events B and C) (Dlugogorski et al., 2014). These minerals are minor components of the ore and undertake different thermal decomposition mechanisms that can produce different mineral phases (Dlugogorski et al., 2014). Therefore, the serpentine mineral will be used as a reference phyllosilicate for the dehydroxilation reaction, as shown on Equation (20). However, this equation cannot be used for the mass loss calculations associated with these thermal transformations.

$$Mg_3(Si_2O_5)(OH)_4 = Mg_2SiO_4 + MgSiO_3 + 2H_2O(g)$$
$$\Delta G^0 = -286T + 136890 \text{ (J/mol)} \qquad (20)$$

The XRD results (Table 6) are evidence that at the temperatures of 520°C to 950°C these minerals are dehydroxylated.

In addition to the thermal decomposition of the phyllosilicates, events B and C are related to the reduction of magnetite and maghemite, as demonstrated by the Equation 21.

$$Fe_3O_4 + 2H_2(g) = 3Fe^0 + 4H_2O(g) \qquad (21)$$

For a sample composed of 68.05% of magnetite + maghemite, the theoretical mass loss associated with the reduction of these minerals is 18.8% (0.2764 X 68.05%). As can be seen on Figure 4, the actual mass loss was found to be 21.02%, which is a bit higher than the theoretical estimation.

Notwithstanding, like the iron oxides, the vanadium and titanium oxides will also be reduced by a reducing atmosphere with $\log(pH_2O/pH_2) = -5$ (Figures 10 and 11). The reduction of oxidized minerals phases of vanadium, titanium and iron is confirmed by the results shown on Table 6.

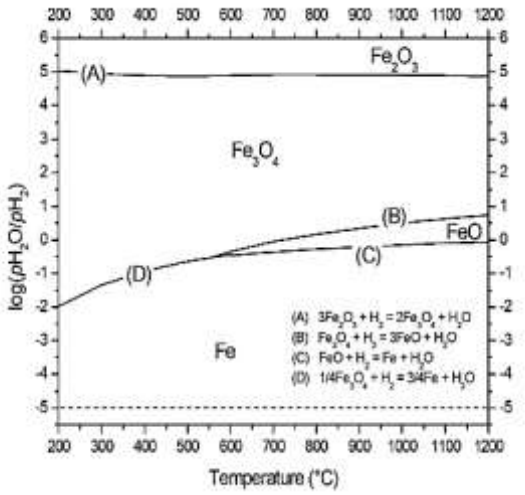

Figure 10. Diagram log(pH_2O/pH_2) vs Temperature for the Fe-O-H system. The dashed red line represents the experimental conditions of this study.

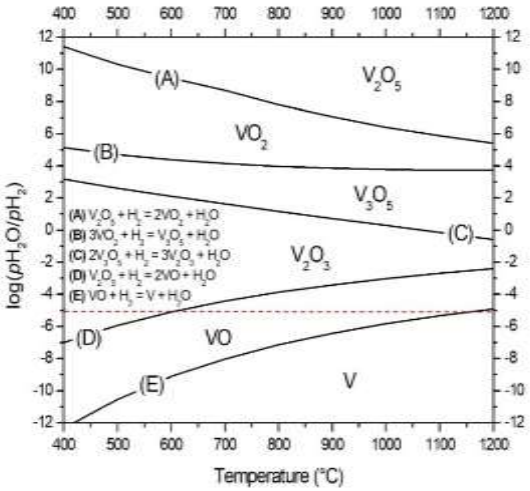

Figure 11. Diagram log(pH_2O/pH_2) vs Temperature for the V-O-H system. The dashed red line represents the experimental conditions of this study.

Figure 12 shows an SEM-EDS image of the ore sample reduced at the temperature of 950°C. It can be noticed the high porosity of the solid particles, and these pores were generated by the gaseous product of the reaction (H_2O).

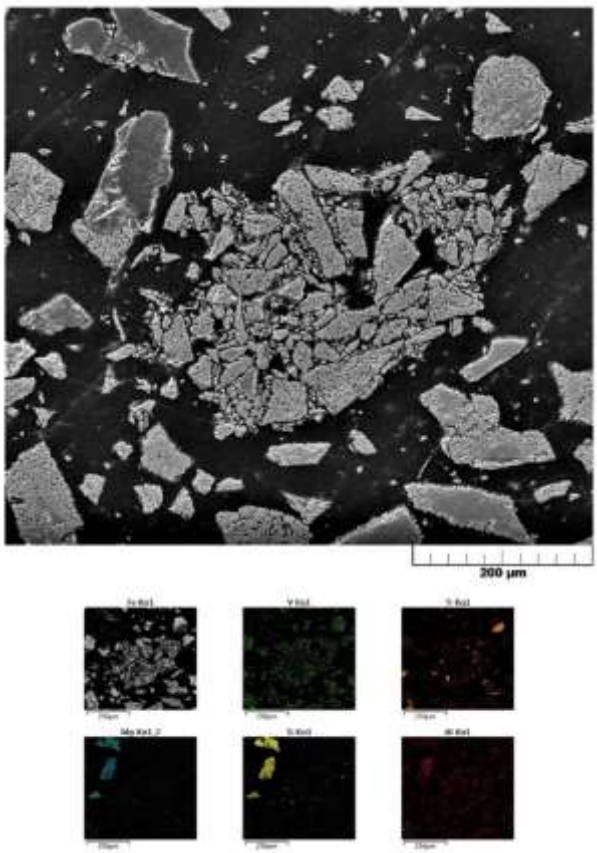

Figure 12. SEM-EDS images of the ore sample reduced at 950°C by hydrogen (1h – 1L/min).

8.3. Isoconversional Kinetics

As mentioned before, the integral isoconversional method was used to evaluate the kinetics of the ore sample reduction. Figure 13 shows the reduction curves at different heating rates (β).

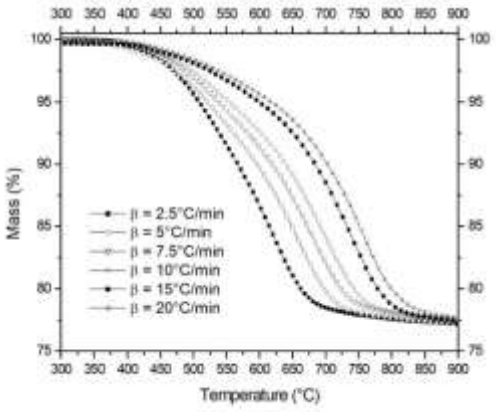

Figure 13. TG curves for the ore sample under different heating rates (β).

The extent of conversion (α) was calculated using the initial content of maghemite and magnetite (P_0 = *68.8%*) in the ore sample, as shown on Equation (22). A value of α 1 indicates that 100% of these minerals have been reduced to metallic iron.

$$\alpha = \frac{w_t}{\left(1-\frac{3\times MM_{Ir}}{MM_{mag}}\right)\times\frac{P_0}{100}} \quad (22)$$

Where MM_{Ir} and MM_{Mag} are respectively the molar masses of iron and magnetite (or maghemite) and w_t is the mass loss at a specific time.

Figure 14 depicts the plots of the integration methods OFW (Equation 4) and KAS (Equation 5), using three different α values. Table 7 shows the apparent activation energy of these plots and the coefficient of determination (R^2) of the linear regression fit.

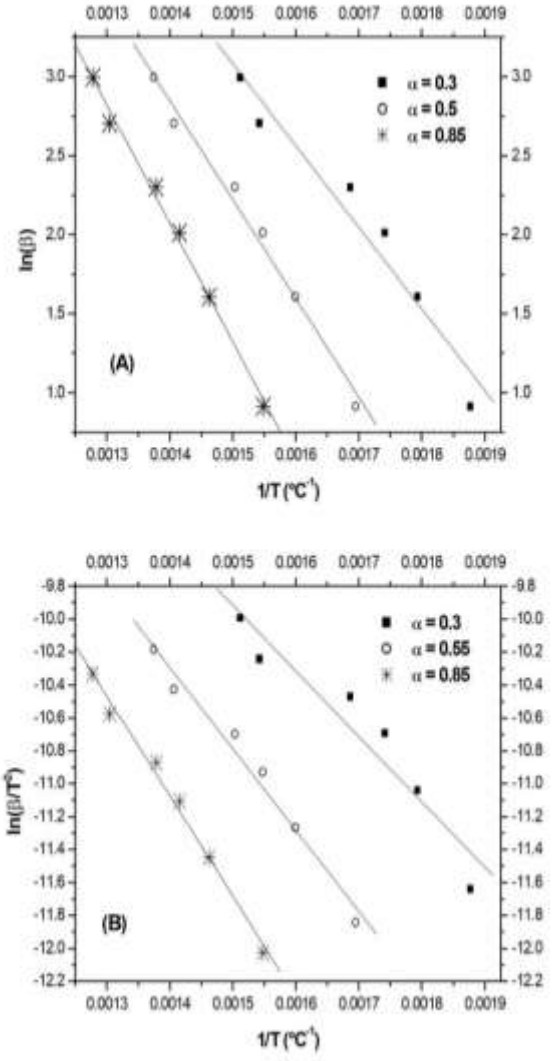

Figure 14. Plots of (A) Ozawa-Flynn-Wall method and (B) Kissinger-Akahira-Sunose methods using three different values of α.

Table 7. Apparent activation energy for different conversion (α) values calculated using the OFW and KAS integration methods.

Conver-sion (α)	OFW		KAS	
	E_a/kJ mol^{-1}	R^2	E_a/kJ mol^{-1}	R^2
0.10	51.66	0.8857	40.56	0.8388
0.15	47.28	0.9015	35.97	0.8513
0.20	44.79	0.9155	33.24	0.8648
0.25	44.28	0.9328	32.44	0.8878
0.30	45.21	0.9506	33.06	0.9152
0.35	46.89	0.9651	34.43	0.9393
0.40	48.86	0.9752	36.09	0.9565
0.45	50.86	0.9815	37.79	0.9674
0.50	52.78	0.9852	39.46	0.9741
0.55	54.70	0.9875	41.08	0.9782
0.6	56.50	0.9891	42.63	0.9811
0.65	58.26	0.9904	44.15	0.9835
0.70	60.03	0.9917	45.68	0.9858
0.75	61.86	0.9928	47.28	0.9878
0.80	63.79	0.9938	48.96	0.9894
0.85	65.75	0.9973	50.67	0.9908
0.90	67.75	0.9950	52.37	0.9916
0.95	70.36	0.9956	54.59	0.9927
1.0	82.47	0.9844	65.54	0.9781

Figure 15 presents a plot of the apparent activation energy (E_a) as a function of the extent of conversion (α). The E_a values ranged from 44.28kJ.mol^{-1} to 82.47kJ.mol^{-1} for the OSW method and from 33.44kJ.mol^{-1} to 65.54kJ.mol^{-1} when the KAS method was applied. The E_a values suggest that the slow process step is a mixed step for low conversion value and a chemical step for high conversion values.

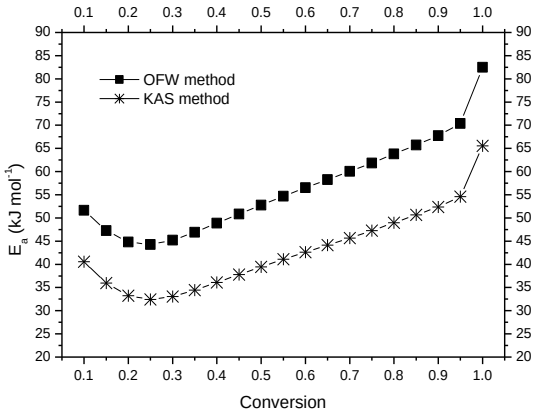

Figure 15. Apparent activation energy (E_a) estimated by the OFW and KAS integration methods.

9. Conclusions

A sample of vanadium ore was extensively characterized by x-ray diffraction, elemental analysis, and Electron Microscopy-Energy Dispersive Spectroscopy (SEM-EDS).

The major mineral phases were found to be maghemite and magnetite. SEM-EDS showed that vanadium is diffused through the crystalline network of almost all minerals of the ore sample.

The ore reduction was assessed by hydrogen thermogravimetry (TG). TG curves revealed that the mineral magnesioferrite is decomposed at temperatures close to 420°C, and its thermal decomposition products are subsequently reduced by the hydrogen gas.

TG curves suggest also that the mineral ulvospinel is decomposed by a redox reaction between this mineral and the different vanadium oxides of the ore sample. In addition, the products of this redox reaction are also reduced by the hydrogen gas at temperatures close to 420°C. The mineral maghemite was reduced to metallic iron and most of the mass loss of the ore as the result of the hydrogen reduction process was related to this reaction.

The use of the integral isoconversional methods KAS and OFW resulted in good linear determination coefficients (R^2). The estimated apparent activation energy (E_a) values ranged from 44.28kJ.mol^{-1} to 82.47kJ.mol^{-1} when the KAS method was used and from 33.44kJ.mol^{-1} to 65.54kJ.mol^{-1} for the OFW method.

These values imply a mixed controlled step for low conversion values and chemical controlled step for high conversion values.

Acknowledgements

The financial support to this research was provided by the agencies Fundação de Amparo à Pesquisa do Estado de Minas Gerais (FAPEMIG) and Conselho Nacional de Desenvolvimento Científico e Tecnológico (CNPq). The characterization analysis was performed by REDEMAT, which is gratefully appreciated.

References

Barth, T. F., & Posnjak, E. (1932). Spinel structures: with and without variate atom equipoints. *Zeitschrift Für Kristallographie-Crystalline Materials*, *82*(1-6), 325-341.

Barth, T.F.W., Posnjak, E. (1934). The crystal structure of ilmenite Locality: Quincy, Massachusetts. *USA Zeitschrift fur Kristallographie*, 88, 265-270.

Bosi, F., Halenius, U., Skogby, H. (2009). Crystal chemistry of the magnetite-ulvospinel series. *American Mineralogist*, 94, 181-189.

Cheng, G.J., Liu, J.X., Liu, Z.G., Chu, M.S., Xue, X.X. (2015). Non-isothermal reduction mechanism and kinetics of high chromium vanadium-titanium magnetite pellets. *Ironmaking and Steelmaking*, 42, 17-26.

Cilgi, G. K., Cetişli, H., & Donat, R. (2014). Thermal and kinetic analysis of uranium salts. *J. of Thermal Analysis and Calorimetry*, 115(2), 2007-2020.

Coats, A.W., Redfern, J.P. (1964). Kinetic Parameters from Thermogravimetric Data. *Nature*, 201, 68-69.

Dlugogorski, B.Z., Balucan, R.D. (2014). Dehydroxylation of serpentine minerals: Implications for mineral carbonation. *Renewable and Sustainable Energy Reviews*, 31, 353-367.

Eggleston, R. A., & Bailey, S. W. (1967). Structural aspects of dioctahedral chlorite. *American Mineralogist: Journal of Earth and Planetary Materials*, *52*(5-6), 673-689.

Fleet, M. E. (1986). The structure of magnetite: Symmetry of cubic spinels. *Journal of Solid State Chemistry*, *62*(1), 75-82.

Flynn, J. H., & Wall, L. A. (1966). General treatment of the thermogravimetry of polymers. *Journal of research of the National Bureau of Standards. Section A, Physics and chemistry*, *70*(6), 487-523.

Ganguly, J., Cheng, W., & O'Neill, H. S. C. (1993). Syntheses, volume, and structural changes of garnets in the pyrope-grossular join: Implications for stability and mixing properties. *American Mineralogist*, *78*(5-6), 583-593.

Gasik, M. (Ed.). (2013). *Handbook of ferroalloys: theory and technology*. Butterworth-Heinemann.

Gilligan, R., & Nikoloski, A. N. (2020). The extraction of vanadium from titanomagnetites and other sources. *Minerals Engineering*, *146*, 106106.

Golovastikov, N. I. (1975). Crystal structure of tricalcium silicate, 3CaOSiO_2= C_3S. *Sov. Phys. Crystallogr.*, 20(4), 441-445.

Guimarâes, D., Oliveira, V.D.A., Leao, V.A. (2016). Kinetics and thermal decomposition of ettringite synthesized from aqueous solutions. *J. of Thermal Analysis and Calorimetry*, 124, 1679-1689.

Hazen, R. M. (1977). Effects of temperature and pressure on the crystal structure of ferromagnesian olivine. *American Mineralogist*, *62*(3-4), 286-295.

Hendricks, S. B. (1939). Random structures of layer minerals as illustrated by cronstedite (2FeO. Fe2O3. SiO. 2.2 H2O). Possible iron content of kaolin. *American Mineralogist: Journal of Earth and Planetary Materials*, *24*(9), 529-539.

Horn, M. S. C. F., Schwebdtfeger, C. F., & Meagher, E. P. (1972). Refinement of the structure of anatase at several temperatures. *Zeitschrift für Kristallographie-Crystalline Materials*, *136*(1-6), 273-281.

Kim, S.M.D.E. (1969). Lattice constants, thermal expansion coefficients, densities, and imperfections in gold and the alphaphase of the gold-indium system, Z. Metallkunde, 69, 272-277.

Konnert, J. A., & Evans, H. T. (1987). Crystal structure and crystal chemistry of melanovanadite, a natural vanadium bronze. *American M.*, *72*(5-6), 637-644.

Le Page, Y., & Strobel, P. (1982). Structural chemistry of the Magnéli phases TinO2n− 1, 4≤ n≤ 9: II. Refinements and structural discussion. *Journal of Solid-State Chemistry*, *44*(2), 273-281.

Li, W., Fu, G., Chu, M., & Zhu, M. (2019). Effect of porosity of Hongge vanadium titanomagnetite-oxidized pellet on its reduction swelling behavior and mechanism with hydrogen-rich gases. *Powder Technology*, *343*, 194-203.

Liu, S. S., Guo, Y. F., Qiu, G. Z., & Jiang, T. (2014). Solid-state reduction kinetics and mechanism of pre-oxidized vanadium–titanium magnetite concentrate. *Transactions of nonferrous metals society of china*, *24*(10), 3372-3377.

Meagher, E.P., Lager, G.A. (1979). Polyhedral thermal expansion in the TiO2 polymorphs: Refinement of the crystal structure of rutile and brookite at high temperature. *The Canadian Mineralogist*, 17, 77-85.

Moskalyk, R. R., & Alfantazi, A. M. (2003). Processing of vanadium: a review. *Minerals engineering*, *16*(9), 793-805.

NEWNHAM, E., & DE HAAN, Y. M. (1962). Refinement of the a Al2O3, Ti2O3, V2O3 and Cr2O3 structures. *Zeitschrift für Kristallographie-Crystalline Materials*, *117*(1-6), 235-237.

Olszak-Humienik, M., & Możejko, J. (1999). Kinetics of thermal decomposition of dolomite. *Journal of thermal analysis and calorimetry*, *56*(2), 829-833.

Ozawa, T. (1965). A new method of analyzing thermogravimetric data. *Bulletin of the chemical society of Japan*, *38*(11), 1881-1886.

Passerini, L. (1930). Ricerche sugli spinelli. II. I composti: CuAl2O4; MgAl2O4; MgFe2O4; ZnAl2O4; ZnCr2O4; ZnFe2O4; MnFe2O4. *Gazz Chim Ital*, *60*, 389-399.

Pecharromán, C., González-Carreño, T., Iglesias, J.E. (1995). The infrared dielectric properties of maghemite, γ-Fe2O3, from reflectance measurement on pressed powders. *Physics and Chemistry of Minerals*, 22, 21-29.

Peng, H. (2019). A literature review on leaching and recovery of vanadium. *Journal of Environmental Chemical Engineering*, *7*(5), 103313.

Pourghahramani, P., & Forssberg, E. (2007). Reduction kinetics of mechanically activated hematite concentrate with hydrogen gas using nonisothermal methods. *Thermochimica acta*, *454*(2), 69-77.

Princivalle, F., Martignago, F., Nestola, F., Negro, A.D. (2012). Kinetics of cation ordering in synthetic Mg(Al, Fe3+)2O4 spinels. *European Journal of Mineralogy*, 24, 633-643.

Redhammer, G. J., Tippelt, G., Roth, G., & Amthauer, G. (2004). Structural variations in the brownmillerite series Ca2 (Fe2− x Al x) O5: Single-crystal X-ray diffraction at 25° C and high-temperature X-ray powder diffraction (25° C≤ T≤ 1000° C). *American M.*, 89(2-3), 405-420.

Rezaee, M., Khoie, S. M. M., & Liu, K. H. (2011). The role of brookite in mechanical activation of anatase-to-rutile transformation of nanocrystalline TiO 2: An XRD and Raman spectroscopy investigation. *CrystEngComm*, *13*(16), 5055-5061.

Schwartz, K. B., Leong, D. B., & McConville, R. L. (1994). Structural chemistry of synthetic cordierite: evidence for solid solutions and disordered

compositional domains in Bi-flux-grown Mg-cordierites. *Physics and Chemistry of minerals*, *20*(8), 563-574.

Shirozu, H., & Bailey, S. W. (1965). Chlorite polytypism: III. Crystal structure of an orthohexagonal iron chlorite. *American Mineralogist: Journal of Earth and Planetary Materials*, *50*(7-8), 868-885.

Sui, Y. L., Guo, Y. F., Jiang, T., & Qiu, G. Z. (2017). Reduction kinetics of oxidized vanadium titano-magnetite pellets using carbon monoxide and hydrogen. *Journal of Alloys and Compounds*, *706*, 546-553.

Tomic-Tucakovic, B., Majstorovic, D., Jelic, D., Mentus, S. (2012). Thermogravimetric study of the kinetics of Co3O4 reduction by hydrogen. *Thermochimica Acta*, 541, 15-24.

Tsirel'Son, V. G., Antipin, M. Y., Strel'Tsov, V. A., Ozerov, R. P., & Struchkov, Y. T. (1988, February). Electron density distribution and electric field gradient in hematite at 153 K determined from precision X-ray diffraction data. In *Soviet Physics Doklady* (Vol. 33, p. 89).

Vyazovkin, S., Isoconversional Kinetics, in: M.E. Brown, P.K. Gallagher (Eds.) *Handbook of Thermal Analysis and Calorimetry*, Elsevier B.V., Amsterdam, 2008, pp. 503-538.

Wang, M., Chen, B., Huang, S., Wang, X., Liu, B., Ge, Q., & Xie, S. (2017). A novel technology for vanadium and chromium recovery from V-Cr-bearing reducing slag. *Hydrometallurgy*, *171*, 116-122.

Wang, X., Gao, D., Chen, B., Meng, Y., Fu, Z., & Wang, M. (2018). A clean metallurgical process for separation and recovery of vanadium and chromium from V-Cr-bearing reducing slag. *Hydrometallurgy*, *181*, 1-6.

Wang, X., Wang, X., Shao, Y., Jin, Z., & Jin, B. (2018). Reactivity of a Chinese lean iron ore as oxygen carrier Kinetics & characterization. *Thermochimica Acta*, *670*, 114-122.

Xiang, J., Huang, Q., Lv, W., Pei, G., Lv, X., & Bai, C. (2018). Recovery of tailings from the vanadium extraction process by carbothermic reduction method: Thermodynamic, experimental and hazardous potential assessment. *J. of hazardous materials*, *357*, 128-137.

Xiao, Y., Jalkanen, H., Yang, Y., Mambote, C. R., & Boom, R. (2010). Ferrovanadium production from petroleum fly ash and BOF flue dust. *Minerals Engineering*, *23*(14), 1155-1157.

Zhang, B., Liu, C., Liu, Z., Li, Z., Jiang, M. (2019). Remediation of the vanadium slag processing residue and recovery of the valuable elements. *Process Safety and Environmental Protection*, 128, 362-371.

Zhang, Y., Zhang, T. A., Dreisinger, D., Lv, C., Lv, G., & Zhang, W. (2019). Recovery of vanadium from calcification roasted-acid leaching tailing by enhanced acid leaching. *Journal of hazardous materials*, *369*, 632-641.

Zhao, W., Chu, M., Wang, H., Liu, Z., Tang, J., & Ying, Z. (2019). Reduction behavior of vanadium-titanium magnetite carbon composite hot briquette in blast furnace process. *Powder technology*, *342*, 214-223.

Živković, Ž. D., & Šesták, J. (1998). Kinetics and mechanism of the oxidation of molybdenum sulphide. *Journal of thermal analysis and calorimetry*, *53*(1), 263-267.

Southern Journal of Research Vol. 3(1), 2023

Financial Analysis of PV-Wind Cogeneration for a Remote Village in Gwadar - Pakistan

Muhammad Muneeb Khan[1]*, Muhammad Aamir Shafi[2,4], Basit Akram[3], Muhammad Usman Tariq[1], Rana Sarmad Mahmood[1], Hafiz Abdul Muqeet[3], Bernabe Mari Soucase[4]

[1] Department of Electrical and Computer Engineering, COMSATS University Islamabad, Islamabad, Pakistan

[2] Department of Electrical Engineering, Glasgow Caledonian University, Glasgow

[3] Electrical Engineering Technology Department, Punjab Tianjin University of Technology, Lahore, Pakistan

[4] Instituto de diseño y Fabricación (IDF), Universitat Politécnica de València (UPV), Valencia, Spain

Abstract. The consumption concern and financial thought of fossil fuel assets around the world have required a basic seek for elective vitality sources to meet up the show vitality requests. Electricity has become a basic need of life for education, medical, transportation etc. In developing countries, the remote villages still have no access to electricity as it is uneconomical for utilities to provide electricity in geographically dispersed load centers. Kappar, a remote village in Gwadar city of Baluchistan province, is taken as a case study that has abundant solar and wind power potential. In this study, a hybrid power generation scheme is proposed for remote villages in Gwadar, Pakistan. A comprehensive study of the technical, economic and financial analysis including Net Present Value (NPV), Internal Rate of Return (IRR), Payback Period (PP), Debt Service Coverage Ratio (DSCR), Benefit-Cost Ratio (BCR) for a hybrid PV-Wind system of said location have been calculated using clean energy management software called RET screen Expert, developed by Natural Resource Canada (NRC). The study of this paper renders an insight to auspicious configuration of PV capacity and wind turbines accessibility needed to meet the energy demand of posit location and their mutual technical, economical, financial and environmental parameters for future decision makings and best manipulations. The annual energy generated by the proposed hybrid system is computed, and an energy economic analysis is carried out based on demand. Using the RET screen tool, the main purpose is to create a hybrid system with an appropriate Levelized Cost of Electricity (LCOE).

Keywords: RET Screen, Hybrid PV, Wind System, Cost Analysis, Financial Analysis.

Email: muneebkhan@isp.edu.pk,

1. Introduction

The development of a country is directly linked to the accessibility of power supply to every citizen from education to health facilities (Aqeel & Butt, 2001). Energy has become a basic need of the day for every citizen to be able to contribute to the development process. Pakistan is an energy deficient nation facing a severe electricity deficit of approximately 4000 MW in supply and demand. A huge amount of the population is living in the south of scattered villages which makes the grid connection even harder and economically unviable. It is also a fact that the country has the indefinite potential for renewable energy resources such as solar, wind, hydro, biomass etc. (Amer & Daim, 2011; Mirza et al., 2009). It has solar PV potential of producing 45 MW to 83MW per hundred-meter squares of area (Adnan et al.,

2012). It encompasses an average daily global range of 19 to 20 MJ per day with an annual mean sunshine duration (Potential of Renewable Energies in Pakistan). There is adequate wind energy to power every coastal village in the country. According to wind resource calculation of Pakistan developed by NREL (National Renewable Energy Laboratory) in collaboration with USAID and Alternative Energy Development Board (AEDB), Pakistan contains a potential of more than 300,000 MW of wind vitality (Potential of Renewable Energies in Pakistan).

Over the years, using RET screen toolkit different scrutinizes have been regulated to discover more about the performance of the renewable energy resources to intuit the profitability and the performance of a projected system. Among these studies, it is worth mentioning the work by MN. Romero et al. (2014), compares the prognostic potential of the wind demonstrated in RET screen with the compelling generation of wind ranches found within the locale of Ontario, Canada, to roll components influencing the quality of these forecasts and thus, to comprehend what aspects of the demonstrate may be upgraded (Romero & Rojas-Solórzano, 2014). The investigation performed by A. Mehmood et al. (2014), conducts the data of six major cities (Islamabad, Karachi Lahore, Multan, Peshawar and Quetta) of Pakistan to fulfill the energy demand domestically by modeling standalone 5kW solar photovoltaic systems on RET screen.

Technical parameters like part of solar irradiance and resultant solar fraction are also observed along with evaluating the system viability based on economic determinants like NPV, IRR, and simple payback period. Software calculations are conducted for how much electric power load reduction is possible and how much Green House Gas (GHG) emission reduction is made authentic (Mehmood, Shaikh & Waqas, 2014). Mufti et al. (2015) searches out the potential and viability of standalone 380watts (0.38kW) solar photovoltaic systems on RET screen for Six major cities (Abbottabad, Chitral, Dera Ismail Khan, Dir, Mardan, and Peshawar) of K.P.K province of Pakistan. In which cost, financial analysis is done to select the optimum location for installation of said system (Akbar, Mufti, & Khurshid, 2015).

With data from measurement stations and the use of Geographic Information System (GIS) software, Zhou et al. (2011) examined the wind resource in Juangsu, a coastal province of China, to choose viable locations for building wind turbines and determine an array of features (Zhou, Wu & Liu, 2011). The study of cost analysis and emission analysis for grid-connected solar photovoltaic systems using RET screen by D. Dwivedy et al. (2015) is also a precedent.

In this simulation, the goal is to determine how much of a decrease in energy consumption cost this hybrid system can achieve, as well as the total cost and environmental impact of the reduction in greenhouse gas emissions (Dwivedy et al., 2015). In this paper,

- Cost analysis of an anticipated hybrid PV-Wind system i.e., 230kW for a proposed location (Kappar Village near Gwadar, Baluchistan) is studied based on climatic conditions to fulfill domestic energy requirements, through RET screen tool.
- Modeled system viability is estimated by relying on technical as well as financial and economic determinants like NPV, IRR, equity payback period and simple payback period. Technical parameters like solar irradiance and wind speed availabilities are also determined.
- Software calculations also revealed how much base case electric power load reduction is possible and how much GHG emissions can be reduced leading

toward green growth hinged on the results of the RET screen.

2. Systems and Methods

2.1. Kappar Village

Kappar village, Gwadar, is a coastal village in the south of Pakistan with the coordinates 25.317342, and 62.753221. It has abundant solar and wind resource potential which is discussed in Sec. 3A. There is only one weather station available for the village which is in Gwadar city. The RET screen Expert can load the required geographical and weather parameters datasheets from NASA (National Aeronautics and Space Administration) stations.

In hybrid PV-wind multi-technology, solar irradiance and wind speed are the main parameters among climatic conditions. A tabulated form of meteorological data measured at 10m is shown in Table I. The environmental data succors the feasibility of the obligation of PV-wind hybrid system installation.

Table 1. Meteorological Data for Kappar village, Gwadar, Pakistan

Months	Average Insolation Incident on A Horizontal Surface (kWh/m^2/day)	Average Direct Normal Radiation (kWh/ m^2/day)	Average Clear Sky Insolation Incident on A Horizontal Surface (kWh/ m^2/day)	Average Daylight Hours (hours)	Average Daylight Cloud Amount (%)	Wind speed (m/s)	Average Atmospheric Pressure (kPa)	Average Surface Albedo (0 to 1.0)
January	3.92	5.62	4.44	10.7	40.4	3.5	98.7	0.13
February	4.61	5.75	5.13	11.3	40.3	4.2	98.6	0.12
March	5.22	4.49	5.95	12	47.8	3.9	98.3	0.12
April	6.1	6.05	6.54	12.7	43.6	4	97.9	0.13
May	6.4	6.03	6.53	13.3	41.2	4.7	97.5	0.13
June	6.46	5.98	6.65	13.6	43.9	4.9	97	0.15
July	5.88	5.04	6.35	13.5	53.5	4.9	97	0.16
August	5.58	4.9	6.12	13	51.3	4.6	97.2	0.16
September	5.36	5.35	5.61	12.3	39.2	4.5	97.7	0.13
October	5	6.11	5.09	11.6	26.9	3.6	98.2	0.12
November	4.19	5.91	4.38	10.9	29.1	3	98.6	0.12
December	3.59	5.24	4.01	10.6	39.4	3.5	98.8	0.12

2.2. PV-wind Hybrid Configuration

The PV-wind crossover framework is well suited where daylight and wind have regular shifts (Subrahmanyam, Sahoo & Reddy, 2012).

Fig. 1 appears the schematic chart of the proposed PV-wind half-breed vitality framework setup. The power generated by the PV modules is DC voltage, which is subsequently converted to AC via a DC-AC inverter.

Through an AC/AC cyclo-converter, the inverter's output sinks with the power provided by wind turbines. A step-up transformer, which is attached to the supply system, boosts the collected power.

In an excess of energy production during a lower demand period, the transformer can feed the excess produced power to the storage (as an option) rather than dump the load. For analyzing the system performance these components are typified individually in section 3B.

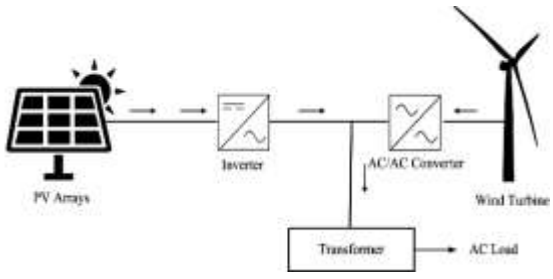

Figure 1. Schematic diagram of the hybrid power generation system

2.3. RET Screen Expert

There are various hybrid renewable energy tools available in the market for designing micro grid hybrid renewable energy systems including the famous Hybrid Optimization of Multiple Energy Resources (HOMER) energy, HYBRID2, System Advisor Model (SAM) developed by the National Renewable Energy Laboratory

(NREL) and RET screen Expert developed by NRC. These software tools are used for technical design, performance and financial modeling to facilitate decision-making for designing hybrid renewable energy systems. Among these tools, HOMER energy and RET screen Expert are the most flexible and user-friendly tools that have the capability of standardized measurements and economic calculations (Li, et al., 2022). The HOMER software programming tool is widely used by many researchers for direct optimization, emission, and economic analyses of all types of designed systems. However, the performance prediction of the designed system is a limitation (Khatib, Mohamed & Sopian, 2012). The study RET screen is preferred for this study

$$NPV = \sum_{t=1}^{T} \frac{Ct}{(1+r)^t} - C_{\square} \qquad (1)$$

because it is provided free of charge by the Canadian Government and to explore its capabilities to design renewable energy schemes for far away loading centers. RET screen Expert analysis is based on five steps; accredit for the comprehensive identification, optimization and assessment software algorithm which is capable of computing technical, economic and environmental viability of different renewable energy, energy-efficient and cogeneration projects in terms of resultant solar irradiance, NPV, IRR, payback periods, GHG emissions reduction and backup fuel savings (Thevenard, Leng & Martel, 2000; Rets, T. ICEDSC).

2.4. Cost Analysis Methodology

The key to the project (PV-wind system) under study is to evaluate the economic viability using RET screen tool

$$DSCR = \frac{Net\ Operating\ Income}{Total\ Debt\ Service} \qquad (3)$$

which has the option of an embedded products cost database. Costs associated with the proposed PV-wind system incorporate costs with feasibility analysis, development, engineering and commissioning of the power system.

2.5. Financial Analysis Methodology

One of the important benefits of using RET screen expert tool is it assists the project valuation process for decision-makers. RET screen expert simulation tool investigates the financial parameters including NPV, the interest rate

$$BCR = \frac{D_b}{D_i} \qquad (4)$$

on debt, IRR, pre-tax IRR, cumulative cash flow, DSCR, BCR etc. Simple definitions and mathematical formulas of these financial parameters are given below.

Net Present Value (NPV): The show esteem of cash inflows short the display esteem of cash outpourings is utilized to calculate the net show esteem (NPV) of expected speculation or extension (Khatib, Mohamed & Sopian, 2012). The formula for calculating NPV is calculated by using the equation (1);

C_t delineates net cash influx amid the period t, Co is added up to starting venture costs whereas *r* limns intrigued rate and *t* informs number of periods.

Internal Rate of Return (IRR): The inside rate of return (IRR) may be a metric utilized in capital arranging to decide the productivity of arranged ventures, as appears in equation (2) (Khatib, Mohamed & Sopian, 2012). Inside rate of return could be a markdown rate that makes the NPV of all cash streams from a specific venture break even with to zero.

$$IRR = \sum \left(\frac{After\ Tax\ Cash\ Flow}{(1+r)^t} \right) - Initial\ Investment \qquad (2)$$

DSCR is a measure of cash flow available to pay current debt obligations, as described in eq. (3).

BCR is a pointer, utilized in an investigation that endeavors to summarize the by and large esteem for cash of a venture or proposition. Acknowledge all ventures with a BCR more prominent than one. The modus operandi of BCR is in equation (4).

D_b depicts the discounted value of incremental benefits and D_t is discounted value of incremental costs.

$$P = \frac{1}{2} k \rho C_p A V^3 \qquad (5)$$

3. Results and Discussions

RET screen software has been developed to shape the possibility of a system in expressions of its technical parameters, economic factors and environmental control (like GHG emission reduction). The annual inflation rate of Pakistan is assumed to be 2%. RET screen conclusions are convoluted in four approaches as shown in Fig. 2.

Figure 2. The maneuver of RET screen analysis

3.1. Feasibility Analysis

Figure 3 shows the data of solar radiation kWh/m²/day VS each month of the year. The average value lies at 5.91 kWh/m²/day of each month. The maximum solar irradiance takes place during April, May, June, and July. As the power generated by a wind turbine is directly proportional to the wind speed m/s (equation below) shows mathematical inference (Rets, T. ICEDSC). A climatic data of projected location produced by RET screen is weighing up the consequences of wind speed in m/s over the year on monthly origin made known in Fig. 3. The power output of wind turbine is given as:

P is power output (kW), k is 0.000133 constant to yield power in kWs, ρ is air density (lb/ft^3), Cp is maximum power coefficient (from 0.25 to 0.45), A is rotor swept area and V is wind speed (mph).

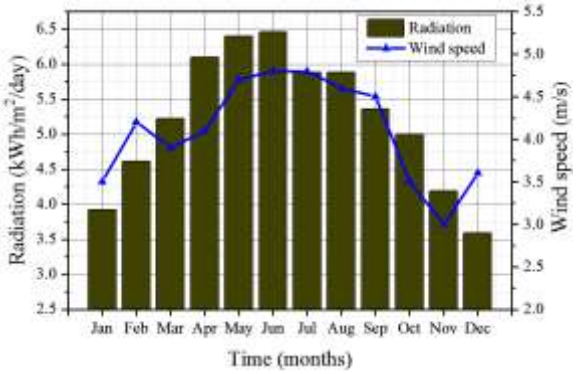

Figure 3. Solar and wind annual resources of Kappar village, Baluchistan

3.2. Technical Analysis

In monetary terms, the specialized examination could be a security examination state of mind of checking the changing in past costs with the expected of estimating future cost and volume (Brealey et al., 2012). But an engineering perspective, technical analysis cop with the restriction of equipment on which the efficiency and efficient consumption depend.

Results show that 484 units of PV (150kW) and 1 unit of wind (80kW) multi-technology are sufficient to provide more than 100% essential power capacity. Tables 2, 3, and 4 compromises the introductory technical parameters of the under-study hybrid power station for inferred capacity.

3.3. Cost Analysis

The initial cost is estimated to be CAD (Canadian dollars) 241,022. Operating and maintenance cost is predicted to be CAD 2795. Grand initial cost includes feasibility study, development, engineering, and power system costs.

Table 5 limns the database cost values in Canadian dollars which the RET screen produced against input parameters of the energy analyzer.

Costs are predicted to be in CAD with 3% contingencies. In the development contract negotiation and permit, approval is included with a per-unit cost of 800 CAD and 1000 CAD respectively. Table 6 shows the detail of the cost calculated in the feasibility study.

Table 2. Precursory Parameters of Proposed System

Base Case PV-Wind Electricity	
Parameters	***Values***
1. Power demand	Stand Alone Load
2. Contracted capacity of PV system	150kw
3. Contracted capacity of wind system	80kw
4. Contracted total capacity	230kW
Proposed Case PV module	
5. Solar PV power plant	150kW
6. Grid type	Hybrid, Stand Alone
7. PV panel type	484 units, 310 W
Proposed case Wind System	
8. Wind power plant	80kW
9. Grid type	Hybrid
10. Wind turbine (horizontal axis)	1 units, 80kW
11. Wind power plant	80kW

Table 3. Characteristics of Selected PV Module

Parameters	**Values**
PV type	Poly-Si
Module	Fixed
Manufacturer	Yingli Solar
Model	poly-Si - YL310P-35b
Capacity	310W
Maximum power (V_{mp})	36.9 V
Maximum current (I_{mp})	8.41 A
Open circuit voltage (V_{oc})	46.4
Short circuit current (I_{sc})	8.98 A
Power tolerance (%)	0~+2 %
Efficiency (%)	16%
No. of units used	484
Nominal operating temperature	- 40°C - +85°C
Frame area	1.94 m²
PV type	Poly-Si

Table 4. Characteristics of Selected Wind Turbine

Parameters	**Values**
Supplier/manufacturer	Wind Energy Solutions BV
Model	WES 18 - 40m (< 2012)
Type	Tubular
Rated power	80 kW
No. of Units	1
Hub Height	40m
Rotor Diameter	18m
Swift Area	254m²
Cut in wind speed	<3 m/sec. (6.7mph)
Cut out wind speed	25 m/sec. (56mph)
Operating temperatures	From -20°C up to +40°C
Degree of protection	IP55

Table 5. Precursory Parameters of Proposed System

Type of Cost	**Cost (CAD)**	**Relative Costs (%)**
Feasibility study	45,000	8.8
Development	40,000	7.8
Engineering	57,000	11.1
Power system		
Photovoltaic	81,022	15.81
Wind turbine	160,000	31.22
Road construction	25,000	4.87
Transmission line	25,000	4.87
Balance and miscellaneous		
Transportation	50,000	9.75
Contingencies	14,491	2.82
Interest during construction	14,925	2.91
Total cost	512,438	100%

Table 6. Feasibility Cost Analysis

Feasibility study	**Unit**	**Unit cost CAD**
Site investigation	p-d	1,600
Resource assessment	Project	15,000
Environmental assessment	p-d	800
Report preparation	p-d	800
Project management	p-d	800
Travel & accommodation	p-trip	300

3.4. Financial Analysis

In the proposed system electricity exported to grid is 437 MWh. We also suppose that the plant receives no government subsidies. Table 7 shows the important financial parameters.

Table 7. Financial Parameter Input

Input parameters	**Values**
Electricity Export rate	CAD 0.15 kW
Electricity export Escalation Rate	2%
Inflation Rate	2%
Discount rate	7%
Gross GHG reductions	73 t CO_2/yr.
Projected life	25 years

Input parameters	Values
GHG reduction cost	CAD -228/tCO_2

DSCR is 3.2 which means the income generated is enough to cover the operating expenses and payments. With a 25-year expected lifetime, the NPV of the PV facility is CAD 460,816. Similarly, if the beginning cost was reduced from CAD 310,670, the NPV would be positive.

The Net Benefit-cost ratio is projected to be 4.7 which is a positive indicator. We can conclude that the benefits would outweigh the costs. The annual life cycle savings (ALCS) represents the PV plant's annual benefit, based on net present value, project lifetime, and discount rate. The project's yearly ALCS is expected to be CAD 46,914.

$$Payback\ Period = \frac{Cost\ of\ project}{Annual\ cash\ flows} \quad (6)$$

The interest collected by the project over its lifetime is represented by the internal rate of return on return. The internal rate of return (IRR) is expected to be 38.7%. The project is financially worthwhile if the IRR exceeds the investor's necessary return on investment.

Given a positive annual income from the PV-Wind system, the simple payback period illustrates how many years it will take to recoup the initial and annual costs, as shown (6) (Devarakonda, 2019). This power plant has a payback period of 4.9 years. Table 8 tabularizes the financial cost.

Table 8. Financial indicator for Plant

Parameters	Values
NPV	CAD 460,816
BCR	4.7
ALCS	CAD 46,914
IRR	38.70%
Payback period	4.9 years

A positive number of cash flows signify that a project generated more cash beneficially. By the use of RET screen analysis, we have negative cumulative cash flows for the first 3 years then we move to positive cash flows for the next 22 years as shown in Fig. 4. which recompenses a good scheme for investment as we generated more cash than we spent.

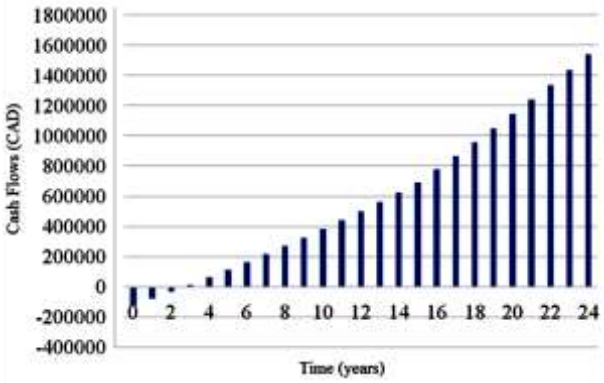

Figure 4. Cumulative Cash Flow

3.5. GHG Emissions

For GHG emission reduction required input data are the transmission and distribution (T&D) losses which are taken as 7% for a proposed location as a developing part of the country and scrutinized fuels are selected as ‘‘All fuel types’’.

GHG emission factor is assumed to be 0.472 tCO2/MWh. Fig. 5 shows the 93% GHG emission reduction possible by the proposed system.

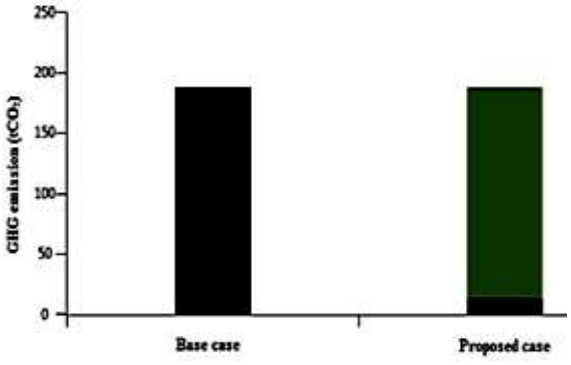

Figure 5. Gross annual GHG emission by RET screen

4. Conclusions

This proffered paper manifests the unit sizing and an economical appraising of a PV-Wind hybrid generation

system and its cost acquisition for a typical assumed location by RET Screen software.

In terms of power delivered to the load, net present value, internal rate of return, benefit to cost ratio, simple and equitable payback times, and GHG emission reduction analysis, an extravagance and utilitarian assessment of the solar system is devised.

The research provides evidence to support an appropriate configuration of PV capacity and wind turbines to suit the energy demand of the area, as well as their mutual cost analysis findings.

This study abets the Government to make certain access to modern and infallible information on the costs and execution of renewable energy resources like hybrid PV-wind systems.

Acknowledgment

The authors acknowledged the support by the European Commission under project Erasmus + (2019-1-ES01-KA107-062073), Coordinator University Polytechnic of Valencia, Spain and Grant PID2019-107137RB-C22 funded by MCIN/AEI/10.13039/501100011033 and by "ERDF A way of making Europe.

References

Adnan, S., Hayat Khan, A., Haider, S., & Mahmood, R. (2012). Solar energy potential in Pakistan. *Journal of Renewable and Sustainable Energy*, 4(3), 032701.

Akbar, T., Mufti, A. U. G. M., & Khurshid, N. (2015). Potential and viability of standalone solar PV systems for rural electrification of Pakistan by using RET screen software. *International Journal of Smart Home*, 9(8), 11-18.

Amer, M., & Daim, T. U. (2011). Selection of renewable energy technologies for a developing county: a case of Pakistan. *Energy for sustainable development*, 15(4), 420-435.

Aqeel, A., & Butt, M. S. (2001). The relationship between energy consumption and economic growth in Pakistan. *Asia-Pacific Development Journal*, 8(2), 101-110.

Brealey, R. A., Myers, S. C., Allen, F., & Mohanty, P. (2012). Principles of corporate finance. *Tata McGraw-Hill Education*.

Devarakonda, S. (2019). Calculating the Economic Viability of Corporate Trainings (Traditional & eLearning) using Benefit-Cost Ratio (BCR) and Return on Investment (ROI). *Int. J. Adv. Corp. Learn.*, 12(1), 41-57.

Dwivedy, D., Singh, S. K., Choudhury, M. K., & Pradhan, S. R. (2015). Study of cost analysis and emission analysis for grid connected PV systems using RETSCREEN 4 simulation software. *Int. J. Eng. Res. Technol*, 4, 203-207.

Khatib, T., Mohamed, A., & Sopian, K. (2012). A software tool for optimal sizing of PV systems in Malaysia. *Modelling and Simulation in Engineering*, 2012.

Kirkpatrick II, C. D., & Dahlquist, J. A. (2010). Technical analysis: the complete resource for financial market technicians. *FT press*.

Li, Y., Li, G., Li, J., Bénard, P., Chahine, R., & Xiao, J. (2022, March). Simulation and optimization of hydrogen-based hybrid renewable energy systems: Software tools and applications. *In Journal of Physics: Conference Series* (Vol. 2208, No. 1, p. 012018). IOP Publishing.

Mehmood, A., Shaikh, F. A., & Waqas, A. (2014). Modeling of the solar photovoltaic systems to fulfill

the energy demand of the domestic sector of Pakistan using RETSCREEN software. *In 2014 international conference and utility exhibition on green energy for sustainable development (ICUE) (pp. 1-7). IEEE*.

Mirza, U. K., Ahmad, N., Harijan, K., & Majeed, T. (2009). Identifying and addressing barriers to renewable energy development in Pakistan. *Renewable and Sustainable Energy Reviews*, 13(4), 927-931.

Potential of Renewable Energies in Pakistan. *https://defence.pk/pdf/threads/potential-of-renewable-energies-in- pakistan.379477/.*

Rets, T. ICEDSC Natural Resources Canada–Canmet ENERGY. *The RET Screen Clean Energy Project Analysis Software*, 4.

Romero, M. N., & Rojas-Solórzano, L. R. (2014). Assessment of the prediction capacity of a wind-electric generation model. *Int. J. Renewable Energy Biofuels*, 2014, 1-16.

Subrahmanyam, J. B. V., Sahoo, P. K., & Reddy, M. (2012). Local PV-Wind Hybrid Systems Development for Supplying Electricity to Industry. *Acta Electrotehnica*, 53(1).

Thevenard, D., Leng, G., & Martel, S. (2000). The RET Screen model for assessing potential PV projects. *In Conference Record of the Twenty-Eighth IEEE Photovoltaic Specialists Conference-2000 (Cat. No. 00CH37036) (pp. 1626-1629). IEEE*.

Zhou, Y., Wu, W. X., & Liu, G. X. (2011). Assessment of onshore wind energy resource and wind-generated electricity potential in Jiangsu, China. *Energy Procedia*, 5, 418-422.

Southern Journal of Research Vol. 3(1), 2023

A Critical Review of Market Basket Analysis on Retail Dataset using Data Mining Techniques

Mubasher H. Malik*, Hamid Ghous, Iqra Rehman

Department of Computer Science, Faculty of Engineering & Technology, Institute of Southern Punjab, Multan, 60000, Punjab, Pakistan

Abstract. The associations between different products can be interpreted using a data mining technique called Market Basket Analysis (MBA). It contributes a vital role to determine the placement of goods, and the design of business strategies for retailers to attract consumer attraction and hence improve the businesses. The relationship among items can be deduced using association rules (AR) from retail datasets. As customer demand changes rapidly and thereby increasing transactional data. So, there is a need to use deep learning (DL) methods along association rules. Therefore, a review is conducted on MBA using AR and DL methods to mine and predict customer purchase patterns from large retail data sets. The objective of the paper is to assist researchers in the implementation of AR and DL methods while conducting MBA to overcome the challenges of large and frequently changing transactional data.

Keywords: MBA; Deep Learning; Association Rules; Mining Pattern; Retail Dataset.

1. Introduction

Nowadays, the size of data is getting large in various areas like medical, banking and retail. But the whole data is not useful to find customer purchase patterns. So, it is necessary to withdraw useful patterns from an immense volume of data. This procedure of fetching important data is known as Knowledge Data Discovery (KDD). The frequent pattern mining helps the retailers to understand customer buying habits and propose new business strategies.

The data mining techniques used to find interesting patterns are an association, clustering, predictions, classification and outlier analysis (Blattberg et al., 2008). The association rules are used to find significant associations in data sets. In the following example, there are transactional data consisting of transactional ID (TID) and Items as shown in Table 1.

Table 1. Transactional data consisting of transactional ID (TID) and Items

TID	Items
1	Bread, Jam
2	Bread, Egg, Jam, Diaper
3	Bread, Jam, Diaper
4	Bread, Milk, Jam, Coke, Diaper
5	Bread, Milk, Coke, Diaper

Dataset is expanding in volume day by day due to expanding requests of clients. The conventional strategy takes more time to discover obtaining behavior due to the huge volume of items and clients. So, there require profound learning strategies for visit design mining (Grewal et al., 2017).

Example of association rules are:
{Bread} ⟶ {Jam}
Left hand side item known as antecedent and right-hand item as consequent.
Customer who buys Bread also buy jam.

{Bread, Jam} ⟶ {Diaper}
customer who buys bread and jam also buy Diaper.

2. Significance of Market Basket Analysis

MBA is a significant technique to enhance profit by monitoring consumer buying habits. The most frequently bought products can be bundled to increase sales at a reduced price. In today's competing market MBA can assist retailers to obtain a forefront benefit so four advantages of conducting an MBA are listed below (Berry & Linoff, 2004):

- Finding high-affinity products,
- To improve visual merchandising,
- Optimized assortment of items on online shop,
- To predict upcoming influencing products.

2.1. Finding high-affinity products

Finding interdependence between two purchased products is an efficient way to uplift profit. Analysis of purchasing patterns helps the retailer suggest new promotions. These promotion increases the sale of one item with another purchasing item if buying behavior is known. These associations also help to predict the new category of product for the future needs of the customer. Traditional methods are not sufficient due to the increasing volume of data and customers so this problem can be solved using market basket analysis in a well-organized way.

2.2. To improve visual merchandising

Placement of a product attracts the customer to purchase a product and increases the sale of the product. Retailers are interested to know the in-store placement of products. Store layout affects sales if most purchasing products are placed fastidiously. If most buying product is known and placed on the shelve with another product, then there are chances to increase the sale of that product. It can also be effective to know the store shelve of the new products. Conventional methods are not easy to apply here because of growing market needs. So, market basket analysis is an efficient way to optimize store and product layout.

2.3. Optimized assortment of items on online shop

The layout of products also affects sales of online stores. To know customer cart and visiting patterns helps in online store layout. An efficient product arrangement in the e-store increases sales of the product. It also helps to predict for cross-selling and upselling of products. Market basket analysis is vital to knowing the e-store layout.

2.4. To predict upcoming influencing product

Due to the growing demands of customers retailers are always interested to introduce new products so they can compete in the market with leading businesses. Finding the interest of the customer and predicting future needs is impossible with conventional methods. Market basket analysis is used to predict stockpiling and introduce new features of the product for the future.

3. Critical Structured Literature Review

3.1. MBA using Association Rules

Affiliation rules utilized to mine visit buy conduct of clients that exist in the value-based dataset (Ahmed, 2004). MBA using Apriori and FP-Growth algorithms retail dataset conducted by Chen et al. (2005), Nafari and Shahrabi (2010), Avcilar and Yakut (2014), Zulfikar et al. (2016), Abusida et al. (2019), Nur et al. (2019), Sutisnawati and Reski (2019), Adali and Balaban (2019), Kavitha and Subbaiah (2020), Liansyah and Destiana (2020), Alfiqra and Khasanah (2020), Yudhistyra et al. (2020), Fang et al. (2018), Ariestya et al. (2019), Anggraeni et al. (2019), Rizqi (2019), Mustakim et al. (2018), Hidayat et al. (2019), Hossain et al. (2019), Unvan (2021), and Choi and Yu (2008).

3.1.1. Apriori

Chen et al., (2005) mined client buy designs utilizing Apriori calculation by joining client statistic factors such as Recency, recurrence, and financial (RFM) values with an exchange dataset of food mart over time. Relatively (Nafari & Shahrabi, 2010) worked on shelf arrangement of products for supermarkets located in Iran. The novel work is considering price effects in a shelf arrangement. The experiment shows that Using Apriori-TdMl 102, 329, and 1579 frequent item sets found for categories, subcategories and products respectively at a minimum support of 0.1 and confidence of 0.1. Cross-selling profit for frequently buying products is shown for 6 products. The shelf space is allocated for high cross-selling products at lift 2.75. For future work use Deep learning methods to predict the shelf arrangement of products using a large transactions dataset. While, (Avcilar & Yakut, 2014) worked on the real transactional dataset of the store to mine patterns between in-category and cross-product categories. The experimental results show that the 8 best rules were extracted using Apriori at a minimum support of 0.05% and confidence of 50%. For future work extracting time base association rules and predicting customer Demographic information using deep learning methods. So also, (Zulfikar et al., 2016) connected advertise bushel investigation to discover visit things utilizing Apriori Calculation at eight clusters of XMART retail company in Indonesia. To review critically graphical visualization, add more value to comprehend statistics inefficient way. So, to explore support and confidence in comprehending the way use of a scatter plot is required. Graph-based visualization of association rules is required to explore frequent item sets. Data mining tool to implement Apriori is not mentioned. The performance of the applied algorithm concerning time and memory is not plotted. The persuasive work of the author is an implementation of CRISP-DM to conduct research. A real dataset is used to find frequent patterns.

Comparatively, (Abusida & Gültepe, 2019) planned a trading technique for arranging and buying datasets of power companies applying apriori calculation. The affiliation rules produced at tall certainty esteem of 100% appearing visit request save parts. Furthermore, (Nur et al., 2019) mined frequent item sets for Fonzu Premium restaurant using the apriori algorithm and built-in system. At confidence 100% If a customer ordered Gyoza Saikoro Yakimeshi and then would order Chicken Teriyaki Don. Results are then verified using built-in systems. Simulation of association rules is shown comprehensively. Graph-based visualization of association rules is not shown properly. Plotting of support and confidence is required to visualize stats using a scatter plot. Likewise, (Sutisnawati & Reski, 2019) applied the apriori algorithm to transactional data of XYZ Restaurants to find purchasing patterns of customers. At confidence 65% 2 pairs of products Nasi-Bakso Ikan purchased frequently. Simulation of applied apriori algorithm is shown comprehensively. A data mining system is designed to analyze data efficiently. To review critically interface of the designed system is not attractive. A visualization interface is required for association rules, support and confidence using graph base and scatter plot. While, (Adalı & Balaban, 2019) developed a dynamic model to mine frequent patterns of X-firm in the electricity sector. A dynamic model can be used to generate rules during any year with dynamic values of support and confidence. The dynamic model is developed using the Apriori algorithm. A Scatter plot of rules is used to examine frequent items. A business strategy for X-Firm is proposed on the obtained results. The interface of the model can be used without any technical knowledge to make business decisions on a dataset in the future. To review critically dynamic model

with other ARM algorithms can be implemented for better analysis of customer buying behavior.

Kavitha & Subbaiah, (2020) implemented an apriori algorithm on the grocery's dataset to mine frequent item sets. Association rules are generated using a rules package in R. Graph-based visualization of association rules is displayed using the rules viz package. The most buying products are yogurt and butter at the support of 0.007 and confidence of 0.6. The research scope is limited because a built-in dataset is used to mine frequent item sets. On the other hand, (Liansyah & Destiana, 2020) worked on the sales dataset of Lotteria Cibubur restaurant to suggest a business strategy. A data mining application Tanagra 1.4 is used to generate association rules using the apriori algorithm. The most buying products are Hot/Ice coffee and float at minimum support 16% and confidence 100%. In the Data visualization phase graph base visualization is not shown of association rules. A large dataset is required to check the reliability of the apriori algorithm. Comparatively (Alfiqra & Khasanah, 2020) developed business strategy for Supermarket X in Yogyakarta.

Using Apriori association rules are generated for each transaction in four periods. The customer purchasing behavior is fluctuating in every period so OCVR implemented to mine frequent rules. Visualization of frequent itemset and association rules using scatter plots and graph-based visualization is required. At 1%<OCVR<30% generated 17 rules are used for bundling and planogram of frequently buying products. While (Yudhistyra et al., 2020) implemented Apriori and CARMA on Big data to design the business strategy of the metal trading company in Indonesia. A standard process CRISP-DM is followed to conduct research. The web graph method is used to visualize association rules. Results are mentioned with the value of confidence and support with frequently generated rules. To review critically there is a need to develop a flexible real-time model so in the future a new business strategy can be designed using the new model in different periods. Similarly, (Rachmatika & Harefa, 2020) analyzed a small sales transaction dataset using the Apriori algorithm to propose a business strategy. To review critically standard process not followed, visualization of itemset and association rule not shown, to conclude results business strategy not defined properly. Similarly, (Fang et al, 2018) proposed dynamic product bundling using Association rules and clustering algorithms. The novel work is dynamic product bundling to save time and energy for customers. The result shows that at a minimum support of 0.1 and confidence of 0.01 three rules were generated using Apriori to find necessary products for bundling. Four clusters of Customers using K-means identified on values of R, F and M to recommend product bundles. The summary table of MBA implementing Apriori is shown in Table 2.

Table 2. Summary Table of MBA using Apriori algorithm

Author Year	MBA using AR	Preprocessing	Dataset	Result	Improvement	Good
Chen et al. (2005)	Association rules with apriori algorithm	Data transformation , integration and segmentation	Transaction data of food Mart including customer, product and transaction database	At minimum support and confidence of 20% generated 111 and 78 rules for first and second periods respectively	Visualizations of results Use of large real transactional dataset	developed an online system to mine customer patterns at different time
Safari and Shahrabi (2010	Association rules using Apriori- TdMl	Not mentioned	Retail dataset of supermarket in Iran of four months with 1241 products 7305 sales transaction.	Using Apriori-TdMl 102, 329, and 1579 frequent item sets were found for categories, subcategories and products respectively at	Deep learning models to predict shelf arrangement of products. Use of large transactions dataset.	Product shelf arrangement considering the price, product cross-category purchase and temporal effects.

				a minimum support of 0.1 and confidence of 0.1. Cross-selling profit effect for frequently buying products. At lift 2.75 shelf space is allocated for high-selling products		
Avcilar and Yakut (2014)	Apriori Algorithm	Calculated Descriptive statistics of data with Mean, Median, Mode, Maximum & Minimum values. Sales & frequency of products	Sales transaction dataset of the store in Turkey with 9.000 products of 35 categories and 42.390 transaction records from 01.01.2012 and 31.12.2012	At minimum support of 0,05% and confidence 50% extracted 8 best rules	Time base mining of association rules. Predicting customer Demographic information using deep learning methods.	Web graphic view to show association among products Association rules defined clearly
Zulfikar et al. (2016)	Apriori Algorithm	Combining different products on Frequency	XMART Retail in Indonesia 25 products 145.548 record	Generated frequent 10 rules at a minimum support of 12% and confidence of 60% for 8 clusters of stores	Considering sale's day and hour effects on sales	Followed standard process CRISP-DM. Worked on Real Dataset
Abusida et al. (2019)	Apriori Algorithm	Data selection, Data splitting, Data filtering, and Data Transformation to ARFF format.	General electricity company of Libya (GECOL) Dataset properties order number	At confidence 100% 10 best rules are generated for each site	Data visualization of association rules Scatter plot for confidence and support values	Simulation of results
Nur et al. (2019)	Apriori Algorithm	Binarization	Sales transaction data of Fonzu Premium restaurant of month June 2018	With manual calculation at confidence 100% Chicken Teriyaki Don and Gyoza Saikoro Yakimeshi With built-in system calculation at confidence 100% Chicken Teriyaki Don and Gyoza Saikoro Yakimeshi	Considering Seasonal and holidays effects on sales of food	Results are mentioned Simulation of association rules shown Defined research methodology clearly
Sutisnawati and Reski (2019)	Apriori Algorithm	Removed unnecessary Attributes Date, Price, Amount, Total, Location.	XYZ dataset with 157 transactions and 32 items with smallest frequency 2 and largest frequency 68	At minimum confidence, 65% and support 23% 2 pairs are often purchased	Considering Seasonal and holidays effects on sales of food Use of large transaction dataset	Comprehensive Simulation of Results Dynamic analysis of association rules using the developed application
Adali and Balaban (2019)	Apriori Algorithms	missing values, Outlier Analysis, Duplicated Observations, Binarization	Dataset1 from January 2014 to December 2014 with 19 attributes 177393 transaction Dataset2 (2015) with 23 attributes183401 transaction	At support of 0.1% and leverage 185.0291 products, HESNYA-03 & HESNYA-02 in different color packages can be used for promotions	More than one dynamic model can be added by applying different algorithms	Followed CRISP-DM methodology Dynamic model for rules independent of time and region Association rules can be downloaded for analysis
Kavitha and Subbaiah (2020)	Association rules with matrix incidence	Data Cleaning, Data Aggregating, Deleted duplicate data for each transaction	Surabaya restaurant sales with 15087 records from March 23 to June 30, 2018, and September 23 to October 16, 2018 May 17 until June 16, 2018	At minimum support and confidence of 4% and 15% 10 rules	Use of Dimension reduction or feature selection method on a dataset	Data visualization using Power BI Business strategy discussed briefly Research method and flow defined clearly Results mentioned properly Dashboard for making business strategies in the different period

						Data analysis using matrix incidence Considering transaction day week, month and food type on customer purchase
Liansyah and Destiana (2020)	Association rules using apriori	Not mentioned	Dataset from period 2 February 2019	At minimum support, 15% extracted 12 best association rules	Dataset not mentioned with dimensions Considering Seasonal effects on purchase of clothes	Results are not mentioned briefly with Support and confidence
Alfiqra and Khasanah (2020	Apriori Algorithm	Not mentioned	Groceries Dataset 9835 transactions and 169 items.	At support of 0.007, the confidence of 0.6 butter and yogurt most frequent item	Limited Research scope	Visualization of association rules Use of scatter plot to show support, confidence and lift values
Yudhistyra et al. (2020)	Apriori, CARMA	Measuring central tendency, removing null tuples, sorting hashing, Exploring Aggregating and visualizing the relationship. Dataset transformed to 80 variables	3,986,872 observations from 248,856 customers	Apriori: At minimum support of 1% and confidence of 50% 21 rules CARMA: At minimum support of 1% and confidence of 50% 5 rules	A flexible model for development of new model to propose business strategy in different period	Web graph visualization of item sets with weak, medium and strong link Worked on real dataset performance plot of two algorithms
Fang et al. (2018)	Apriori algorithm	Data cleaning, Data reduction, Data integration	Supermarket X dataset of 57784 transactions in a month including 41248 items	At 1%<OCVR<30% generated 17 rules	Scatter plotting of confidence and support. Graphical visualization of association rules	Followed standard research methodology Results mentioned Proposed Business strategy
Ariestya et al. (2019)	Association rule using Apriori Algorithm, K-means clustering finds customer segment using RFM values	Integration data from four database customer, Transaction, products and products classed. Z-score normalization	Electronic Sales Transaction dataset with10281 customers, 251396 records, 1560 products and 110 product categories.	At minimum support 0.1 and confidence 0.01 three rules were generated using Apriori to find necessary products for bundling. 4 clusters of Customers using K-means identified on values of RFM.	Proposing price bundling method by using customer attribute and demands.	Dynamic product bundling to save both time and energy of customer

3.1.2. FP-Growth

While (Ariestya et al., 2019) mined frequent patterns to propose marketing schemes for small grocery stores. ARM, FP-Growth and Apriori algorithms are implemented on a dataset of 602 transactions. To review critically dataset is not mentioned with proper dimensions and source. Performance comparison of applied algorithms not shown. Results are mentioned with support and confidence clearly to propose a new marketing strategy. Anggraeni et al., (2019) worked on a sales dataset of an electronic company in Indonesia. FP-Growth and Apriori implemented using Weka to find frequent item sets for sale promotions. The final results are shown using the Apriori algorithm with support and confidence. The best rules generated by FP- Growth are not mentioned in the results section. Visualization of rules, support and confidence using scatter plot and graph base visualizations are not used. Comparatively (Rizqi, 2019) worked on the product bundling strategy of Retail Z in Indonesia. The research methodology is defined

briefly. Dataset of 5 departments with 58 products is used to mine frequent items using FP-Growth. Association rules with confidence, support and lift are mentioned properly. Results are mentioned clearly to bundle products for Retail Z. To review critically Visualization of support, confidence and association rules are required using scatter and graph-based plotting.

A study (Mustakim et al., 2018) observed the most interesting pattern of Berka Mart applying Apriori and FP growth. To review critically Comparison of both algorithms in terms of memory should be plotted to examine performance. To critically analyze values of support and confidence scatter plotting is essential. Graph-based representation of association rules enhanced the understanding of frequent item sets in the finding of patterns. So, graph-based visualization of association rules is required to implement. A comparison of the two algorithms shows FP takes less time in the generation of the rule than Apriori. FP growth scans the database two times to generate frequent items. A standard method is followed and shown pictorially to find patterns. Findings are mentioned with the most frequent rule at specific support and confidence.

Hidayat et al., (2019) describe the application and evaluation analysis of the Apriori and FP-growth algorithm for the Market Basket analysis of brilliant shop. Regarding this article, the authors do not mention which methodology was used for data understanding and pre-processing and also do not describe which tool was used for the results. Authors directly put results in tables rather than showing them in diagrams or graphs and in the results of both algorithms processing time is not mentioned because authors in this research show that the Apriori algorithm takes time enough its scan the database many times but in FP-growth algorithm, it just takes less time and only scan database two times to generate frequent item set. Maliha et al., (2019) in this study used market basket analysis with Association rules and two algorithms respectively Apriori and FP-growth. Researchers used two datasets obtained from Kaggle website 1: French Retail Store 2: transaction of bakery items processed this data by using python tool. In the end, FP- growth and Apriori algorithm comparison regarding time shows in good form. But still needs some improvement on this to improve the accuracy of the algorithm and need to apply it to different transaction datasets to determine the percentage for product reduction. (€Unvan, 2020) in this research doing market basket analysis with Association rules and applying two algorithms Apriori and FP-growth. The researcher used the sales data of any supermarket received from the Vancouver Island University website and processed this data by using Weka tool and finding patterns. In this article results not shown in table forms or graphics need to be shown. The summary table of MBA using FP-Growth is shown in Table 3.

Table 3. Summary table of MBA using FP-Growth

Author Year	MBA using AR	Preprocessing	Dataset	Result	Improvement	Good
Anggraeni et al. (2019)	FP-Growth, Apriori Algorithms	Data cleaning from 620 to 577 data, Data integration, Data selection, Data Transformation	Dataset of 620 items	FP-Growth: At minimum support of 45% and confidence 60% 5 rules Apriori: At minimum support 45% and confidence 60% 3 rules	Dataset with proper dimensions Performance plot of two algorithms Use of the large dataset	Followed standard Research Methodology Results mentioned with support and confidence
Rizqi (2019)	Apriori, FP-Growth Algorithms	Not mentioned	Electronic Sales data from January 2016 to December 2016 116 transactions	Using Apriori at a minimum support of 9% and confidence of 40% 10 best rules	Association rules with FP-growth not mentioned properly Performance plot of two algorithms	Use of the real dataset

			containing 14 items		Visualization of association rules Use of the large dataset	
Mustakim et al. (2018)	FP-Growth	Data cleaning, recapitulating data, removing duplicate data, checking inconsistent data, Data Transformation, cleaning of noise and missing data	Retail Z dataset of 5 Departments with 58 transactions	At minimum support of 30% and 60% generated 6 rules.	Scatter plotting of confidence and support. Graphical visualization of association rules Use of Large dataset Considering price attribute for product bundling	Problem statement mentioned Results with support and confidence Research methodology defined Worked on the real dataset Proposed business strategy on mined frequent patterns
Hidayat et al. (2019)	FP Growth, Apriori	Not mentioned	Berkah Mart Dataset 8,307 items 400 transactions at a day in 2017 October, November, December	Apriori: Frequent itemset found at support 13.02 and confidence 48.37. FP Growth: Frequent item set found at support 13.11 and confidence 48.42	Use of scatter plot for graphical visualization of support and confidence. Graphical visualization of Association rules. Pruning of dataset. Comparison of the algorithm in terms of memory	Comparison of two applied techniques in terms of memory and speed. Use of real dataset. Frequent patterns were mentioned with support and confidence in the result. Standard process followed to mine patterns
Hossain et al. (2019)	FP Growth, Apriori	Not mentioned	sales transaction data of cosmetics in Brilliant Store during November 2018	support value of 8.8% and 30% confidence value, with a filtering time of 0.036 seconds	This research does not show data exploration and does not explain which tool is used to mine the dataset	A good thing in this article is authors used the original dataset to find frequent item sets and patterns.
Unvan (2021)	FP Growth, Apriori	Not mentioned	Two datasets obtained from Kaggle 1: French Retail Store 2: transaction of bakery items	Minimum support=1% and Minimum confidence =50%,	Need to apply to different transaction datasets to determine the percentage of product reduction	FP-growth and Apriori algorithm comparison regarding time shows good form
Choi and Yu (2008)	FP Growth, Apriori	Not mentioned	The sales data of any supermarket is received from the Vancouver Island University website.	21.06 Conviction and 1 (100%) confidence values	Results not shown in table forms or graphics	Good thing authors well describe the association

3.2. MBA using Deep Learning

Deep learning utilized to mine visit buy conduct of clients that covered up in retail dataset (Ahmed, 2004). Market basket analysis using NN and LSTM algorithms on retail dataset conducted by:

3.2.1. Neural Networks

Whereas (Choi & Yu,2008) proposed deals estimating show for mold retail utilizing Developmental Neural Arrange (ENN). The proposed approach outflanks SARIMA show when variances of season impact mold retail. Future attributes of product size and color can be considered to forecast sales more accurately. Essentially, (Chen et al, 2010) proposed determining deals demonstrate utilizing Standard day and occasion moving normal strategy and back engendering neural arrange. The test performed on deals dataset of new nourishment deals at store appears that BPNN outflanks with less MSE and tall accuracy. For future work deals estimating can be done by taking into number the impact of occasions, summer excursions, modern years and autonomy day. So also, (Wang et al, 2016) proposed a multi errand multi-course forecast show for the general store Retail dataset in China. The novel work is the forecast of multi errand and multi-course statistic properties of the client on buying conduct. The pack of thing representation is utilized to discover the visit itemset. The proposed demonstrate Organized Neural Implanting (SNE) performs best utilizing normal amassing pooling work

with tall Exactness 0.371, Audit 0.289, F1 0.324 Hamming Misfortune 0.411 and for energetic clients with tall Exactness 0.361, Survey 0.299, F1 0.327 Hamming Misfortune 0.410 and dynamic clients with tall Accuracy 0.361, Review 0.299, F1 0.327 Hamming Loss 0.410. For future work Testing Model efficiency using more datasets with large transactions considering Seasonal and time stamp effects on purchase of items, integrating association rules to find frequent itemset with Deep learning methods. Using deep neural architecture than shallow and Prediction of more demographic attributes to measure the efficiency of the proposed model. Comparatively (Salehinejad & Rahnamayan, 2016) predicted customer shopping patterns utilizing Repetitive Neural Arrange. The novel work is desire of Recency, Repeat and Cash related (RFM) values utilizing RNN to anticipate client shopping plans. The auto- encoding procedure is utilized to remove highlights of input variables Client ID, R, F and M. The proposed illustrate RNN-ReLU outflanks than LSTM-RNN and SRNN to predict RFM values with 80%. Future work can be conducted to use location and age variables for feature extraction. The next item recommendation system can be proposed using predicted RFM values.

Likewise, (Massaro et al, 2018) worked on Walmart's 45 stores sales dataset to predict sales using an Artificial Neural Network (ANN). The preprocessing step is performed using different Operators in Rapidminer. The Profound learning with ANN beats as best deals anticipating calculation with Relationship 73% / 97,4%, Normal Outright Blunder 2000 +/- 1250 and Relative Normal Blunder 12,9% +/- 9,9% than other strategies Slope Boosted Trees, SVM, KNN, Choice Trees and Irregular Woodland. To review critically the following improvement required proposing a Hybrid model using Association Rules and Deep learning to predict sales, use of other deep learning methods LSTM and CNN, and use of dimension reduction algorithm. The persuasive work of the author is the use of a real sales dataset and graphical performance plot comparison of deep learning with other strategies Angle Boosted Trees, SVM, KNN, Choice Trees, and Irregular Woodland. (Lismont et al, 2018) proposed demonstrate to foresee fewer buying items utilizing Client- Item organize as preprocessing strategy. The half-breed Irregular Timberland predicts fewer buying items with tall AUC than neural organize.

Kim et al, (2002) proposed deals forecast show utilizing hereditary based classification of neural systems on deals dataset. The Integration comes almost from three neural frameworks NN1, NN2, and NN3 into a single GA-based procedure that shows up to figure target thing purchase with a classification rate of 76.5% and a botch rate of 13.5. For future work, classification can be extended to abstract and rank levels. So too, (Pale et al, 2015) proposed a novel neural organize approach NN-Rec to foresee the following bushel proposal of two Honest to goodness Retail datasets Tafeng and Beirne. The proposed framework contains three layers embedding, hidden, and output layers. The user id and items id’s transformed into the matrix to form a feature vector. The feature vector feed into the embedding layer. The hidden layer transforms h1 to h2 using the activation function. The SoftMax operator is applied at the output layer to predict the probability of the next purchased item. This demonstrates captures long conditions and input layer more adaptable to include other highlights than previous methods. Experiment for Beiren dataset appears precision is underneath 0.1 when wicker container k= 2 and for Tafeng dataset precision is underneath 0.06 when wicker container k=2 using NN-Rec novel neural network approach. Likewise, (Yu et al, 2016) proposed a novel show named Energetic Repetitive Wicker Container Show (DREAM), based on RNN.

The novel work is thought of dynamic user's interest and global intuition of all wicker containers of the client over time. The Max and Avg pooling operation are performed on items in the basket to get basket representation. These basket representations feed as input into the input layer. Energetic representations of the client get in the covered layer. The yield layer appears with scores of clients for all items. The result appears nonlinear operation max-pooling outflanks than Avg pooling strategy since it measures the intuitively relationship of wicker container things. Gangurde et al., (2017) a proposed a novel predictive model for MBA by using data cleaning and a neural network approach. To find frequent item sets for seasonal dataset MBA algorithm takes more time and repeated scans of the database. So, this may be accomplished by changing the weights through backpropagation. This strategy makes a difference minimize the time and taken a toll of performing as often as possible MBA on an expansive database. A handmade dataset was used to simulate the proposed method. Valid four combinations are generated using a threshold of 0 and 1 in the handmade dataset. The proposed framework is implemented on the transaction dataset of online shopping. Analysis of proposed framework with other MBA methods evaluated using metrics of precision, recall and accuracy. Results from the online shopping dataset achieved an accuracy of 0.90. To review critically the source of the dataset and data visualization not mentioned. While (Li et al, 2018) designed an engine to combine current and past transactions to dynamically predict preference for the next item for making real-time business strategies. The obtaining data of clients extricated utilizing Individual Acquiring Inclination Design (PPPP). The Repetitive Neural Arrange (RNN) is connected to the extraction data of PPPP to discover another obtaining thing of the client. Top 100 orders taken as input for each customer. For training data, 97 orders and the remaining 3 orders are considered as testing data. The result shows that PPPP achieves 18.29% higher Individual Prediction Accuracy than Baseline (Apriori). To review critically simulation of the proposed method and prediction results are not shown using RNN on the transactional dataset. The persuasive work of the author is to propose an engine for making real-time business strategies using RNN. The performance of PPPP is shown with metrics.

Comparatively, (Wang et al,2018) proposed an attention-based proposition appear utilizing a neural organize approach. The novelty of work is recommending novel items other than rigid order assumptions using attention base recommendations. ATEM comprises three layers input layer, the thing implanting layer, the Consideration Layer, the setting inserting layer, and the yield layer. The execution of ATEM was assessed utilizing two genuine deals value-based datasets of Insights IJCAI-15 and Ta-Fang. The ATEM performs at REC@10 0.3542, REC@50 0.5134, and MRR 0.2041 on the IJCAI-15 dataset. The ATEM performs at REC@10 0.1089, REC@50 0.2016, and MRR 0.0347. Whereas (Yu et al, 2016) proposed a novel demonstration named Energetic Repetitive Bushel Show (DREAM), based on Repetitive Neural Arrange (RNN). The novel work is thought of energetic user's intrigued and worldwide intuitive of all bushel of the client over the time. The Max and Avg pooling operation are performed on things in the bushel to induce bushel representation. These basket representations feed as input into the input layer.

Energetic representations of the client are gotten within the covered-up layer. On the other hand, (Sreenivasa & Nirmala, 2019) proposed half breed appear to mine client buying conduct on a retail dataset of the T-Mall online shopping store. The novel work is considering zone base information of the client and utilizes lively brief- and

long-term consider of the client. To achieve brief-term purposeful move networks are utilized from past exchanges of clients. The hybrid model is designed using RNN and FNN to attain the short- and long-term behavior of customers. The proposed model outperforms other hybrid models with HR 0.08547365 and MRR 0.12935566. In future work, the model can be evaluated using the Amazon dataset with high HR, and MRR values and considering the time-centric information of the customer.

Comparatively, (Lee et al, 2020) proposed a multi-period proposal show utilizing RNN. The system is assessed by different periods since the client obtains conduct changes over time but the conventional proposal demonstrates assessed as it were once. An experiment was performed on a Real dataset of a Fresh Food delivery company with 7716 customers and 10 shopping carts. The result shows that LSTM based recommendation model outperforms the collaborative filtering-based model with an accuracy of 21% high at T and 10% high at T+4. To review critically the use of diverse transactional datasets and propose a hybrid model using CF and RNN-based recommendation models required as improvement in current work.

Changchien et al. (2001) proposed an online suggestion system for electronic stores utilizing clustering and running the appear extraction module. The SOM neural arrange-based plan utilized to find 9 clusters from O-ID, Buyer, Recipient, Item table, and 99 affiliation rules are extricated at least certainty 0.25. For future work proposed approach can be applied to sales and product datasets considering Seasonal effects. The summary table of MBA applying NN is depicted in Table 4.

Table 4. Summary table of MBA using NN

Author Year	MBA using AR	Preprocessing	Dataset	Result	Improvement	Good
Chen et al. (2010)	Evolutionary Neural Network	Not mentioned	Sales data for two fashion products T-shirts and Jeans from 2002 to 2003	ENN outperforms SARIMA when seasonal trend fluctuates in fashion retail	Taking into count the attribute of products color and size	An experiment performed on the real dataset
Wang et al. (2016)	Back Propagation Neural Networks (BPNN) And Logistic Regression (LR)	Not mentioned	35 days of fresh food sales at Hi-Life convenience stores. Fresh foods herein are comprised of four kinds of sandwiches, three kinds of hand-made rolls, two kinds of rice balls, sushi.	The BPNN outperforms with smaller MSE and high precision to forecast sale	Demand forecasting takes into count the holidays, summer vacation, new year and Independence Day	Plotting Sale predictions applying BPNN
Salehinejad and Rahnamayan (2016)	Structured Neural Embedding (SNE)	Filtered dataset with the user who has five demographic attributes. Extracted transaction history of users and removed the items bought less than five times	BeiRen retail dataset of supermarkets in China from 2012 to 2013 with 49, 290, 149 transactions, 220, 828 items and 1, 206, 379 users.	The proposed illustrates SNE performs best utilizing ordinary storing up pooling work with tall Precision 0.350, Audit 0.281, F1 0.312 and Hamming Misfortune 0.431 for Torpid clients. For medium clients with tall Accuracy 0.371, Audit 0.289, F1 0.324 and Hamming Misfortune 0.411. For energetic clients with tall Exactness 0.361, Review 0.299, F1 0.327 and Hamming Hardship 0.410.	Using deep neural architecture than shallow to predict demographic attributes from purchase history. Prediction of more demographic attributes to measure the efficiency of the proposed model Integrating Association rules to find frequent itemset with the deep learning method.	Correlation between demographic attributes. Incorporating Multi-task and multi-class prediction problems. Turning Multiple prediction tasks into a single structured prediction task.
Massaro et al. (2018)	Recurrent Neural Network (RNN)	Splitting the dataset into 50% training,	Ta-Feng grocery shop transaction sales dataset with 817,741	The ReLU-RNN predicts R, F and M values by 80% more	Conducting Experiment on Large Training	Customer behavior

		25% validation and 25% testing.	transactions 32,266 users and 23,812 items.	than LSTM-RNN and SRNN.	dataset. Using location and age variables for feature extraction. Proposing a recommendation system using predicted RFM	prediction using RFM values.
Lismont et al. (2018)	Artificial Neural Network (ANN)	Using "Join" operator to make single dataset, Nominal to Binominal conversion, Split data into training and testing	Walmart 45 store sales forecasting dataset 140000 sales records for each store features.csv scores.csv train.csv test.csv	Profound learning with ANN outperforms as best sales predicting calculation with Correlation 73% / 97,4%, Normal Absolute Error 2000 +/- 1250 and Relative Normal Mistake 12,9% +/- 9,9% than other methods Gradient Boosted Trees, SVM, k-NN, Decision Trees and Random Woodland	Hybrid model to predict sales using AR and Deep Learning. Use of Dimension reduction algorithm on dataset. Applying LSTM OR CNN to predict sales with more high correlation and less absolute and relative Errors.	Worked on Real sales dataset. Comparison of Deep Learning with other methods. Graphical performance comparison plot of applied method ANN with other algorithms Gradient Boosted Trees, SVM, k-NN, Decision Trees and Random Forest.
Kim et al. (2002)	Customer product network for extracting features, predicting less sold product using classification method Random Forest, Decision tree, Logistic regression, Neural network	Customer-Product network used to extract feature of product and customer	European Grocery shop transactional dataset with 6355 products, 406,678 customers ,100 million transactions during the period of 12 months	Random forest outperforms with average values of AUC using local features 0.6616, Network features 0.6902 and Hybrid features 0.6989. The hybrid Random Timberland predicts fewer buying items with high AUC esteem.	Considering long period effects on customer buying behavior and seasonal effects on product purchase. Conducting current research on online dataset of retail. In local feature considering price and promotion other than RFM values.	First customer product network-based study on offline retail dataset.
Wan et al. (2015)	Genetic based classification of neural networks	Not mentioned	Sales dataset of EC company in Korea. Data set consists of 10 demographic features, 5 transactional feature during one year.	Integration of comes about from three neural networks NN1, NN2, and NN3 into Single GA-based method show expectation of target product buy with classification rate 76.5% and error rate 13.5	Applying rank and abstract level classifiers	Experiment performed on two datasets
Salehinejad and Rahnamayan (2016)	Dynamic Recurrent basket Model (DREAM), based on Recurrent Neural Network (RNN)	Dataset preprocessed for each item purchased by at least k users. For Ta-Feng k=10 and For T-mall k=3	Ta-Feng: 817,741transactions belonging to 32,266 users and 23,812 items. T-mall: 4,298 transactions of 884 users and 9,531 brands	Using Avg-Pooling: For Ta-Feng dataset with dimensions {50, 100, 150} f1-Score 0.061 NDCG 0.082, f1-score 0.064 NDCG 0.081, f1-score 0.067 NDCG 0.083 respectively. For T-mall dataset with dimensions {10, 15, 20} f1-Score 0.058 NDCG 0.141, f1-score 0.063 NDCG 0.154, f1-	Heterogeneity of Basket Recommendation Problem. Effects of season and time on datasets.	Use of linear and nonlinear pooling methods for basket representation Performance plot of applied methods with metrics on two datasets

				score 0.066 NDCG 0.160 respectively. **Using Max Pooling:** For Ta-Feng dataset with dimensions {50, 100, 150} f1-Score 0.065 NDCG 0.084, f1-score 0.068 NDCG 0.085, f1-score 0.070 NDCG 0.086 respectively. For T-mall dataset with dimensions {10, 15, 20} f1-Score 0.070 NDCG 0.162 , f1-score 0.071 NDCG 0.168, f1-score 0.073 NDCG 0.173, respectively		
Massaro et al. (2018)	Market basket Analysis with Feed forward Neural network	Data cleaning using the proposed EHC leaner algorithm	Handmade 4 inputs Biscuit, Cold drinks, Tea and Fast food	4 Valid combinations for rainy phase is (1,3,4), (1,3), (1,4) and (3,4)	Source of dataset not mentioned Visualization of data is missing using graph base and scatter plot	Performance plot of FFNN with MBA algorithm Simulation on Transactional dataset
Yu et al. (2016)	Market Basket Analysis using Recurrent Neural Network with Long Short Term Memory	Splitting transactional data into purchase history and shopping cart data	InstaCart Online Grocery Shopping Dataset1 in 2017 206,209 Customer's transaction history including 3,421,083 orders categorizes 49,685 products into 21 departments and 134 aisles	RNN based Personal Purchasing Preference Pattern achieves 18.29% higher Individual Prediction Accuracy than Baseline	Simulation of proposed method using transactional dataset Visualization of data Prediction results of The next item not shown	Performance metrics of proposed method. Real-time marketing strategies using Proposed model
Sreeniasa and Nirmala (2019)	Attention-based neural network	Removed Transactions that contains only one item	Two Real-world transaction dataset IJCAI-15 and Ta-Fang **IJCAI-15:** #Transactions144,936, #Items27,863, Avg. Transaction Length2.91, #Training Transactions 141,840, #Training Instances 412,679, #Testing Transactions 3,096, #Testing Instances 9,030 **Ta-Fang:** #Transactions 19,538, #Items 5,263, Avg. Transaction Length 7.41, #Training Transactions 18,840, #Training Instances 141,768, #Testing Transactions 698, #Testing Instances 3,150	For IJCAI-15Attention Based Transaction Embedding Model performs at REC@10 0.3542, REC@50 0.5134, MRR 0.2041. For Ta-Fang Attention Based Transaction Embedding Model performs at REC@10 0.1089, REC@50 0.2016 , MRR 0.0347.	Proposing Hybrid model using Attention-based mechanism With RNN and CNN	Dataset mentioned with proper dimensions Worked on Recommending novel item other than rigid order assumption using attention mechanism
Lee et al. (2020)	Sequential Hierarchical Attention Network (SHAN)	Items observed by less than 10 users are removed from dataset	T-Mall #user 20,648 #Item 25,129 avg. session length 2.73 #Train session 71,892 #Test session 3,534 Gowalla #user 15,171 #Item 13,193 avg. session length 2.97 #train session 129,225 #Test session 3,635	SHAN performs best on Gowalla dataset with AUC 0.987, Recall 0.439. On the T-Mall dataset SHAN performs best with high AUC 0.801 and SHAN-S	Capturing Feature in long and short term intentions Worked on large datasets	Combining user dynamic long and short term intentions. Hierarchical attention network to capture long and short term intentions.

				performs best with high Recall 0.156 on T-Mall.		Capture high level complex interactions between item-item and user-item factors.
Changchein and Lu (2001)	Multitask Long Short-Term memory-based model	Splitting attributes into four bins morning, afternoon, night, and dawn time splitting data into 90% for training and 10% for testing	InstaCart online grocery shopping cart sales transaction data from 2017 with 3,421,083 millions of orders	LSTM predicted single transaction Embedding of next day purchase accuracy 44%, next hour 56%, and next purchase category 82%. Predicted multiple transactions embedding for the next day 30%, next purchase 57% and purchase category 81% Predicted pre-trained embedding for next day 32%, next hour 62%, and purchase category 82%	An experiment conducted on multi-context embedding using additional dimensions as location, customer age and gender. Use of large dataset to evaluate embedding strategies.	Guide to preprocess customer multi-intention behavior using embedding strategies for customer multi-intent embedding. Multitask LSTM model to learn embedding of multitasking
Changchein and Lu (2001)	Recurrent Neural Network (RNN)	Not mentioned	Real dataset of Fresh Food delivery company with 7716 customers and 10 shopping carts	The LSTM-based recommendation model outperforms the collaborative filtering-based model with an accuracy of 21% high at T and 10% high at T+4.	Use of diverse transactional dataset Proposing hybrid model using CF and RNN based recommendation model	Multi-period product recommender Results mentioned clearly Use of real dataset with proper dimensions
Auon et al. (2015)	Clustering module using neural networks, Self-organization map and rule extraction module using rough set theory	Creating fact table, from database for mining, selecting dimensions and attributes, filtering data with noise and handling missing values Data transformation, normalization	Electronic store dataset for online marketing	using SOM find 9 clusters from O-ID, Buyer, Receiver and product. 99 association rules extracted at minimum confidence 0.25	Applying proposed approach on sales and product dataset considering seasonal effects	Use of the hybrid approach for online recommendation Dimension reduction of dataset

3.2.2. LSTM

Auon et al., (2015) proposed an expectation demonstrate extricating worldly and total highlights utilizing LSTM and QR individually. The novel work is the integration of LSTM and QR models into a Blend of Specialists (ME) to classify rehashed and non-repeated clients.

The tests on the exchange dataset of 9 markets appear that a Blend of Specialists (ME) performs best with less MSE as compared to person Quantile Relapse and LSTM models to classify rehashed and non-repeated clients for 9 markets. For future work, the large dataset can be used to measure the efficiency of the proposed model and use association rules to mine frequently and non-frequently products.

Wang et al., (2016) proposed Multi-Task Representation Learning Demonstrate (MTRLM) to foresee users' statistic properties. The novel work is extricating highlights automatically rather than manually and learning from shared representations. The experiment on a retail dataset of supermarkets shows that MTRL

predicts client statistic characteristics from buy history with a tall weighted F1 degree for the medium gather of clients Sex 0.645, Conjugal status 0.802, Instruction Foundation 0.647. For future work Prediction of more demographic attributes to measure the efficiency of the proposed model and use of association rules to find more frequent item sets than the Bag of items method.

Comparatively (Sakar et al, 2019) proposed a cross breed demonstrate utilizing Multilayer Perceptron Organize (MLP) and RNN-LSTM to anticipate the acquiring behavior of clients. The primary module anticipated client deliberates to visit online shops utilizing MLP.

The novel work is utilized filter-based include choice strategies. The MLP beats than base classifiers at a Precision of 87.24, F1-score 0.86, True-positive rate of 0.84 and True-negative rate of 0.92. In the second module, LSTM-RNN estimated visitors' intention to leave the site without a transaction.

Chen & Li, (2019) proposed Consideration Base Repetitive Neural Arrange to suggest a thing for repurchase. The oddity of work is presenting a self-attention component instead of a highlight building base suggestion show. The other recognizing figure is the utilize of LSTM to mine the intermittent buy conduct of clients. The Result appears that AttRNN beats LSTM at a certainty level of 0.2 with an F1 score of 0.4723.

While (Cirqueira et al, 2019) predicted single, multiple, and pre-trained embedding of next day, hour, and purchase category using the LSTM model on InstaCart shopping store. The novel work is a guide to preprocess multi-intent customers using neural network embedding strategies. The result shows that LSTM anticipated single exchange implanting of following day buy exactness at 44%, another hour at 56%, and another buy category at 82%. The LSTM Anticipated numerous exchanges implanting of another day 30%, Following buy 57% and buy category 81%.

The LSTM Anticipated Pre-trained inserting of the following day 32%, following hour 62% and buy category 82%. Long-term work is conducting a Test on Multi setting inserting utilizing extra measurements such as area, client age and sex. The precision of LSTM can be moved forward employing an expansive dataset to assess inserting procedures. The summary table of MBA using LSTM is illustrated in Table 5.

Table 5. Summary Table of MBA using LSTM

Author Year	MBA using AR	Preprocessing	Dataset	Result	Improvement	Good
Wang et al. (2016)	Classification of temporal features using Long Short-Term Memory (LSTM) Classification of aggregate features using Quantile Regression (QR)	Customer-based feature, product-based feature. customer product-based feature extraction	Transaction dataset obtained from Kaggle Acquire Valued Shoppers Challenge with 1-year transaction history of shoppers including 9 markets and 38k customers.	A blend of Specialists (ME) performs best with less MSE as compared to person Quantile Relapse and LSTM strategies to classify rehashed and non-repeated clients for 9 markets.	Use of association rules to mine frequently and non-frequently buying customers Use of a large dataset to measure the efficiency of the proposed model	Integration of deep learning and machine learning methods.
Sakar et al. (2019)	Multi-Task Representation Learning Model (MTRLM) using Feed forward Neural networks	Filtered dataset with items bought by less than 10 times.	BeiRen retail transaction dataset of Chinese supermarkets from 2012 to 2013 with 64097 items, and 80540 users.	MTRL predicts client statistic characteristics from buy history with a tall weighted F1 degree for a medium bunch of clients Sex 0.645, Conjugal status 0.802, Education Background 0.647.	Prediction of more demographic attributes to measure the efficiency of the proposed model. Use of association rules to find frequent item sets than Bag of items representations	Multitask Representation Learning model is based on automatically extracting features than manually defining features

Chen and Li (2019	Multilayer perceptron (MLP), Long Short Term Recurrent Neural Network (LSTM)	Oversampling and feature selection	Online Retail data consisting of 185,000 Web pages visited in 9800 sessions of 3500 visitors.	In the first module, MLP performs best than SVM and Random Forest to predictpurchasing intention of the visitor at an Accuracy of 87.24, F1-score 0.86, positive rate 0.84 and True-negative rate0.92. second module LSTM-RNN estimated visitor intention to leave site without a transaction.	Integrating recommendation system on user or item based.	Real-time customer behavior analysis using a hybrid model.
Cirqueira et al. (2019)	Attention Recurrent Neural Network (AttRNN) Long Short-Term Memory	Not mentioned	InstaCart Dataset with 10,000 shopping records of users, an average of 4 to 100 shopping baskets per user.	attend performs better than LSTM with an F1-score of 0.4723 at a confidence level of 0.2	Hybrid model to mine periodic purchase rules Attention-based mechanism with CNN	Periodic purchase rule Use of self-Attention mechanism
Bai et al. (2019)	Long short-term (LSTM) to predict next recommendation	In Tafeng and BeiRen datasets removed the product bought less than 15 times.	Ta-Feng transaction dataset from December 2000 to 2017 with 7,044 items 1,951 users total 90,986 purchase records. Average purchase record of users 50 average purchase time 14. BeiRen online shopping dataset from April 2013 to July 2013 with 211,519 purchase records 3,264 users and 5,818 items. Purchase record 65. Amazon product from January 1st, 2014 to June 30th, 2014. 6,092 items 1,443 users with 15,811 purchase record average products reviewed by 11.	LSDM performance metrics are On Ta-Feng dataset Hit@5 0.1194, Hit@10 0.1281, NDCG@5 0.0824, NDCG@10 0.0890. On BeiRen dataset Hit@5 0.2187, Hit@10 0.2290, NDCG@5 0.1617, NDCG@10 0.1646. Amazon dataset Hit@5 0.0182, Hit@10 0.0265, NDCG@5 0.0119, NDCG@10 0.0147.	Incorporating attributes of the item as price and category. Detecting best time scale from dataset automatically.	incorporated user's demand towards products over a specific time/ Experiment performed on three real datasets. Considering multiple time scales for long demands using hierarchical neural structure. Use of attention mechanism to capture user's intentions.

5. Conclusions & Future Work

The application of information mining strategies in showcase wicker container investigation is a rising slant in retail. This paper distinguished articles related to advertise wicker container examination in retail distributed between 2000 to 2020. It points to provide an organized survey of showcase wicker container examination in retail utilizing affiliation rules and profound learning strategies.

The restrictions recognized as the require for measurement decrease strategies on the retail dataset utilizing affiliation rules, utilize of consideration, and implanting layers in profound learning strategies on retail datasets to realize more exact comes about. Within the future, more inquire about work is required to create a half breed system due to the developing retail dataset at quick speed and as often as possible changing client buying propensities.

References

Abusida, A. M., & Gültepe, Y. (2019). An Association Prediction Model: GECOL as a Case Study. *Int. Journal of Info. Technology and Computer Science*, 11(10), 34-39.

Ahmed, S. R. (2004) 'Applications of Data Mining in E-Business and Finance', *Proceedings of Int. Con. on Info. Technology: Coding and Computing* (ITCC'04), p. 157.

Alfiqra, & Khasanah, A. U. (2020). Implementation of Market Basket Analysis based on Overall Variability of Association Rule (OCVR) on Product Marketing Strategy. *IOP Conf. Materials Science and Engineering*, 722(1).

Anggraeni, S., Iha, M. A., Erawati, W., & Khairunnas, S. (2019). Analysis of Sales by Using Apriori and FP- Growth at PT. Panca Putra Solusindo. *Riset Dan E-Jurnal Manajemen Informatika Komputer* Volume 3, Number 2, April 2019, 3(2), 41–47.

Ariestya, W. W., Supriyatin, W., & Astuti, I. (2019). Marketing Strategy for the Determination of Staple Consumer Products Using Fp-Growth and Apriori Algorithm. *Jurnal Ilmiah Ekonomi Bisnis*, 24(3), 225–235.

Auon, G. A., Kazmi, H., Malhotra, P., Vig, L., Agarwal, P., & Shroff, G. (2015). Deep Temporal Features to Predict Repeat Buyers. *NIPS 2015 Workshop: Machine Learning for ECommerce*, February 2016.

Avcilar, M. Y., & Yakut, E. (2014). Association Rules in Data Mining: An Application on a Clothing and Accessory Specialty Store. *Canadian Social Science*, 10(3), 75–83.

Bai, T., Du, P., Zhao, W. X., Wen, J. R., & Nie, J. Y. (2019). A long-short demands-aware model for next-item recommendation.

Berry, M.J.A., Linoff, Gordon. S. (2004) Data Mining Techniques: for Marketing, Sales and Customer Relationship Management (second edition), *Hungry Minds Inc*.

Blattberg R.C., Kim BD., Neslin S.A. (2008) Market Basket Analysis. In: Database Marketing. *International Series in Quantitative Marketing, vol 18. Springer*, New York, NY.

Changchien, S., & Lu, T. C. (2001). Mining association rules procedure to support on-line recommendation by customers and products fragmentation. *Expert Systems with Applications*, 20(4), 325–335.

Changchien, S., & Lu, T. C. (2001). Mining association rules procedure to support on-line recommendation by customers and products fragmentation. *Expert Systems with Applications*, 20(4), 325–335.

Chen, C., Lee, W., Kuo, H., Chen, C., & Chen, K. (2010). Expert Systems with Applications The study of a forecasting sales model for fresh food. *Expert Systems with Applications*, 37(12), 7696–7702.

Chen, M. C., Chiu, A. L., & Chang, H. H. (2005). Mining changes in customer behavior in retail marketing. *Expert Systems with Applications*, 28(4), 773–781.

Chen, P., & Li, J. (2019). A recurrent model with self-attention for product repurchase recommendation. *ACM International Conference Proceeding Series*, 10, 199–203.

Choi, T., & Yu, Y. (2008). Fashion retail forecasting by evolutionary neural networks, 114, 615–630.

Cirqueira, D., Helfert, M., & Bezbradica, M. (2019). Towards Preprocessing Guidelines for Neural Network Embedding of Customer Behavior in Digital Retail. *ACM International Conference Proceeding Series*.

Fang, Y., Xiao, X., Wang, X., & Lan, H. (2018). Customized bundle recommendation by association rules of product categories for online supermarkets.

Proceedings - 2018 IEEE 3rd International Conference on Data Science in Cyberspace, DSC 2018, 472–475.

Grewal, D., Motyka, S., & Levy, M. (2018). The evolution and future of retailing and retailing education. *Journal of Marketing Education*, 40(1), 85-93.

Hidayat, A. A., Rahman, A., Wangi, R. M., Abidin, R. J., Fuadi, R. S., & Budiawan, W. (2019). Implementation and comparison analysis of apriori and fp-growth algorithm performance to determine market basket analysis in Breiliant shop. *Journal of Physics: Conference Series*, 1402(7).

Hossain, M., Sattar, A. S., & Paul, M. K. (2019, December). Market basket analysis using apriori and FP growth algorithm. *In 2019 22nd International Conference on Computer and Information Technology (ICCIT)* (pp. 1-6). IEEE.

Karahan Adalı, G., & Balaban, M. E. (2019). A Dynamic Application of Market Basket Analysis with R and Shiny in The Electric Materials Sector. *Bilişim Teknolojileri Dergisi*, April, 93–102.

Kavitha, M. & Subbaiah, D. S. (2020). Association Rule Mining using Apriori Algorithm for Extracting Product Sales Patterns in Groceries. *International Journal of Engineering Research and Technology (IJERT)*, 8(3), 5–8.

Kim, E., Kim, W., & Lee, Y. (2002). Combination of multiple classifiers for the customer's purchase behavior prediction. 34, 167–175.

Lee, H. I., Choi, I. Y., Moon, H. S., & Kim, J. K. (2020). A multi-period product recommender system in online food market based on recurrent neural networks. *Sustainability (Switzerland)*, 12(3).

Liansyah, O., & Destiana, H. (2020). The Use of Apriori Algorithm in the Formation of Association Rule Lotteria Cibubur. *SinkrOn*, 4(2), 76.

Lismont, J., Ram, S., Vanthienen, J., Lemahieu, W., & Baesens, B. (2018). Predicting interpurchase time in a retail environment using customer-product networks: An empirical study and evaluation. *Expert Systems with Applications*, 104, 22-32.

Massaro, A., Maritati, V., & Galiano, A. (2018). Data Mining Model Performance of Sales Predictive Algorithms Based on Rapidminer Workflows. *Int. Journal of Computer Science an Information Technology*, 10(3), 39-56.

Massaro, A., Maritati, V., & Galiano, A. (2018). Data Mining Model Performance of Sales Predictive Algorithms Based on Rapidminer Workflows. *Int. Journal of Computer Science and Information Technology*, 10(3), 39-56.

Mustakim, Herianda, D. M., Ilham, A., Daeng Gs, A., Laumal, F. E., Kurniasih, N., Iskandar, A., Manulangga, G., Indra Iswara, I. B. A., & Rahim, R. (2018). MB Analysis Using Apriori and FP-Growth for Analysis Consumer Expenditure Patterns at Berkah Mart in Pekanbaru Riau. *Journal of Physics: Conference Series*, 1114(1).

Nafari, M., & Shahrabi, J. (2010). A temporal data mining approach for shelf-space allocation with consideration of product price. *Expert Systems with Applications*, 37(6), 4066–4072.

Nur, Y., Triayudi, A., & Diana, I. (2019). Implementation of Data Mining to Predict Food

Sales Rate Method using Apriori. *International Journal of Computer Applications*, 178(35), 22–28.

Rizqi, Z. U. (2019). Implementation of association rule-market basket analysis in determining product bundling strategy: Case study of retail businesses in Indonesia. *Proceedings of the International Conference on Industrial Engineering and Operations Management*, 153.

Sakar, C. O., Polat, S. O., Katircioglu, M., & Kastro, Y. (2019). Real-time prediction of online shoppers' purchasing intention using multilayer perceptron and LSTM recurrent neural networks. *Neural Computing and Applications*, 31(10), 6893–6908.

Salehinejad, H., & Rahnamayan, S. (2016). Customer shopping pattern prediction: A recurrent neural network approach. *2016 IEEE Symposium Series on Computational Intelligence*, SSCI 2016.

Salehinejad, H., & Rahnamayan, S. (2016). Customer shopping pattern prediction: A recurrent neural network approach. *2016 EE Symposium Series on Computational Intelligence*, SSCI2016.

Sreenivasa, B. R., & Nirmala, C. R. (2019). Hybrid location-centric e-Commerce recommendation model using dynamic behavioral traits of customer. *Iran Journal of Computer Science*, 2(3), 179–188.

Sutisnawati, Y., & Reski, M. (2019). Looking for Transaction Data Pattern Using Apriori Algorithm with Association Rule Method. *IOP Conference Series: Materials Science and Engineering*, 662(2).

Ünvan, Y.A (.2021). Market basket analysis with association rules. Communications in Statistics-Theory and Methods, 50(7), pp.1615-1628.

Wan, S., Lan, Y., Wang, P., Guo, J., Xu, J., & Cheng, X. (2015). Next basket recommendation with neural networks. *CEUR Workshop Proceedings*, 1441(2), 1–2.

Wang, P., B, J. G., Lan, Y., Xu, J., & Cheng, X. (2016). Multi-task Representation Learning for Demographic Prediction. 88-99.

Wang, P., B, J. G., Lan, Y., Xu, J., & Cheng, X. (2016). Multi-task Representation Learning for Demographic Prediction. 88–99.

Yu, F., Liu, Q., Wu, S., Wang, L., & Tan, T. (2016). A dynamic recurrent model for next basket recommendation. SIGIR 2016. *Proceedings of the 39th Int. ACM SIGIR Conference on R&D in Information Retrieval*, 729– 732.

Yudhistyra, W. I., Risal, E.M., Raungratanaamporn, I., & Ratanavaraha, V. (2020). Using Big Data Analytics for Decision Making: Analyzing Customer Behavior using Association Rule Mining Metal Trading Comp. Indonesia. *International Journal on Data Science*, 1(2), 57–71.

Zulfikar, W. B., Wahana, A., Uriawan, W., & Lukman, N. (2016). Implementation of association rules with apriori algorithm for increasing the quality of promotion. *Proceedings of 2016 4th International Conference on Cyber and IT Service Management*, CITSM 2016, 4–8.

Southern Journal of Research Vol. 3(1), 2023

Computed Optical Analysis of an Antimicrobial Sulfanilamide Drug

Abrar Ul Hassan and Sajjad Hussain Sumrra*

Department of Chemistry, University of Gujrat, 50700 Gujrat, Pakistan

Abstract. We are reporting the theoretical studies on Sulfanilamide (SA) which is an important antibacterial drug. The molecular geometry was optimized at its lowest quantum mechanical energy using Density Functional Theory (DFT) at the B3LYP level with the 6-311+G (d, p) basis sets. The first principle examination of electronic characteristics, molecule electrostatic abilities, and quantum chemical identities has been studied. The UV-Vis analysis was carried out using the CAM-B3LYP/6-311+G (d,p) function and Time Dependent Density Functional Theory (TD-DFT). The natural bond orbital show that the maximum stabilization energy went up to 19.34kJ/mol, therefore was accountable for the molecule's added stability. The negative (red and yellow) zones on MEP have been linked to the possibility of electrophilic engagement, whereas the positive (blue) regions had been linked to the possibility of nucleophilic addition.

Keywords: Sulfanilamide, Density Functional Theory, UV-Vis, TD-DFT and MEP,

Email: sajjadchemist@uog.edu.pk,

1. Introduction

Sulfanilamide is an antibacterial organic Sulphur compound with a structure comparable to p-amino benzoic acid (PABA) (Sharaby, Amine and Hamed, 2017). Sulfanilamide competes with PABA for the bacterial enzyme dihydropteroate synthase, preventing PABA from being incorporated into dihydrofolic acid, the direct precursor of folic acid (Alaghaz *et al.*, 2014). This inhibits bacterial folic acid production as well as de novo purine and pyrimidine synthesis, ultimately leading in cell growth arrest and cell death (Thiede *et al.*, 2016). It is a sulfonamide with a 4-position sulfonyl functional group linked to aniline. It is an EC 4.2.1.1 (carbonic anhydrase) inhibitor, antibacterial agent, and drug allergen (Sumrra *et al.*, 2020). It is also a sulfonamide antibiotic, with a modified aniline, and a sulfonamide (Buldurun *et al.*, 2020). Following topical application or administration as a vaginal cream or suppository, a limited quantity of sulfanilamide is absorbed (through the vaginal mucosa). Like other sulfonamides, it is metabolized via acetylation and eliminated in the urine. It is also associated with antimicrobial resistance and is potentially hazardous to aquatic creatures (Hassan and Sumrra, 2021). It has also been found primarily in surface water (Johnson *et al.*, 1998). As a result, finding sensitive techniques for determining (**SA**) is crucial. Mass spectrometry, gas chromatography, fluorescence polarization immune assays, high performance liquid chromatography, and electrochemical procedures are examples of traditional detection methods. These procedures, however, are typically time-consuming, difficult, and costly (Fig 1).

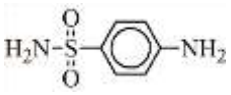

Fig 1: Chemical structure of Sulfanilamide

QSAR investigations are used to anticipate endpoints of interest in organic compounds that function as medicines (Sumrra *et al.*, 2020). The composition and structure of molecules can influence several physiological processes (Adam *et al.*, 2021). QSAR analysis employs molecular descriptors, which are numerical representations of molecular structures. In

the literature, semi-empirical approaches such as AM1 and PM3 have mostly been employed to calculate the quantum mechanical molecule descriptors used in QSAR research. However, recent QSAR investigations have demonstrated that using DFT instead of AM1 or PM3 leads in a greater correlation across computed and experimental findings. By combining the semi-empirical approaches, the DFT technique is projected to produce a statistically more accurate model.

The DFT approach has seen considerable application in recent years for estimating molecular characteristics of somewhat big compounds (Komjáti *et al.*, 2016). DFT can determine molecular parameters like optimal shape and energy with the same precision as electron-correlated ab initio approaches like MP2, but it takes significantly less computing time. The selection of the basis set and technique for calculating molecular characteristics is a significant undertaking that varies depending on the kind of molecules of interest.

The current original study goal is to develop a technique for investigating the molecular characteristics of sulfonamide (SA) compounds.

2. Computational methodology

Lee, Yang, and Parr employed Becke's three-parameter hybrid (B3LYP) exchange as also as a semi linkage functional to perform the various theoretical estimates (Lee, Yang and Parr, 1988). We had employed some functions in addition to the B3LYP function to get the required findings across the density functional theory experiments (Sumrra *et al.*, 2022). Without the presence of single-crystal information, the (SA) was configured at their ground state (S°) energy levels to get insight onto their geometric forms (Hassan and Guleryuz, 2021). More exact values for Frontier Molecular Orbitals (FMO) and Natural Bond Orbitals (NBO) studies have been achieved by doing single-point studies with a rather robust basis set of 6–31+G* (d,p) (Sumrra, Zafar, *et al.*, 2021).

The Gaussian 9 program was used to do these computations (Frisch *et al.*, 2013). To perceive the optimized structure, theoretical FT-IR and UV–Vis spectra, and descriptions of geometric forms such as bond angles and related length, *Chemcraft* (V 1.6) and *Gaussview* (V 5.0.9), along with *Gaussum* (V 3.0.2), were developed. The HOMO/LUMO energy band gap was used to investigate the global reactivity characteristics (Noreen and Sumrra, 2021).

3. Results and discussion

3.1. Optimized molecular structure

The SA geometry was optimized using the DFT/B3LYP scheme 6–31+G (d, p) sets. The vibrational frequency of molecule in the gaseous state was calculated using a B3LYP approach with a 6-31+G(d, p) basis set in the FT-IR spectrum with no negative values (Hassan *et al.*, 2021). DFT-optimized bond lengths were found to be 1.40–1.41, all through the phenyl (C–C) ring, with bond angles ranging from 119.9° to 120.6°. Based on the optimized geometric morphologies of the assessed sulfonamide molecule (**SA**), the S=O and S–N bond ranges were determined to be, 1.51–1.52, and 1.69–1.71, respectively, and their dihedral angles were determined to be 105–126°, respectively (Sumrra *et al.*, 2018)(Fig 2).

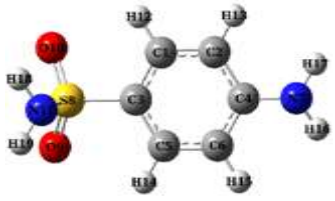

Fig 2: Optimized structure of SA at B3LYP/6-31 G+(d,p) level

Because the SA contained two nitrogen atoms in the molecular plane, their bonding was established at same length as its structure. Its stiffness influenced its consistency, leading the bond angles to deviate from 90°. The electron density contribution by active centers was also anticipated to lessen the conventional charge (Jacob *et al.*, 2020).

The vibration frequency of the title molecule in the gas phase was calculated using a B3LYP technique with a 6-31+G(d, p) basis set. In the FT-IR spectrum, the specified vibrational band values lacked any negative value. The phenyl system resembled the C-H vibrations of organic heterocyclic units and their derivatives. This comprises of several weak bands in the 3100-3000 cm-1 region, which correspond to the twisting C-H vibrations (Fig 3).

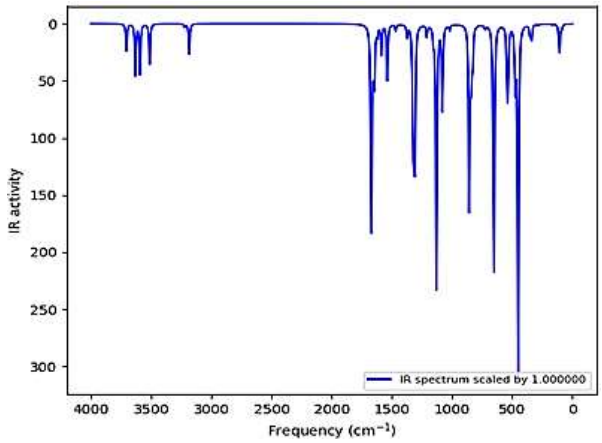

Fig 3: Computed FT-IR spectra of SA

3.2. Molecular orbitals

One of the primary goals of computational chemistry is to approximate the responsiveness of chemical entities, and much research has been done in this regard (Mahmoud *et al.*, 2019). The density functional theory (DFT) has been significant in establishing a theoretical foundation for the agreement of qualitative chemical terminology. FMOs and their quantum chemical features are being utilized to explain various sorts of processes and find the most responsive regions via conjugated arrangements. The calculations showed the charge dispersal to be mostly over HOMOs is frequently resolute by N and S containing lone pairs, as well as the phenyl moietiety. In contrast, the LUMOs vitality had the charge which was thoroughly dispersed over the phenyl moiety with an anti-bonding worth (Fig 4). The FMO mechanism, which can also be seen in the electronic transition, has confirmed intramolecular electrostatic interactions. Various quantum chemistry reactivity classifiers have been anticipated and used to study physicochemical characteristics and site specificity (Kutty *et al.*, 2020).

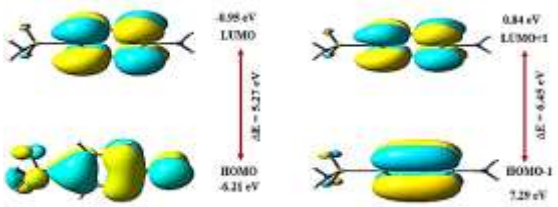

Fig 4: FMOs analysis of SA at B3LYP/6-31G+(d,p) level

The greater energy level of E_{HOMO} denotes how easy it can be to transfer an electron to an empty orbital, although the low quantity of E_{LUMO} indicates the low liability to accept electrons (Hassan *et al.*, 2020), showing that it might accept electrons easily (Table 1).

Table 1: Global reactivity parameters of SA

Parameter (eV)	Value
Ionization potential (*IP*)	6.25
Electron Affinity (*EA*)	0.94
Electronegativity (χ)	3.60
Potential (μ)	-3.60
Hardness (η)	2.66
Softness (σ)	0.19
Electrophilicity index (ω)	2.43

Chemical potential, μ, is really a propensity for electrons to leave out of a structural system; a minus chemical potential indicates that the solid is difficult to be and would not spontaneously breakdown into its constituents. SA had a value (-0.181eV) in the range

that justifies their robust existence and capacity to withstand small external environment. *Hardness* measures a molecule's resistance to changes in electron distribution. The link between hardness and electronic structure is the same. The aromaticity of a range of non-substituted aromatics can be connected to general toughness (both absolute and relative), therefore "molecules should be as robust as feasible." Substances with such low E_{HOMO} values often have vulnerable exciton capacities, implying that (SA) had a superior electron-donating ability. As a result, they can contribute to their improved antioxidant as well as biological features. Antioxidant chemicals donate an electron to a free radical, causing it to form a radical charge.

3.4. Natural bond orbitals

This approach is a good tool for investigating hyper-conjugative involvement and electron transference by lone pairs present any chemical implications. The DFT/B3LYP/6-31G(d, p) method was used to assess the natural bond orbitals (Sajjad H Sumrra *et al.*, 2021), and a detailed description of the information acquired from the second order petulances analysis for this theory was estimated (Glendening, Landis and Weinhold, 2012). This is a powerful tool for analyzing charge transitions or conjugation in diverse parts of the molecule structure with higher accuracy. The quantity of stabilizing energy is related to the frequency of the hyper conjugative interaction between electron transfers.

Similarly, stronger interactions involving lone pairs (LP) were observed in another aromatic ring that exhibits substantial electron delocalization across the molecule. The same sort of binding energy, equivalent to molecular resonance, would be an electron transition with enormous stabilization energies (Sumrra, *et al.*, 2021). Significantly, the molecule's stabilization energy was around 81.03 kJ/mol, demonstrating the stability of the electron molecular system (Table 2).

Table 2: NBO analysis of title molecule SA

Donor (i)	Ty-pe	Acce-ptor (j)	Ty-pe	E(2) [kcal /mol]	E(J) E(i) (a.u)	F (I,j) (a.u)
C1-C2	π	1-C3	π^*	3.13	1.28	0.056
C1-C3	π	C1-C2	π^*	2.39	1.31	0.050
C1-C3	π	C1-C3	π^*	0.54	0.28	0.011
C1-H12	π	C1-C2	π^*	0.91	1.10	0.028
C2-C4	π	C1-C2	π^*	2.47	1.31	0.051
5-C6	π	C1-C3	π^*	15.04	0.28	0.059
S8-O9	π	C1-C3	π^*	1.28	1.56	0.040
S8-O10	π	C3-C5	π^*	1.39	1.56	0.042
S8-N11	π	2C1-C3	π^*	0.60	0.82	0.022
O9	LP	C3-S8	π^*	1.01	0.97	0.029
O10	LP	C3-S8	π^*	0.97	0.97	0.029
N11	LP	C3-S8	π^*	3.80	0.58	0.043
C1-C3	π	C5-C6	π^*	293.35	0.01	0.080
C3-S8	π	C1-C2	π^*	1.05	0.38	0.056
S8-O9	π	C1-C3	π^*	0.78	0.25	0.042
S8-O10	π	C1-C3	π^*	0.70	0.25	0.040
S8-N11	π	C3-S8	π^*	12.98	0.02	0.034

3.5. UV-Vis analysis

The UV-Visible (UV-Vis) interpretation was estimated using optimized designs, leveraging the CAM-B3LYP attribute as part of a TD-DFT simulation, at the same 6-31G(d,p)++ assumption.

The hypothetical UV-Vis spectra show the absorption spectrum, excitation energies, and oscillator strengths, with H→L (55%) as a major transformation (Table 3).

Table 3: Computed electronic analysis of SA				
No.	E (cm^{-1})	λ (nm)	O.S	Major contribs
1	37787	264	0.02	H→L+1 (50%)
2	40234	248	0.13	H→L (55%)
3	41072	243	0.19	H→L+2 (47%)

The calculated wavelength (max) was seen in the 264, 248, and 243 nm regions.

The first band was orientated to π* and n* transitions, with minor involvement from * and dd transitions (Fig 5). The second and third bands were attributed to π→π* shifts, separately.

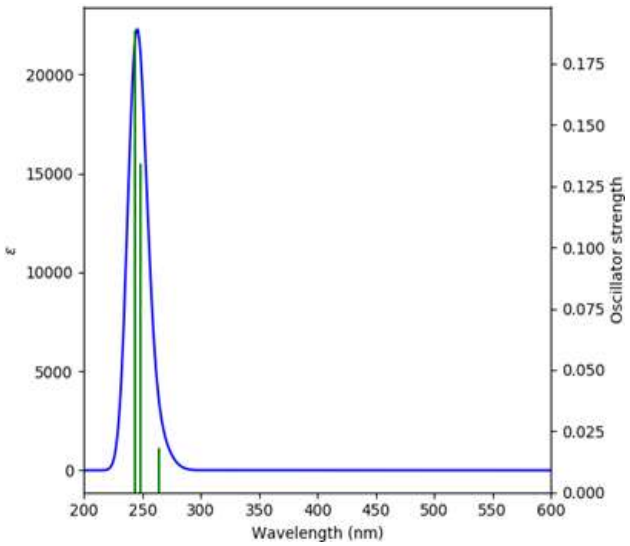

Fig 5: Computed UV-Visible spectra of (SA)

3.6. Electron density

The electrostatic molecular potential (MEP) is related to charge density and provides a very useful indication for electron donating target sites and nucleophilic engagements with hydrogen bonds (Sumrra *et al.*, 2021). The surfaces have also been used to characterize reactive behavior, with negative domains referred to as potential electrophilic spots and positive sectors referred to as nucleophilic centers (Fig 6).

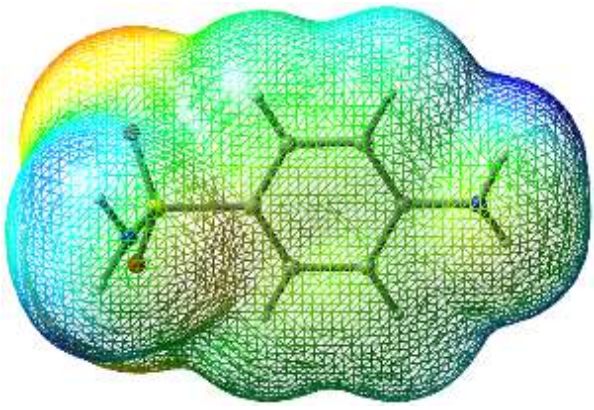

Fig 6: MEP plot of (SA)

During the current investigation, the electron donating sites had negative (red) regions and the electrophilic sites had positive (blue) portions over through the molecule (Kusmariya *et al.*, 2016). The negative charge density positions in (**SA**) were found on the title portion of sulfonamide Skelton. Positive charge was found in the confined vicinity of hydrogen atoms.

The current study discovered that nitrogen atoms had the most reactive impact. According to FMOs, this molecule has lower hardness and higher softness values. These results suggest that the chemical may be bioactive.

4. Conclusions

The current report reveals that the optimized bond lengths and bond angles agree well with the published X-ray and current DFT results.

The molecular chemical reactivity identifiers, electrostatic potentials, frontier molecular orbital analysis, one electrochemical response process, energy gap with electron transfer competence of this title molecule (**SA**) suggested that it is an efficient biological active drug.

The maximal stabilization potential is two times lower than the published work.

The FT-IR frequencies have increased as compared to stated values in all techniques, however there is considerable agreement across the evaluated methods.

Acknowledgments

Authors are thankful to higher education commission of Pakistan for assisting their research by financial means (NRPU 7800).

References

Adam, M.S.S. *et al.* (2021) 'Enhanced catalytic (ep)oxidation of olefins by VO(II), ZrO(II) and Zn(II)-imine complexes; extensive characterization supported by DFT studies', *Journal of Molecular Structure*, 1236, p. 130295.

Alaghaz, A.-N.M.A. *et al.* (2014) 'Synthesis, spectral characterization, thermal analysis, molecular modeling and antimicrobial activity of new potentially N2O2 azo-dye Schiff base complexes', *Journal of Molecular Structure*, 1074, pp. 359–375. doi:https://doi.org/10.1016/j.molstruc.2014.05.078.

Buldurun, K. *et al.* (2020) 'Synthesis, spectroscopic properties, crystal structures, antioxidant activities and enzyme inhibition determination of Co(II) and Fe(II) complexes of Schiff base', *Research on Chemical Intermediates*, 46(1), pp. 283–297.

Frisch, J.M. *et al.* (2013) 'Gaussian 09, Revision D. 01, Gauss', *Inc., Wallingford CT* [Preprint].

Glendening, E.D., Landis, C.R. and Weinhold, F. (2012) 'Natural bond orbital methods', *Wiley Interdisciplinary Reviews: Computational Molecular Science*, 2(1), pp. 1–42.

Hassan, A.U. *et al.* (2020) 'Design, facile synthesis, spectroscopic characterization, and medicinal probing of metal-based new sulfonamide drugs: A theoretical and spectral study', *Applied Organometallic Chemistry*.

Hassan, A.U. *et al.* (2021) 'New organosulfur metallic compounds as potent drugs: synthesis, molecular modeling, spectral, antimicrobial, drug likeness and DFT analysis', *Molecular Diversity* [Preprint].

Hassan, A.U. and Guleryuz, C. (2021) 'Theoretical evaluation of the permeability o discharge item (LiOOH) in Li-O_2 batteries', *Latin American Applied Research*, 51(3), pp. 153–157.

Hassan, A.U. and Sumrra, S.H. (2021) 'Exploring the Bioactive Sites of New Sulfonamide Metal Chelates for Multi-Drug Resistance: An Experimental Versus Theoretical Design', *Journal of Inorganic and Organometallic Polymers and Materials*.

Jacob, J.M. *et al.* (2020) 'Mixed ligand copper(II) chelates derived from an O, N, S- donor tridentate thiosemicarbazone: Synthesis, spectral aspects, FMO, and NBO analysis', *Polyhedron*, 189, p. 114736.

Johnson, T. *et al.* (1998) 'Quantitative structure-activity relationship studies of a series of sulfa drugs as inhibitors of Pneumocystis carinii dihydropteroate synthetase', *Antimicrobial agents and chemotherapy*, 42(6), pp. 1454–1458.

Komjáti, B. *et al.* (2016) 'Systematic study on the TD-DFT calculated electronic circular dichroism spectra of chiral aromatic nitro compounds: A comparison of B3LYP and CAM-B3LYP', *Spectrochimica Acta Part A: Molecular and Biomolecular Spectroscopy*, 155, pp. 95–102.

Kusmariya, B.S. *et al.* (2016) 'Theoretical and experimental studies of Cu(II) and Zn(II) coordination compounds with N,O donor bidentate Schiff base ligand containing amino phenol moiety', *Journal of Molecular Structure*, 1119, pp. 115–123.

Kutty, A.A. *et al.* (2020) 'A system thinking approach for harmonizing smart and sustainable city initiatives

with United Nations sustainable development goals', *Sustainable Development*, 28(5), pp. 1347–1365.

Lee, C., Yang, W. and Parr, R.G. (1988) 'Development of the Colle-Salvetti correlation-energy formula into a functional of the electron density', *Phys. Rev. B*, 37(2), pp. 785–789.

Mahmoud, W.H. *et al.* (2019) 'Transition metal complexes of nano bidentate organometallic Schiff base: Preparation, structure characterization, biological activity, DFT and molecular docking studies', *Applied Organometallic Chemistry*, 33(1), p. e4556.

Noreen, S. and Sumrra, S.H. (2021) 'Aminothiazole-Linked Metal Chelates: Synthesis, Density Functional Theory, and Antimicrobial Studies with Antioxidant Correlations', *ACS omega*, 6(48), pp. 33085–33099.

Sharaby, C.M., Amine, M.F. and Hamed, A.A. (2017) 'Synthesis, structure characterization and biological activity of selected metal complexes of sulfonamide Schiff base as a primary ligand and some mixed ligand complexes with glycine as a secondary ligand', *Journal of Molecular Structure*, 1134, pp. 208–216.

Sumrra, S.H. *et al.* (2018) 'AC SC', *Journal of Molecular Structure* [Preprint].

Sumrra, Sajjad Hussain *et al.* (2020) 'A review on the efficacy and medicinal applications of metal-based triazole derivatives', *Journal of Coordination Chemistry*, 0(0), pp. 1–40.

Sumrra, Sajjad H *et al.* (2020) 'Synthesis, characterization, and biological screening of metal complexes of novel sulfonamide derivatives: Experimental and theoretical analysis of sulfonamide crystal', *Applied Organometallic Chemistry*, 34(7), p. e5623.

Sumrra, S., Zafar, W., *et al.* (2021) 'Computational investigation of molecular structures, spectroscopic properties, cholinesterase inhibition and antibacterial activities of triazole Schiff bases endowed metal chelates', *Journal of Molecular Structure*, 1238, p. 130382.

Sumrra, S.H *et al.* (2021) 'Facile synthesis, spectroscopic evaluation and antimicrobial screening of metal endowed triazole compounds', *BioMetals* [Preprint].

Sumrra, S. H, Arshad, Z., *et al.* (2021) 'Metal incorporated aminothiazole-derived compounds: synthesis, density function theory analysis, in vitro antibacterial and antioxidant evaluation', *Royal Society Open Science*, 8(9), p. 210910.

Sumrra, S.H. *et al.* (2022) 'Metal incorporated sulfonamides as promising multidrug targets: Combined enzyme inhibitory, antimicrobial, antioxidant and theoretical exploration', *Journal of Molecular Structure*, 1250, p. 131710.

Thiede, J.M. *et al.* (2016) 'Targeting intracellular p-aminobenzoic acid production potentiates the anti-tubercular action of antifolates', *Scientific Reports*, 6(1), p. 38083.

Reduction of Power losses by Repetitive Controller and Phase Modulation based DVR

Shabbab Zahra[1]*, Saffe Ullah Mughal[2], Nashitah Alwaz[3]

[1]Department of Electrical Engineering, School of Engineering and Technology, NFC-Institute of Engineering & Technology, 60000 Multan, Punjab, Pakistan

[2]Department of Biomedical Engineering, School of Engineering and Technology, Foundation University, 44000 Islamabad, Punjab, Pakistan

[3]Department of Electrical Engineering, School of Engineering and Technology, NFC-Institute of Engineering & Technology, 60000 Multan, Punjab, Pakistan

Abstract. The utility voltages are experiencing significant power quality problems like grid voltage dip, unbalanced 3-phase voltage, and voltage fluctuations owing to diverse load conditions and increasing disturbances at the distribution side of the power system. Among all other Custom power devices to solve grid control issues, the dynamic voltage restorer (DVR) consisting of a power electronics converter can nurture the load amid grid voltage variations; hence protect the sensitive electronic equipment, whereas current quality can be improved using Hybrid Active Power Filter. The purpose of this article is to address the issues related to grid voltage sag and swell compensation and the diminishment of total harmonic distortion. In this paper power, quality improvement through DVR with two control methods is investigated and the results are compared for both techniques. The outcomes of proposed control techniques, DVR and HAPF are discussed, correlated, and validated using MATLAB simulation software.

Keywords: Dynamic Voltage Restorer; Power Quality; Phase Modulation, Repetitive Controller, MATLAB.

Email: shababzahra@isp.edu.pk

1. Introduction

Electricity plays a vital role to run machinery in factories and industrial units, to light our metropolises and powering equipment, H. Arango (2002). To maintain the power quality maintain is the real challenge as the large current carrying capacity of devices makes them prone to power losses, overheating in contrast to transmission lines which carry high voltages and low current, H.De Keulenaer and Rosli Omar (2003, 2011). The utility voltage dip and surge are the critical grid power quality issues that are dangerous to electric power equipment and cause huge financial loss to industries annually, F.A.L Jowder (2009). The different types of problems related to electric power are voltage flicker, dip, surge, interruption, and distortion (C. Chang, Y. Ho 2000, P. Loh, R. Targosz and J. Manson 2007). Usually, around 10 to 90% of PQ issues are produced by voltage sags and swells J. Y. Chan and J. V. Milanovic (2015). Inrush currents, faults, lightning strokes are the reasons for voltage sags whereas voltage swells are caused due by a single line to ground fault or sudden lowering of loads F. C. Trindade, K. V. do Nascimento, and J. C. Vieira (2013). Voltage dip is the drop in voltage amplitude for 1 min that lasts for half cycle can be from 0.1 Pu to 0.9 Pu (A. M. Rauf and V. Khadkikar 2015, C. Benachaiba and B. Ferdi 2008, P. Li and Y. Hu 2017). Even if these defects last for a short interval, they can cause damage to computer and electrical equipment E. Babaei, M. F. Kangarlu (2012).

Voltage surge is the rise in voltage level for 1 min that lasts for half cycle can be from 1.1 pu to 1.8 pu. Electrical loads during grid voltage variations, a dynamic voltage restorer DVR is usually employed F. Z. Peng, L. Chen, and F. Zhang (2003).

Furthermore, (PLL) control is utilized for the compensation of nonlinear voltages with DVR. FUZZY control-based DVR is suggested for the enhancement of voltage stability in a grid-connected system. Similarly, DVR structure based on buck-boost converter topology is utilized to overcome voltage disturbances M. R. Banaei, R. Alizadeh, N. Jahanyari, and E. S. Najmi, (2016). Effective utilization for the transfer of bulk power on an existing transmission line is done with the help of using Matrices converter-based DVR by injecting desired voltage M.-K. Nguyen, Y.-G. Jung, and Y.-C. Lim (2009). PWM direct converter-based DVR is used for fast control of voltage flicker, harmonics current, frequency, and voltage regulation 4Rosli Omar, et al (2011). The cascaded topology is employed to provide improved stability of system J. Anderson and F. Z. Peng (2008).

DVR is presented by A. M. Rauf and V. Khadkikar (2015) with the main focus of the design of urgent, voltage, active power, and characteristics, and the design is explained and discussed. In the structure work of H. Kim and K. Sul (2005) DVR, the design considerations of the DVR line filter are also explained. Repetitive control was introduced to ameliorate recurring interference and keep track of periodical reference signals with null tracking errors. Repetitive control was used to diminish speed variations in the electrical motors, although, later was widely used in the applications of power electronics. A complete investigation of the several repetitive control methods is being manifested. In a three-phase PWM inverter with constant voltage and constant frequency, repeated control is employed to achieve voltage at the output with less perversion. With a repeatable controller, the current at the output of the three-phase rectifier is utilized to reach zero tracking error and improve the PF. The RC introduced in this article can be applied more widely to improve voltage drop, harmonic voltage imbalance with the DVR system. Unlike other solutions that have significant applicability, only one of the controllers is required to overcome the three interferences synchronously. The control structure includes a network voltage feed-forward technique to ameliorate the nonlinear response of the system. In this paper DVR and HAPF accomplishing two control methods are modeled in MATLAB.

Several researchers have proposed different control approaches for improving power quality. In this paper, comparative analysis between phase modulation control and the repetitive controller is being manifested for the efficient performance of DVR. The proposed techniques for power quality improvement contains the following objectives,

- Power quality improvement (voltage dip/ surge and harmonics mitigation) using DVR.
- Comparative analysis of Phase modulation control method and HAPF based Repetitive Control method.

2. Dynamic voltage resistor

The typical circuit of a DVR that comprises of a 1-phase ac to ac converter and its input is connected to parallel with line voltage V-load load voltage and V-line line voltage are in series with its output through a line frequency transformer which provides essential electrical isolation and safety Z. Qin, P. C. Loh, and F. Blaabjerg (2016). Amid utility voltage dip and surge, the converter is supposed to inject positive and negative voltage in series with line voltage, respectively, to balance the Vload J. Kaniewski, Z. Fedyczak, and G. Benysek (2014). It is

primarily positioned between the supply side and the load. Other than overcoming voltage dips and swells, DVR can also compensate for harmonics, transients, and fault currents restrictions J. Anderson and F. Z. Peng (2008). DVR is a FACTS device that maintains a stable load voltage by compensating the supply voltage at the time of a dip or swell.

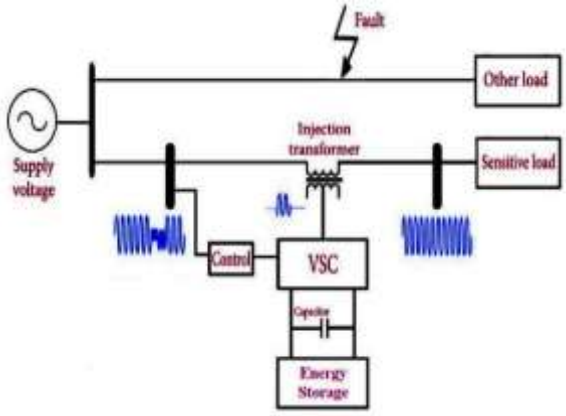

Figure. 1. Typical configuration of DVR

When the supply voltage decreases from a standard value caused by any defects, series voltage VDVR is infused via DVR, and the voltage is regulated to the required value.

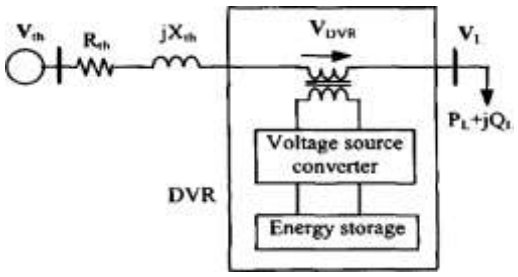

Figure 2. DVR Equivalent Circuit

$$V_{DVR} = V_{Load} + Z_S * \mathrm{I}_{Load} - V_S$$

Where, Vload is Voltage at load, Zs = Source impedance, Iload = Load Current, Vs is Source voltage. Considering Iload as IL, Vload as VL, Zs as ZTh, and Vs as VTh. The load current IL is given as

$$I_L = \frac{[P_L + jQL]}{V} \qquad (2)$$

The equation (2) can be rewritten by considering VL as a reference:

Where ∝, β and δ are the angles of VDVR, ZTh, and VTh respectively. Θ is the power angle.

$$\theta = \tan^{-1}\frac{Q_L}{P_L}$$

DVR injecting complex power injection is calculated as:

$$S_{DVR} = V_{DVR} I *$$

3. Hybrid Active Power Filter (HAPF)

Harmonic filters are used to control harmonics in a system. They are classified into 3 categories passive, active and hybrid. Passive filters are programmed to work on specific frequencies using an LC circuit and they are simple but unstable to change voltage and current. Active filters use inverter circuits to filter harmonics, they are very stable in the case of harmonics. Fig. 3 shows the 3 phase HPAF used in the proposed system.

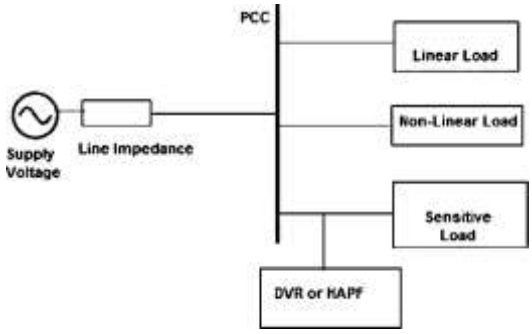

Fig. 3. Three Phase Active Power Filter

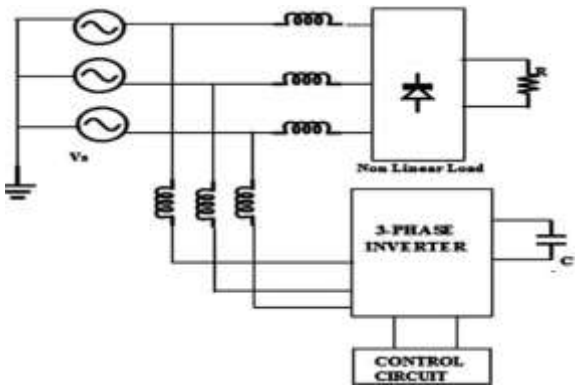

Fig. 4 displays the modeling of the tested system across the sensitive load with DVR.

4. Hybrid Active Power Filter (HAPF)

4.1. Phase Modulation Control method

The suggested method utilizes the error signal which is the distinction between the real data and the calculated data to provoke the inverter's switches.

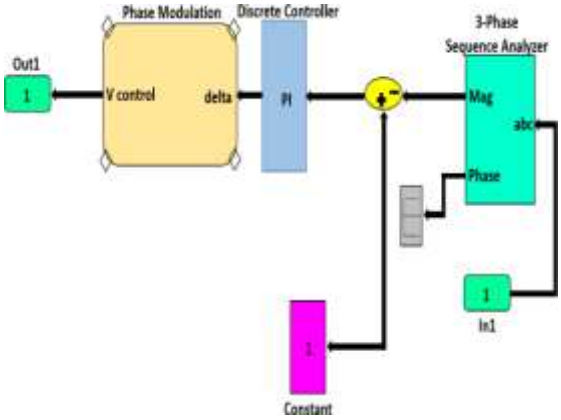

Fig. 5. Control Circuit

It employs a feed-forward approach that utilizes the above error signal to generate gate pulses. The values of load are determined by the sequence analyzer and are then compared with the reference value. PCC fed the desired voltage and current using the Pulse Width Modulation method. The control circuit is shown in Fig. 5. Three-phase fault causes sag/swell of voltage on load terminals. A sequence analyzer usually passes and senses the load voltage. The reference voltage (*Vref*) is compared with the magnitude, whereas (PWM) pulse width modulation is a technique that is validated for switching of inverter and causes 3-phase 50 Hz sinusoidal voltage on load side as well as maintaining 1 p.u across load terminals resulting in 1 p.u as base voltage. Fig. 6 shows the circuit of phase modulation.

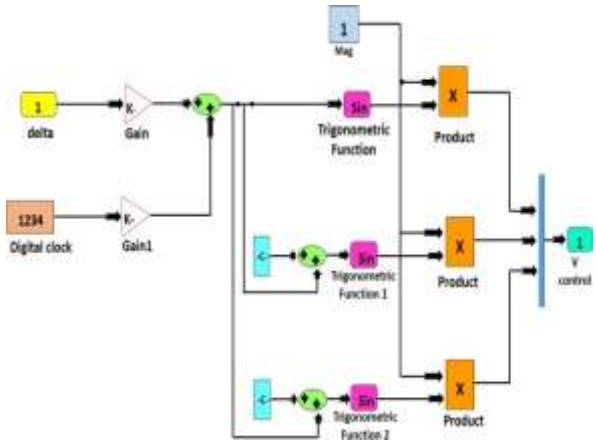

Fig. 6. Phase Modulation Control Circuit

4.2. Repetitive Controller

The fundamental use of this controller is to mitigate the voltage disturbances in case of occurrence of any faults.

$$V(S) = e^{\frac{(-2\pi)S}{(W1)}} V^{*}(S) + \left[1 - e^{\frac{(-2\pi)S}{(W1)}}\right] e^{-t_0 S}$$

$$+ \left[1 - e^{\frac{(-2\pi)S}{(W1)}}\right] e^{-t_0 S} \left[(1 - e^{-t_0 S}) V_{pcc}(S) - P_2(S) I(S)\right]$$

transfer function of the low-pass filter, where D (D) is the estimated value of the DVR time delay, where,

$$T = \frac{(2\pi)}{(W1)} - \beta$$

The transfer functions F(S), Fw(S), Fi(S) with the new modified controller C(S) are:

$$F(S) = \frac{\left[e^{-t_0 S} + Q(S) e^{TS} (e^{\delta S} - e^{-t_0 S})\right]}{1 + Q(S) e^{-TS} (e^{-\delta S} - 1)}$$

$$Fw(S) = \frac{\left[1 - e^{-t_0 S}\right]\left[1 - Q(S)\, e^{-TS}\right]}{1 + Q(S) e^{-TS} (e^{-\delta S} - 1)}$$

$$Fi(S) = \frac{\left[1 - Q(S) e^{-Ts}\right] P_2(S)}{1 + Q(S) e^{-TS} (e^{-\delta S} - 1)}$$

$$1 + Q(S) e^{-TS} (e^{-\delta S} - 1) = 0$$

$$G(S) = Q(S)\, e^{-TS} (e^{-\delta S} - 1)$$

With $\delta = t_0 - t_0\wedge$

The characteristic equation of the resulting closed-loop system is:

To ensure stability, the term G(s) in formula (11) must conform to the Nyquist criterion: if the number of unstable poles of the open-loop system G(s) is equal to zero (p = 0), then the term G (jω). The number of points (-1, 0) counterclockwise must be zero (N = 0. Since all poles of Q(S) are stable, which means that P = 0, then N must be zero to ensure stability, and sufficient conditions for Q(S) can be obtained by the following formula:

The load voltage equation is given as (6) by using this controller, the delay t_0 is not exactly known and the closed-loop system will not be stable. To check this problem a modified controller, C(S) is given.

By implementing this controller, the delay t0 is not

$$C(S) = \frac{Q(S)e^{-(t-t0)S}}{1-Q(S)\,\mathrm{e}^{-Ts}}$$

exactly known and the closed-loop system will not be stable. To check this problem a modified controller, C(S) is given Where Q(S) is the transfer function of a low pass filter to is the estimated value of the time delay for DVR with

By implementing this controller, the delay t0 is not fully known and the closed-loop system will be unstable. To check the problem, a modified controller P(C) is given, where T(F) is the

$$2\,|\sin\left(\frac{\partial}{2}\omega\right)\|\,\mathrm{Q}(j\omega)|<1\forall\omega$$

5. Simulation Results

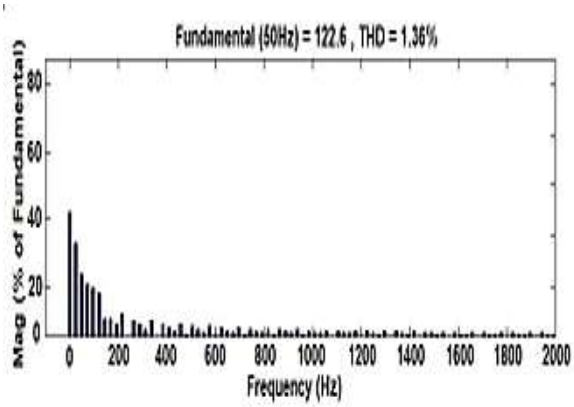

Fig. 6a. Via Phase Modulation

The test system of the DVR consists of a 3-phase, 415V, 50 Hz supply system. The output from the supply unit feeds the primary of a 3-winding transformer. Two parallel feeders are drawn. DVR is connected in series to one of the feeders whereas the other feeder is kept as it is. The parameters are given in Table 1.

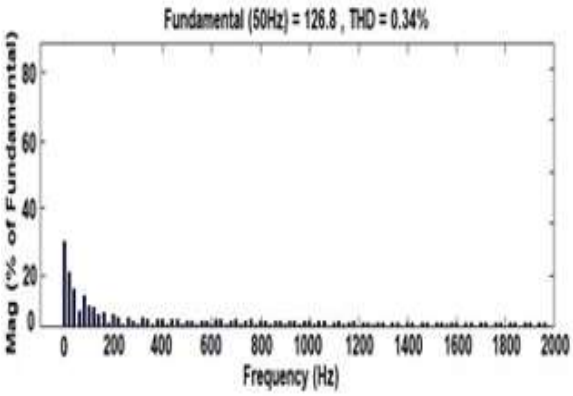

Fig. 6b. Via HAPF RC based DVR

Table 1. DVR Parameters

Supply voltage	3-phase, 415V
Supply frequency	50 Hz
Inverter parameters	IGBT based 3 arms, 6 pulses
Carrier frequency	1080Hz
Sample time	5μsec

The system is analyzed for voltage sag, voltage swell conditions. Fig. 7 shows the 50% of voltage sag. Voltage Sag of 0.5 p.u magnitudes is initiated for 0.3 seconds and the magnitude reduces from 1 p.u. to 0.5 p.u. during this period.

The three-phase programmable source was programmed to produce a 50% voltage sag that is to generate the voltage of amplitude 0.5 p.u. for 0.3 seconds. DVR in this mode injects the required voltage to overcome voltage dip and to give a balanced voltage at the load side.

6. Total Harmonic Distortion (THD)

Total Harmonic distortion is a measure of the degree of perversion in the signal. In the control system, the deadly interruption can cause serious damage. According to standard IEC 61000-3-2, the total harmonic distortion (THD) should be less than 7%. Figs 6, 7 & 8. shows that the THD with traditional DVR is 14.94% which is not acceptable for the stable operation of the system. The THD for Repetitive Controller is 0.34 % that is better than Phase modulation Control and traditional DVR as shown in Figs. 6-8.

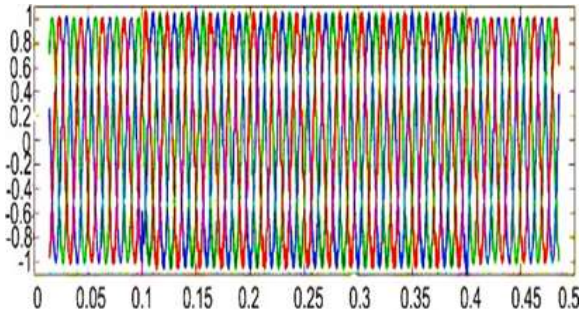

(a) Source voltage with sag 0.5pu

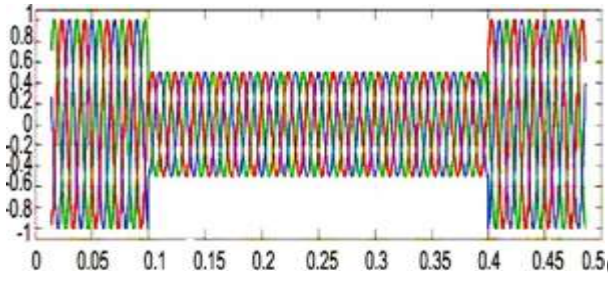

(b) Compensated Voltage via RC

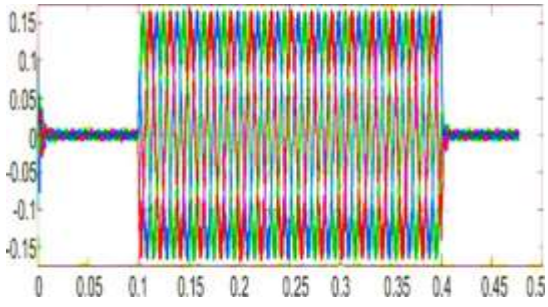

(c) Compensated Voltage via PM

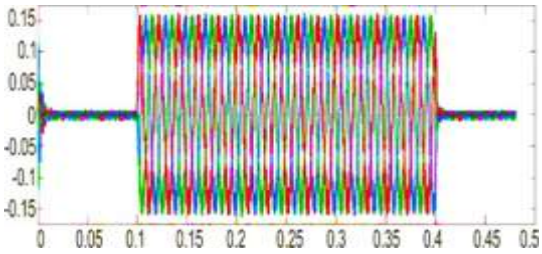

(d) Injected Voltage

Fig. 7. Voltage dip compensation using RC and PM

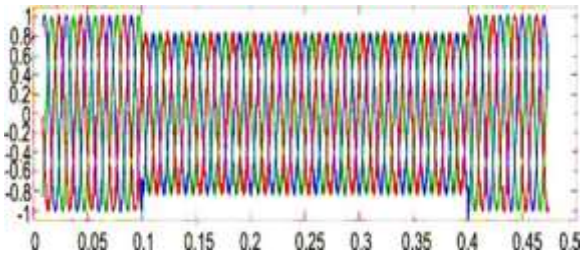

(a) Source voltage with swell 0.5pu

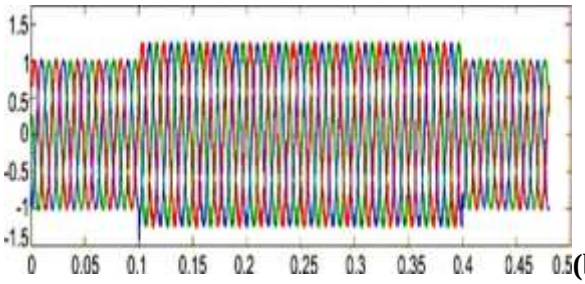

(b) Compensation of Voltage Via RC

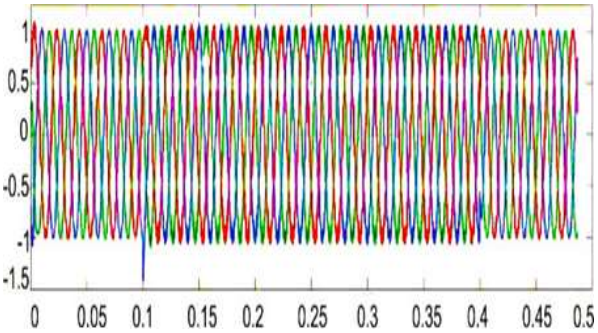

(c) Compensation of Voltage Via PM

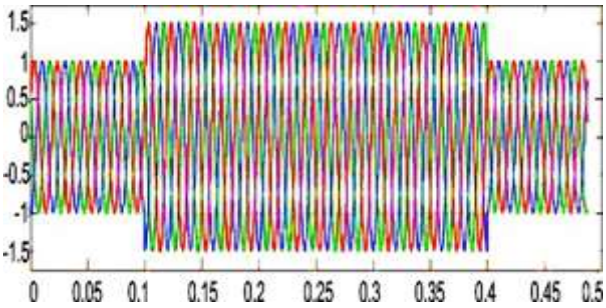

(d) Injected Voltage

Fig. 8. Voltage surge compensation using RC and PM

7. Conclusions

This paper deals with two control techniques for a grid-connected system. DVR is utilized to overcome variations in voltages and thence ameliorate the power quality.

HAPF based Repetitive Controller is used to overcome the harmonics injected due to unbalance loads and hence makes the current drawn to be sinusoidal. MATLAB/SIMULINK is used to structure the proposed DVR and HAPF.

Two techniques, phase modulation, and Repetitive control are compared for voltage THD of source and load. By employing the Repetitive control technique, the THD value has decreased from 4.94% of the phase control method to 3.36%.

By contrasting the phase modulation method with the Repetitive control method, it is obvious that the Repetitive control method is more efficient for compensating the voltage dips using DVR and also harmonics with HAPF.

Nomenclature

DVR Dynamic Voltage Restorer
PQ Power Quality
RC Repetitive Controller
PCC Point of Common Coupling
P(C) Modified ControllerK(S) Voltage gain
T(F) Transfer Function
PM Phase Modulation
HAPF Hybrid Active Power Filter
PLL Phase-Locked Loop
Zs Source Impedance
View Reference Voltage
Vlin Line Voltage
THD Total harmonic distortion
VDVR Series Voltage
IL Load Current

References

Ahmed, H. F., Cha, F., Khan, A. A. and Kim, H. G. (2016). A novel buck-boost ac–ac converter with both inverting and noninverting operations and without commutation problem. *IEEE Transactions on Power Electronics*, vol. 31, no. 6, pp. 4241–4251.

Anderson, J. and Peng, F.Z. (2008). A class of quasi-z-source inverters. *In Industry Applications Society Annual Meeting, IAS'08. IEEE*, pp. 1–7, Sept 2005.

Arango, H., Domingues, E.G., Abreu, J.P.G. and Camposilvan, D.M. (2002). "Applying real options methodology to value electrical power quality projects. In *Harmonics and Quality of Power, 10th International Conference on*, vol. 1, pp. 385–389, IEEE, 2002.

Babaei, E. and Kangarlu, M. F. (2012). Sensitive load voltage compensation against voltage sags/swells and harmonics in the grid voltage and limit downstream fault currents using DVR. *Electric Power Systems Research*. 83(1), 80-90.

Banaei, M. R., Alizadeh, R., Jahanyari, N. and Najmi, E. S. (2016). An ac Z-source converter based on gamma structure with safe-commutation strategy. *IEEE Transactions on Power Electronics*, vol. 31, no. 2, pp. 1255–1262.

Benachaiba, C. and Ferdi, B. (2008). Voltage quality improvement using DVR. *Electrical Power Quality and Utilization. Journal*, vol. 14, pp. 39– 46.

Chan, J. Y., & Milanović, J. V. (2015). Assessment of the economic value of voltage sag mitigation devices to sensitive industrial plants. *IEEE Transactions on power delivery*, 30(6), 2374-2382.

Chang, C., Ho, Y. and Loh, P. (2000). Voltage quality enhancement with power electronics-based devices.

In Power Engineering Society Winter Meeting, IEEE, vol. 4, pp. 2937–2942, IEEE, 2000.

De-Keulenaer, H. (2003). The hidden cost of poor power quality. *European copper institute*.

Georgakas, K. and Safacas, A. (2010). Modified sinusoidal pulse-width modulation operation technique of an ac–ac single-phase converter to optimize the power factor. *IET Power Electronics*, vol. 3, no. 3, pp. 454–464.

Jowder, F. A. L. (2009). Design and analysis of dynamic voltage restorer for deep voltage sag and harmonic compensation. *IET generation, transmission & distribution*, 3(6), 547-560.

Jothibasu, S. and Mishra, M. K. (2015). An improved direct ac–ac converter for voltage sag mitigation. *IEEE Transactions on Industrial Electronics*, vol. 62, no. 1, pp. 21–29.

Kaniewski, J., Fedyczak, Z. and Benysek, G. (2014). Ac voltage sag/swell compensator based on a three-phase hybrid transformer with buck-boost matrix-reactance chopper. *IEEE Transactions on Industrial Electronics*, vol. 61, no. 8, pp. 3835–3846.

Kim, H. and Peng, K. S. (2005). Compensation voltage control in dynamic voltage restorers by use of feedforward and state feedback scheme *IEEE Trans*. on P. E., vol. 20, no. 5, pp. 1169 – 1177.

Li, P. and Hu, Y. (2017). Unified non-inverting and inverting PWM ac–ac converter with versatile modes of operation. *IEEE Transactions on Industrial Electronics*, vol. 64, no. 2, pp. 1137– 1147.

Nguyen, M. K., Jung, Y. G. and Lim, Y.C. (2009). Voltage swell/sag compensation with single-phase Z-source ac/ac converter. *In Power Electronics and Applications, 2009. EPE'09. 13th European Conference on, pp. 1–8, IEEE*.

Peng, F.Z., Chen, L. and Zhang, F. (2003). Simple topologies of PWM ac-ac converters. *IEEE Power Electronics Letters*, vol. 1, no. 1, pp. 10– 13.

Qin, Z., Loh, P.C. and Blaabjerg, F. (2016). Modulation schemes with enhanced switch thermal distribution for single-phase ac–dc–ac reduced-switch converters. *IEEE Transactions on Power Electronics*, vol. 31, no. 4, pp. 3302– 3313.

Rauf, A.M. and Khadkikar, V. (2015). An enhanced voltage sag compensation scheme for dynamic voltage restorer. *IEEE transactions on industrial electronics*, vol. 62, no. 5, pp. 2683– 2692.

Rosli, O., Rahim, N. A., & Sulaiman, M. (2011). Dynamic voltage restorer application for power quality improvement in electrical distribution system: An overview. *Australian Journal of Basic and Applied Sciences*, 5(12), 379-396.

Targosz, R. and Manson, J. (2007). Pan-European power quality survey. *In Electrical Power Quality and Utilization, EPQU 2007. 9th International Conference* on, pp. 1–6, IEEE, 2007.

Trindade, F.C., Nascimento, K.V. and Vieira, J.C. (2013). Investigation on voltage sags caused by dg anti-islanding protection. *IEEE transactions on power delivery*, vol. 28, no. 2, pp. 972–980.

A Study on Structural and Transport Properties of Neodymium Doped La_2CoMnO_6

Javed Ahmad*[1], Muhammad Awais[1], Umair Nissar[1], Jamshaid Alam Khan[1], Hammad Abbas[1], Maryam Hina[1] and S. H. Bukhari[2]

[1]Department of Physics, Bahauddin Zakariya University 60800, Multan Pakistan.

[2]Department of Physics, GC University Faisalabad, Sub-Campus, Layyah 31200, Pakistan

Abstract

Doped rare-earth polycrystalline $La_{2-x}Nd_xCoMnO_6$ (x=0.0, 0.5, 1.0, 1.5 & 2.0) double perovskites have been synthesized by sol-gel auto-combustion method. X-ray diffraction analysis confirms the single phase with a monoclinic structure having the *P2₁/n* space group in all samples. The resistivity measurements show the semiconducting behavior with increasing current in the temperature range 303-493K. The activation energy values i.e., 0.15, 0.23, 0.28, 0.28, and 0.22 eV have also been calculated by Arrhenius plot. The dielectric measurements have shown as the frequency increases the dielectric constant increases smoothly and becomes constant at high frequency.

Keywords: Sol-gel; XRD; Resistivity measurements; Dielectric constant

* Corresponding Author: javedahmad@bzu.edu.pk,

1. Introduction:

Double perovskites oxides (DPOs) having formula $A_2BB'O_6$ (where A = Rare Earth alkaline metal, B & B' are transition metals) have numerous applications due to crystal structure and interesting physical properties which are owed to combinations of different transition elements. Depending upon symmetry of crystal structure, they have different structures like cubic, rhombohedral, monoclinic etc. Due to various synthesis conditions, different structures can also co-exist in same composition of crystal (Singh, Truong, Jandl, & Fournier, 2009). These materials have interesting features such as magneto-electric and magneto-dielectric effect which are produced by the coupling between ferroelectric and ferromagnetic parameters. Since charge ordering process provides a hope in a direction toward novel multiferroics, La_2CoMnO_6 (LCMO) double perovskites having Co^{2+} and Mn^{4+} at B-site is also believed to exhibit a local polar behavior that can be the reason of ferro-electricity in LCMO (Nasir et al., 2019). Interestingly, the ferro-magnetic semiconductor LCMO with high Curie temperature T_c has monoclinic structure with space group *P2₁/n* in which octahedral with Co^{2+} and Mn^{4+} centers stack along (111) alternatively. At room temperature LCMO has magneto dielectric behavior which makes it significant in advancement of electronic devices (N. Bajpai et al.). The effect of doping on structure and physical properties of LCMO has so far been focused at rare-earth site substitution. However partial substitution at Co^{2+} ions with magnetic or non-magnetic ions is expected to regulate physical properties of LCMO compound. The doping of LCMO with Nd^{3+} changes the crystal structure because of size effects (Niketa Bajpai,

Saleem, & Mishra). Moreover, LCMO and doped elements has orthorhombic, monoclinic and rhombohedral phases. These phases are due to the mixing of valence states Co^{2+}/Mn^{4+} and Co^{3+}/Mn^{3+}. LCMO shows multiferroics properties where ferro-electricity coexists with ferromagnetism at very high temperature (Kobayashi, Kimura, Sawada, Terakura, & Tokura, 1998). Additionally, Nd_2CoMnO_6 has multiphase magnetic states with monoclinic symmetry having space group $P2_1/n$. It is noted that Ni/Co-Mn bond angle depends upon Lanthanide ionic radius (R_{LN}). In case of ferromagnetic materials, the Curie temperature (T_c) decreases on decreasing this bond angle (Guo, Shi, Zhou, Zhao, & Liu, 2013).

In this article, a detailed study on $La_{2-x}Nd_xCoMnO_6$ (x = 0.0, 0.5, 1.0, 1.5 & 2.0) DPOs synthesized by sol-gel auto-combustion method has been explored. The single-phase nature of all DPOs is confirmed by XRD patterns. The temperature dependent resistivity curves have shown semiconducting nature as well as confirmed small polaron hopping (SPH) conduction in these materials. At last, the temperature and frequency dependent dielectric constant trend have also been discussed.

2. Experiment:

Sol-gel based auto-combustion method is preferred due to its cost efficiency and low energy consumption. The advantage of this method is to control particle size and homogenize the distribution of particles. $La_{2-x}Nd_xCoMnO_6$ (x=0.0, 0.5, 1.0 & 2.0) DPOs have been synthesized by conventional sol-gel method. High purity reagent-grade chemicals such as $LaN_3O_9.6H_2O$; $Nd_2(NO_3)_2$; $Co(NO_3)_2.6H_2O$ and $MnN_2O_6.4H_2O$ were used as precursor materials. A solution in 100 ml distilled water was made of all nitrates and dissolved completely with help of magnetic agitator after maintaining ph. After 7 hour and 40 minutes keeping temperature of stirrer at 343 K, a gel was formed and then on crushing the ignited material it was converted into fine black powder which was used as precursor in all the materials. All the samples (powdered form) were sintered by placing in a furnace for about 6 hours at 1223 K to remove all the impurities and developing the pure phase. The sintered powder was ground by hand in an agate mortar for about 10 minutes to achieve homogeneity and limited quantity of polyvinyl chloride was added as it behaves like a binder. Paul Otto Weber Hydraulic press was used to make disc like pellets of 13 mm diameter at 50 kN pressure for 3 minutes. Powder was used in X-Ray diffraction method. LCR-8101 was used to investigate dielectric measurements, Keithley source meter 2400 was used to investigate electrical measurements of these samples.

3. Results and Discussions

3.1. X-Ray Diffraction

The structural analysis has been accomplished by X-Ray diffraction analysis. All the patterns were fitted by JANA2006 software using the Rietveld refinement. Moreover, Pseudo-Voigt function has considered different groups like monoclinic $P2_1/n$, tetragonal $I4/m$, orthorhombic $Pbnm$ and orthorhombic $Pnma$. It can be examined that sample has monoclinic structure and space group is $P2_1/n$ for values: x=0.0, 0.5, 1.0, 1.5, and 2.0. The indication of series sample has monoclinic structure with $P2_1/n$ space group. The values of lattice parameters, volume, and goodness of fitting (GOF), R_p and R_{wp} were evaluated after refinement (see **Table 1**). All the samples possessed single phase that shows purity of sample (N Bajpai et al., 2019). XRD refinement of LCMO

confirmed that it belongs to monoclinic ($P2_1/n$). Bragg's reflection at $2\theta = 33°$ peaks were identified in monoclinic structure.

XRD analysis also gives information about particle size, cell parameters and volume of the crystal. All these measurements were calculated for $La_{2-x}Nd_xCoMnO_6$ (x=0.0, 0.5, 1.0, 1.5 & 2.0). The Scherer's formula is given as (Ahmad et al., 2018):

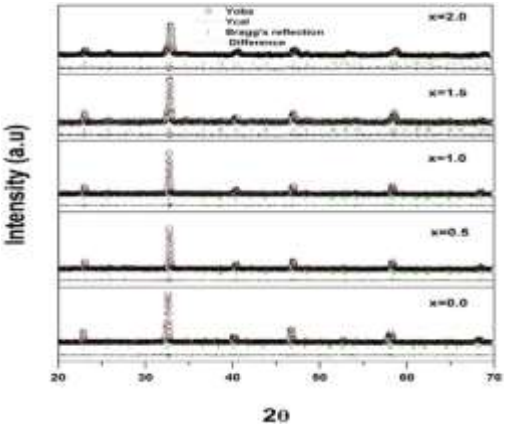

Fig. 1: XRD stack of $La_{2-x}Nd_xCoMnO_6$ (x = 0.0, 0.5, 1.0, 1.5 &2.0) DPOs.

$$D = k\lambda/\beta \cos\theta \quad (1)$$

where, k is the constant depending upon the shape of crystallite size (k=0.9), β is the full width at half maximum (FWHM) of the intensity with the profile of 2θ, λ is the wavelength of Cu-kα_1 radiations (0.15409 Å) and the θ is the Bragg's diffraction angle for most intense peaks.

3.2. Electrical Properties:

These measurements were taken by using Keithley source meter 2400 in a voltage range of 0 to 20 V and temperature range 303-413K. I-V measurements were taken by using two probe methods. Graph between voltage and current is depicted in **Fig. 2** voltage is plotted along x-axis and current along y-axis. If we increase voltage then current is rapidly increased that shows material has semi-conductor like behavior (Asghar et al., 2015).

Table 1: XRD refinement parameters of $La_{2-x}Nd_xCoMnO_6$ (x = 0, 0.5, 1.0, 1.5 &2.0) DPOs.

Material	**La_2CoMnO_6**	**$La_2Nd_{0.5}CoMnO_6$**	**$La_{1.0}Nd_{1.0}CoMnO_6$**	**$La_{0.5}Nd_{1.5}CoMnO_6$**	**Nd_2CoMnO_6**
Structure	Monoclinic	Monoclinic	Monoclinic	Monoclinic	Monoclinic
Space Group	$P2_1/n$	$P2_1/n$	$P2_1/n$	$P2_1/n$	$P2_1/n$
a(Å)	5.5190	5.4623	5.4654	5.4420	5.4765
b(Å)	5.4779	5.4857	5.4933	5.5001	5.5132
c(Å)	7.7588	7.7095	7.7255	7.7018	7.7534
V(Å)^3	234.6	231	231.9	230.5	230
B (∘)	90.00	90.103	90.161	90.183	90.170
R_p (%)	6.34	6.93	6.79	7.16	7.23
R_{wp} (%)	8.03	8.81	8.54	9.01	9.12
GOF	0.90	0.92	0.95	0.95	0.95
Grain size (nm)	84	62.98	44.38	34.07	28.88

I-V graphs have also shown that by increasing temperature current shows maximum values. This can be interpreted as if voltage and temperature increase the value of current also increases that means there are a greater number of electrons jumping from valence band to conduction band. At fixed voltage i.e., V_o =15V increase in temperature results in increasing the current (**see inset of Fig. 2**) which again confirm these DPOs semi-conducting nature.

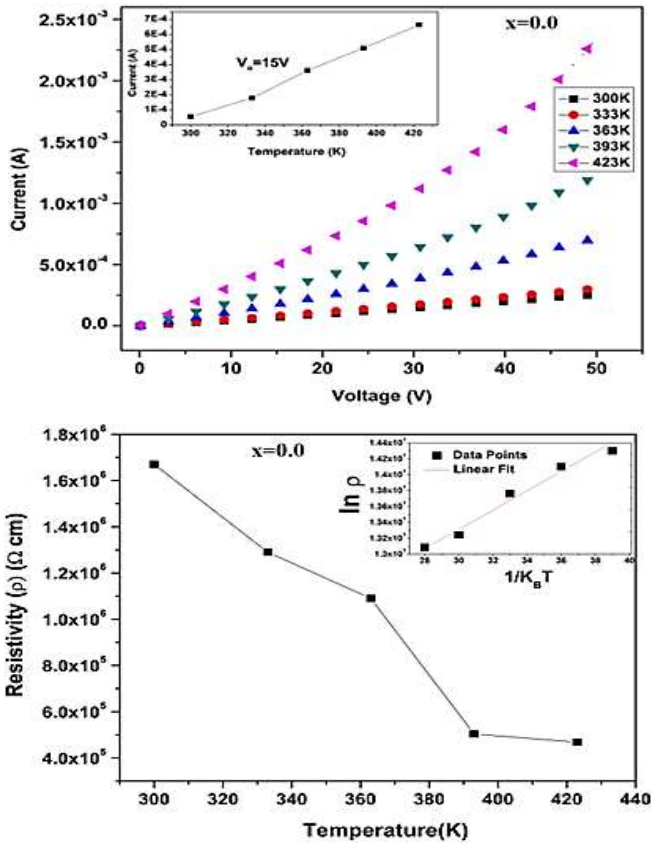

Fig. 2: Graph between I-V of $La_{2-x}Nd_xCoMnO_6$(x=0, 0.5, 1.0, 1.5 &2.0) at different temperatures with inset

Activation energy values for $La_{2-x}Nd_xCoMnO_6$ (where x =0.0 0.5, 1.0, 1.5, and 2.0) is measured from Arrhenius plot and the values are given in the **Table 2**. The slope between $1/K_BT$ and $ln\ \rho$ (see inset of **Fig. 3**) gives activation energy (E_a) values of all DPOs (Krustok, Collan, & Hjelt, 1997).

graph between Temperature (T) and Current (A) at V_o=15V.

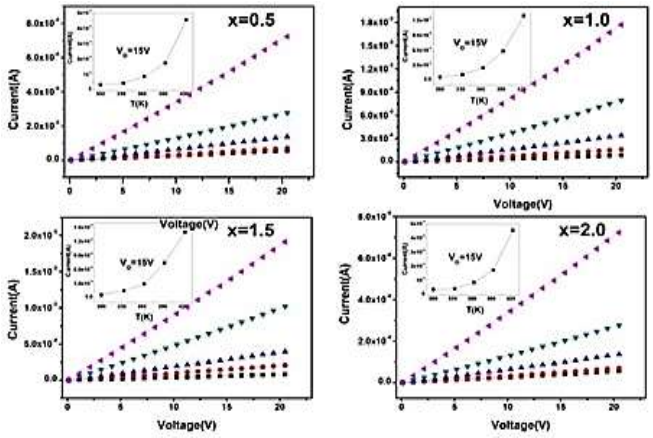

Fig. 3 gives the behavior of resistivity of all samples which can be measured by the given formula:

$$\rho = \frac{R\,A}{L} \qquad (4)$$

while measuring *R*, we have to first find value of 1/R from I-V graph of each sample. Area '*A*' is calculated by using formula $A = \pi r^2$, radius is taken from formula $r = d/2$ and '*L*' is thickness of sample.

Resistivity of pure semiconductor decreases when temperature is increased because dispersion phenomenon occurs in the pure semi-conductor material also on doping same behavior is observed i.e., resistivity decreases on increasing temperature. From **Fig. 4,** it can also be verified that resistivity is decreased on increasing the temperature for all DPOs so all the materials are semiconductors.

The Arrhenius equation is given below:

$$\rho = \rho_\circ \exp\left({}^{E_a}/_{K_B T}\right) \qquad (5)$$

where $'\Delta E'$ activation energy and K_B is Boltzmann constant. 'T' is absolute temperature. Activation energy is minimum amount of energy that is required by a reacting material to get converted into the products. In

given samples E_a is maximum for x = 1.0 whereas lowest for x = 2.0. From the graph it can be noted that with increasing temperature, resistivity decreases which is experimental evidence of semiconducting nature of materials. Furthermore, the hopping mechanism is controlled by temperature which tells us that resistivity decreases with increased temperature (Bosson, Gutmann, & Simmons, 1950). Activation energy was obtained from the graph between $1/K_BT$ vs. $ln\ p$ of $La_{2-x}Nd_xCoMnO_6$ (x = 0, 0. 5, 1.0, 1.5 & 2.0). There is slightly different trend in the values of activation energy (Nissar, Ahmad, Bukhari, & Iqbal, 2020).

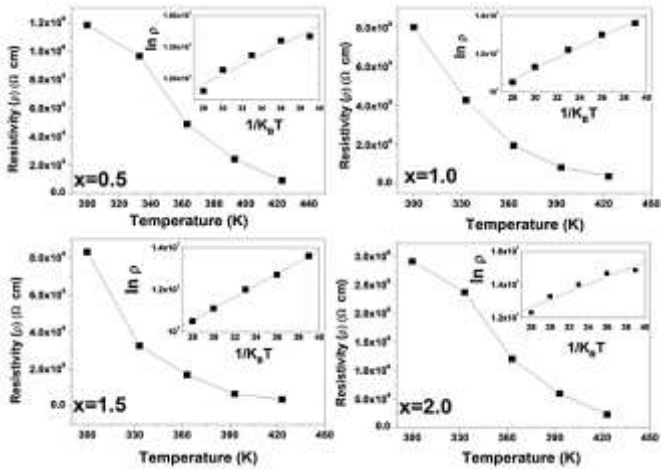

Fig. 4: Graph between temperatures vs. resistivity. Inset shows Arrhenius plot of $La_{2-x}Nd_xCoMnO_6$ (x = 0, 0.5, 1.0, 1.5 & 2.0).

Table 2: shows the values of activation energy (*Ea*) of $La_{2-x}Nd_xCoMnO_6$ (x = 0, 0.5, 1.0, 1.5 & 2.0)

Samples	Activation Energy (eV)
La_2CoMnO_6	0.15
$La_{1.5}Nd_{0.5}CoMnO_6$	0.23
$La_{1.0}Nd_{1.0}CoMnO_6$	0.28
$La_{0.5}Nd_{1.5}CoMnO_6$	0.28
Nd_2CoMnO_6	0.22

3.3. Dielectric Properties:

The graph is plotted between the log of dielectric constant and frequency for $La_{2-x}Nd_xCoMnO_6$ (x=0, 0.5, 1.0, 1.5 & 2.0) as depicted in **Fig. 5**, graph shows that the values of the dielectric constant increases monotonously at low frequency but after certain increase in frequency the dielectric constant becomes almost invariant at higher frequency.

The higher value of dielectric constant at lower frequencies is due to contribution of different polarizations i-e space charge, ionic, dipole, electronic, atomic as well as interfacial (Hong, Ho, Hsu, & Liu, 2004). However, large dielectric constant values for low frequency are related to ionic polarization and also Maxwell-Wagner interfacial type of polarization (Catalan, 2006).

At higher frequencies, the value of dielectric constant becomes frequency independent which shows rotational motions of the polar molecule of dielectric and the equilibrium cannot be attained with field. The observed independent behavior at higher frequency depicts the normal behavior of dielectrics which is followed by complete dielectric materials.

The explanation of this kind of performance is that the dipoles only follow applied field at low frequencies. The lagging behavior of dipoles at high frequency is responsible for decrease in value of dielectric constant (Sayed et al., 2014).

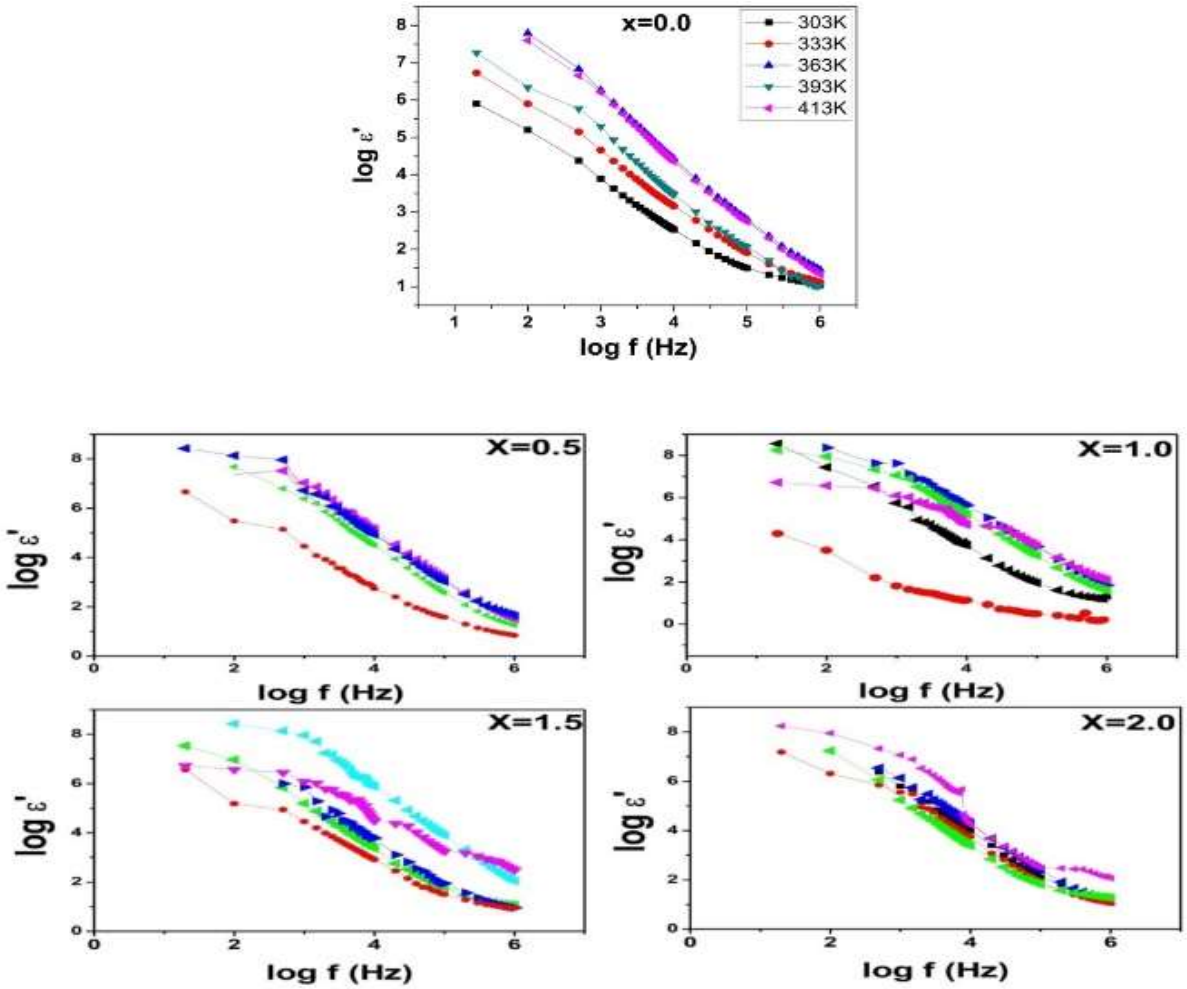

Fig. 5: Graph between log f (Hz) and log έ of La2-xNdxCoMnO$_6$ (x=0.0, 0.5, 1.0, 1.5, 2.0).

4. Conclusions

The polycrystalline $La_{2-x}Nd_xCoMnO_6$ (x=0.0, 0.5, 1.0, 1.5 & 2.0) DPOs were synthesized and investigated in detail. XRD analysis confirms the single phase with monoclinic structure having $P2_1/n$ space group in all samples. The resistivity measurements confirm semiconducting nature of all these DPOs as well as calculated the activation energy values. Moreover, we have also confirmed small polaron hopping conduction (SPH) in these materials. In addition, the dielectric measurements exhibit the dependency at low frequency, however dielectric constant become nearly saturate at high frequency.

References

Ahmad, J., Abbas, H., Bukhari, S. H., Jamil, M. T., Nissar, U., Khan, J. A., & Ali, S. A. (2018). Infrared Reflectivity Analysis of Y3+ Substituted LaMnO3. *Journal of Ovonic Research, 14*(6).

Asghar, Z., Zahid, G., Ahmad, E., ud Din, R., ul Haq, M. N., Subhani, T., . . . Badshah, S. (2015). Effect of particle morphology and coating thickness on fluorescent behavior of Ce doped yttrium aluminium garnet phosphor screens. *Journal of Materials Science: Materials in Electronics, 26*(9), 6744-6749.

Bajpai, N., Saleem, M., & Mishra, A. (2021). *Analysis of structural and dielectric behaviour of La1. 95Y0. 05NiMnO6 and La1. 9Y0. 05Sm0. 05NiMnO6 double perovskites*.

Bajpai, N., Saleem, M., Soni, M., Padole, M., Varshney, M. D., & Mishra, A. (2019). *Bismuth doped double*

perovskite La2CoMnO6: Analysis on structural, dielectric and modulus character.

Bajpai, N., Saleem, M., Soni, M., Padole, M., Varshney, M. D., & Mishra, A. (2019). *Bismuth doped double perovskite La2CoMnO6: Analysis on structural, dielectric and modulus character.* Paper presented at the AIP Conference Proceedings.

Bosson, G., Gutmann, F., & Simmons, L. (1950). A relationship between resistance and temperature of thermistors. *Journal of Applied Physics, 21*(12), 1267-1268.

Catalan, G. (2006). Magnetocapacitance without magnetoelectric coupling. *Applied Physics Letters, 88*(10), 102902.

Guo, Y., Shi, L., Zhou, S., Zhao, J., & Liu, W. (2013). Near room-temperature magnetoresistance effect in double perovskite La2NiMnO6. *Applied Physics Letters, 102*(22), 222401.

Hong, Y. S., Ho, C. M., Hsu, H. Y., & Liu, C. T. (2004). Synthesis of nanocrystalline Ba (MnTi) xFe12− 2xO19 powders by the sol–gel combustion method in citrate acid–metal nitrates system (x= 0, 0.5, 1.0, 1.5, 2.0). *Journal of magnetism and magnetic materials, 279*(2-3), 401-410.

Kobayashi, K. I., Kimura, T., Sawada, H., Terakura, K., & Tokura, Y. (1998). Room-temperature magnetoresistance in an oxide material with an ordered double-perovskite structure. *Nature, 395*(6703), 677-680.

Krustok, J., Collan, H., & Hjelt, K. (1997). Does the low-temperature Arrhenius plot of the photoluminescence intensity in CdTe point towards an erroneous activation energy? *Journal of Applied Physics, 81*(3), 1442-1445.

Nasir, M., Khan, M., Kumar, S., Bhatt, S., Patra, N., Bhattacharya, D., . . . Sen, S. (2019). The effect of high temperature annealing on the antisite defects in ferromagnetic La2NiMnO6 double perovskite. *Journal of Magnetism and Magnetic Materials, 483*, 114-123.

Nissar, U., Ahmad, J., Bukhari, S. H., & Iqbal, Y. (2020). Impact of A-site rare earth substitution on structural, magnetic, optical and transport properties of double perovskites. *Materials Research Bulletin, 127*, 110844.

Sayed, F. N., Achary, S. N., Deshpande, S. K., Rajeswari, B., Kadam, R. M., Dwebedi, S., Tyagi, A. K. (2014). Role of annealing atmosphere on structure, dielectric and magnetic properties of La2CoMnO6 and La2MgMnO6. *Zeitschrift für anorganische und allgemeine Chemie, 640*(10), 1907-1921.

Singh, M. P., Truong, K. D., Jandl, S., & Fournier, P. (2009). Long-range Ni/Mn structural order in epitaxial double perovskite La 2 NiMnO 6 thin films. *Physical Review B, 79*(22), 224421.

INSTITUTE OF SOUTHERN PUNJAB MULTAN, PAKISTAN

EMAIL US AT
patroninchief.sjr@isp.edu.pk
editorinchief.sjr@isp.edu.pk

CALL US AT
+92 61 111 477 786

www.isp.edu.pk